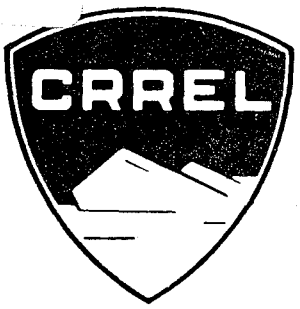

Research Report 345

BRINE DRAINAGE AND INITIAL SALT ENTRAPMENT IN SODIUM CHLORIDE ICE

G.F.N. Cox and W.F. Weeks

December 1975

CORPS OF ENGINEERS, U.S. ARMY
COLD REGIONS RESEARCH AND ENGINEERING LABORATORY
HANOVER, NEW HAMPSHIRE

Unclassified

SECURITY CLASSIFICATION OF THIS PAGE *(When Data Entered)*

REPORT DOCUMENTATION PAGE

READ INSTRUCTIONS BEFORE COMPLETING FORM

1. REPORT NUMBER: Research Report 345
2. GOVT ACCESSION NO.:
3. RECIPIENT'S CATALOG NUMBER:

4. TITLE *(and Subtitle)*: BRINE DRAINAGE AND INITIAL SALT ENTRAPMENT IN SODIUM CHLORIDE ICE

5. TYPE OF REPORT & PERIOD COVERED:

6. PERFORMING ORG. REPORT NUMBER:

7. AUTHOR(s): G.F.N. Cox and W.F. Weeks

8. CONTRACT OR GRANT NUMBER(s):

9. PERFORMING ORGANIZATION NAME AND ADDRESS: U.S. Army Cold Regions Research and Engineering Laboratory, Hanover, New Hampshire 03755

10. PROGRAM ELEMENT, PROJECT, TASK AREA & WORK UNIT NUMBERS:

11. CONTROLLING OFFICE NAME AND ADDRESS: U.S. Army Cold Regions Research and Engineering Laboratory, Hanover, New Hampshire 03755

12. REPORT DATE: December 1975

13. NUMBER OF PAGES: 88

14. MONITORING AGENCY NAME & ADDRESS *(if different from Controlling Office)*:

15. SECURITY CLASS. *(of this report)*: Unclassified

15a. DECLASSIFICATION/DOWNGRADING SCHEDULE:

16. DISTRIBUTION STATEMENT *(of this Report)*

Approved for public release; distribution unlimited.

17. DISTRIBUTION STATEMENT *(of the abstract entered in Block 20, if different from Report)*

18. SUPPLEMENTARY NOTES

19. KEY WORDS *(Continue on reverse side if necessary and identify by block number)*

Brine	Salts	Thickness
Desalination	Sodium chloride	
Growth	Solidification	
Ice	Solutions	
Salinity	Structure	

20. ABSTRACT *(Continue on reverse side if necessary and identify by block number)*

To obtain a better understanding of the desalination of natural sea ice, an experimental technique was developed to measure sequential salinity profiles of a growing sodium chloride ice sheet. Using radioactive ^{22}Na as a tracer, it was possible to determine both the concentration and movement of the brine within the ice without destroying the sample. A detailed temperature and growth history of the ice was also maintained so that the variation of the salinity profiles could be properly interpreted. Since the experimental salinity profile represented a smoothed, rather than a true salinity distribution, a deconvolution method was devised to restore the true salinity profile. This was achieved without any significant loss of end points. In all respects, the salinity profiles are similar to those of natural sea ice.

DD FORM 1 JAN 73 1473 EDITION OF 1 NOV 65 IS OBSOLETE

Unclassified

SECURITY CLASSIFICATION OF THIS PAGE *(When Data Entered)*

20. Abstract (cont'd)

They have a characteristic *C*-shape, and clearly exhibit the effects of brine drainage. Not knowing the rates of brine expulsion or gravity drainage, the variation of the salinity profiles during the period of ice growth could be explained by either process. To determine the relative importance of the desalination mechanisms, a theoretical brine expulsion model was derived and compared to the experimental data. As input for the model, equations describing the variation of some properties of NaCl brine with temperature were derived. These included the brine salinity, viscosity, specific heat, thermal conductivity, and latent heat of freezing. The theoretical brine expulsion model was derived by performing mass and energy balances over a control volume of NaCl ice. A simplified form of the model, when compared to the experimental results, indicated that brine expulsion was only important during the first several hours of ice growth, and later became a minor desalination process relative to gravity drainage which continued to be the dominant mechanism for the remainder of the study period (up to 6 weeks). The rate of gravity drainage was found to be dependent on the brine volume and the temperature gradient of the ice. As either the brine volume or temperature gradient was increased, the rate of change of salinity due to gravity drainage increased. The equation commonly used to calculate the effective distribution coefficient (Weeks and Lofgren 1967) was modified and improved by taking brine drainage into account. An expression was also derived to give the distribution coefficient at very low growth velocities.

PREFACE

This report was prepared by Dr. G.F.N. Cox, formerly of the Department of Earth Sciences, Dartmouth College and currently of the Research Department of Amoco Production Company, Tulsa, Oklahoma, and by Dr. W.F. Weeks, Glaciologist, Snow and Ice Branch of the U.S. Army Cold Regions Research and Engineering Laboratory.

The research was supported by the Polar Continental Shelf Project, Department of Energy, Mines, and Resources, Canada, and by the U.S. Army Cold Regions Research and Engineering Laboratory, Hanover, New Hampshire.

This report was technically reviewed by Dr. W.D. Hibler III and Dr. S.C. Colbeck of USA CRREL and by Dr. S. Martin of the Department of Oceanography, University of Washington.

The authors wish to thank Drs. S. Colbeck, G. Wallis, W. Hibler III, George Hobson and J. Lyons for the advice, criticism, and time given throughout the different phases of this research.

CONTENTS

ILLUSTRATIONS

TABLES

LIST OF SYMBOLS

A	activity of sample (counts/sec)
$C(x)$	activity of sample at position x (counts/sec)
C_1	activity of upper cylinder (counts/sec)
C_2	activity of lower cylinder (counts/sec)
Cp	specific heat (cal/g °C)
D	diffusion coefficient (cm^2/sec)
d	total differential
E	internal energy (cal)
EC	electron capture
$F(x)$	fraction of concentration difference
f	frequency (cycles/data interval)
H	latent heat of freezing of pure water (cal/g)
h	height of freezing chamber (cm)
I	rate of mass production per unit volume of ice and brine (g/cm^3 sec)
J^*	diffusive mass flux relative to the mass average velocity (g/cm^2 sec)
k	thermal conductivity (cal/cm sec °C)
k_{eff}	effective distribution coefficient
k^*	effective distribution coefficient at $v = 0$
k	data interval (cm)
L	latent heat of fusion of ice coexisting with brine (cal/g)
Li_b	latent heat of freezing of brine (cal/g)
L	partial molal enthalpy of water in a NaCl solution (cal/g)
ℓ	ice thickness (cm)
m	mass (g)
n	porosity
q	heat flux (cal/cm^2 sec)
$R(f)$	frequency response at f
S	salinity ($^0/_{00}$)
$\bar{S}$	average salinity ($^0/_{00}$)
$S_e(X)$	experimental salinity at position X ($^0/_{00}$)

$S_t(X)$	true salinity at position X (‰)
T	temperature (°C)
t	time (sec)
$t_{1/2}$	half-life of radioisotope (sec)
U	volume consisting of ice and brine (cm^3)
U_α	volume of species α (cm^3)
V	velocity (cm/sec)
V^*	mass average velocity (cm/sec)
v	growth velocity of ice (cm/sec)
v^*	velocity of the bridging layer (cm/sec)
w	mass fraction
$w(k)$	smoothing function weight at position k
X	arbitrary function
x	data interval (cm)
Y	arbitrary function
Z	arbitrary function
z	data interval (cm)
α	species
α	least squares coefficient
β^+	positive beta decay
∇	divergence operator
δ	boundary layer thickness (cm)
v_b	relative brine volume (‰)
ρ	density (g/cm^3)
ρ'	mass per unit volume of ice and brine (g/cm^3)
ρ''	mass per unit volume of brine (g/cm^3)
μ	viscosity (centipoise)
ϕ	phase shift (degree)

Subscripts

0	initial
1	at time 1
2	at time 2
b	brine
c	calculated
e	experimental
i	ice
s	salt
t	true
w	water
α	of species α

BRINE DRAINAGE AND INITIAL SALT ENTRAPMENT IN SODIUM CHLORIDE ICE

by

G.F.N. Cox and W.F. Weeks

INTRODUCTION

One of the most important and basic properties of a sea ice cover is its salinity profile. The salinity and temperature of the ice uniquely determine the amount of liquid brine and solid salts present in the ice. It is the brine volume v_b that has the dominant role in determining the mechanical, electrical and thermal properties of the ice. The failure strength of sea ice is proportional to $\sqrt{v_b}$; Young's modulus is proportional to v_b (Weeks and Assur 1967); and the dielectric constant is proportional to $[1/(1 - 3v_b)]$ (Hoekstra and Cappillino 1971).

During the formation and eventual decay of an ice sheet there appears to be a continuous decrease in ice salinity. The liquid brine, which is initially trapped within the sea ice structure, drains out into the underlying water. Thus, the mechanical, electrical, and thermal properties change accordingly. Various mechanisms have been suggested to explain brine drainage. However, it has been difficult to ascertain the relative effectiveness of these mechanisms because of a lack of controlled experimental data. Field data have not been helpful in this regard because of large natural variations in several possible controlling parameters.

The main objective of this investigation was, therefore, to perform a series of carefully controlled experiments that would assist in determining which brine drainage mechanisms are responsible for the time variations in the salinity of sea ice. The study involved a controlled laboratory simulation of the growth and evolution of a sea ice sheet. The initial freezing solution was tagged with radioactive ^{22}Na so that both the concentration and the movement of the brine within the ice could be remotely followed using a scintillation detector. Since the quantity of radioisotope was proportional to the amount of entrapped salt, the salinity of the ice could be determined at any specified time or position without destroying the sample. Thermistors were inserted in the freezing chamber so that temperature profiles could be measured. From the sequential temperature and salinity profiles, brine volume profiles were calculated and studied as a function of temperature gradient and time.

PREVIOUS WORK

The realization that brine drainage occurs in sea ice is certainly not a recent discovery. The knowledge that the near-surface layers of sea ice in pressure ridges and multiyear floes are potable when melted has been useful to arctic travelers for many hundreds of years. It is, however, only recently that detailed salinity measurements have given a clear picture of the general nature of these changes (Fig. 1). For instance, young sea ice consistently has a high salinity as well as a *C*-shaped

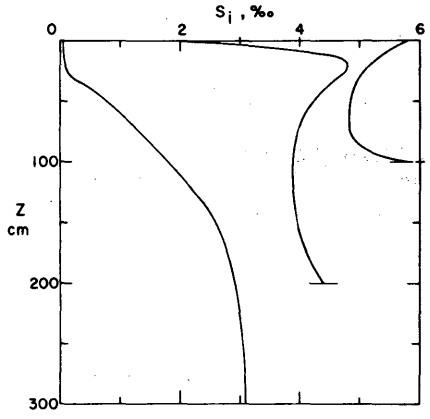

Figure 1. Schematic salinity profiles for sea ice samples that are 100, 200, and 300 cm thick. The low salinity values at the top of the 200-cm profile indicate that this ice has been through a period of summer melt. The 300-cm profile is the steady state salinity distribution in old sea ice (Weeks and Assur 1969).

salinity profile. As a sea ice sheet grows, the mean salinity decreases and the *C*-shaped profile becomes less pronounced, becoming almost flat in the spring. The salinity profile of old ice (i.e. ice that has survived a summer's melt period) is also strikingly different from first year ice in that it gradually changes from a fraction of $1‰$ above the water line to a salinity of roughly $3‰$ in the lower portions of the ice sheet (Malmgren 1927; Weeks and Lee 1958, 1962; Schwarzacher 1959; Cox and Weeks 1974).

In attempting to understand sea ice salinity profiles, it must be remembered that there are at least two different aspects to the problem. First one must understand the initial entrapment of salt within the ice. This is a complex function of the morphology of the growing interface and of the composition of the adjacent solute-rich boundary layer. The morphology and composition are, in themselves, dependent upon the degree of partitioning of solute at, and the rate of transfer of solute from, the interface. Although there is much still unknown about the initial entrapment of salt in ice, Weeks and Lofgren (1967) have, with considerable success, applied concepts developed in the metals and ceramics literature to experimental observations on the freezing of salt solutions. Inasmuch as our present experiments have bearing on this initial entrapment problem, more will be said about this later.

The second part of the problem is that, once the ice itself has been formed, desalination occurs. It is this desalination that is the main concern of the present paper. Four primary mechanisms have been proposed to cause desalination: *brine pocket migration, brine expulsion, gravity drainage,* and *flushing.* Historically the first of these ideas to be considered was brine pocket migration. This occurred when, as a result of a suggestion (by Stefansson), Whitman (1926) attempted to discover the process responsible for the desalination of sea ice. Whitman concluded that the reduction of the amount of brine was controlled by the temperature gradient in the ice sheet, in such a manner that the brine inclusions migrated because of the gradient in the direction of higher temperature. Any brine inclusion in winter sea ice has a cold upper portion and a warmer lower portion. This produces a solute concentration gradient in the inclusion since, via phase relations, the brine is both denser and more concentrated in the colder region. Such a situation is unstable. To reach an equilibrium state, salt diffuses from the colder dense end to the warmer less dense end to minimize the imposed gradient. As a result of this diffusion, the concentration of brine in the lower portion becomes greater than that specified by the local ice temperature, and melting occurs to dilute the brine. Conversely, to restore phase equilibrium in the upper region, freezing takes place so that the brine may be concentrated. Thus, the brine pocket migrates to the warmer portion of the ice sheet, which is usually in the direction of the ice/water interface. Although Whitman realized that this process was undoubtedly slow, its postulated importance remained undisputed for nearly forty years.

It was only in the 1960's, when experimental studies were finally made to determine the rate of brine pocket migration, that this process was rejected as the dominant brine drainage mechanism

(Kingery and Goodnow 1963, Hoekstra et al. 1965, Harrison 1965). This is not to say that brine pocket migration does not occur – it does – but only that it is too slow to cause the changes observed in salinity profiles. This is because, as was concluded by these investigators, the process is limited by the very slow rate of diffusion of the salt in the brine. Untersteiner (1967) has even shown that, for multiyear ice, the downward migration of brine produced by brine pocket migration between August and April (about 2 cm) is compensated by an similar upward migration between May and July when the temperature gradient is usually reversed.

The possibility of brine expulsion being an effective desalination mechanism was first suggested by Bennington (1963). He pointed out that during the ice growth season the temperature at any given level in the ice sheet is, in general, continuously decreasing as the ice sheet thickens. Because of this, freezing occurs on the interior of the brine cavities, so that the brine composition can reach the more concentrated value required by phase equilibria at the lower temperature. Associated with this phase change is a volume increase of approximately 10% which produces a pressure gradient driving the brine down and ultimately out of the ice sheet. Near the ice surface, some brine is also rejected upward during the initial stage of ice growth, giving the new ice a wet, slick appearance.

It is quite reasonable that brine expulsion should occur, in that it is basically a simple continuity relation. However, its relative effectiveness is another matter. Based on qualitative arguments it has been suggested that brine expulsion is probably the most important desalination mechanism during the initial stages of ice growth (Cox and Weeks 1974, Eide and Martin 1975). At present the only quantitative support for brine expulsion as an effective mechanism comes from a series of calculations by Untersteiner (1967). His model is, in principle, capable of producing a multiyear salinity profile that roughly approximates observed multiyear profiles. However, in his analysis, Untersteiner neglected to maintain continuity during warming periods, when a net increase in salinity can actually result. In fact his success in producing a multiyear salinity profile is largely irrelevant, because brine expulsion should be evaluated on the basis of comparisons between sequential salinity profiles from first year ice. In addition (as shown by Untersteiner) flushing, a mechanism that is undoubtedly important in the first year-to-multiyear ice transition, gives a significantly better agreement with the steady-state multiyear ice salinity profile than does brine expulsion.

Gravity drainage includes all processes where brine, under the influence of gravity, drains out of the ice sheet into the underlying sea water. As an ice sheet increases in thickness, its surface rises higher and higher above sea level to maintain isostatic equilibrium. The accumulation of brine above sea water level thereby produces a pressure head which drives the underlying brine out of the ice (Eide and Martin 1975). This process, together with flushing, presumably accounts for the low salinity of the upper portion of multiyear sea ice (Cox and Weeks 1974). In addition, because the density of the brine in equilibrium with ice is determined by the ice temperature, an unstable vertical density distribution also exists in the brine in a growing ice sheet. This results in a convective overturn of brine within the ice, as well as the exchange of the denser brine within the ice with the underlying less saline sea water. For instance, Eide and Martin (1975) have described oscillatory flow in brine channels of the lower part of NaCl ice that was grown in a very thin plastic tank. First they observed the upward uniform flow of the underlying sea water into the brine channels, which was then followed by the downward flow of brine in many small streamers. The regular temperature variations observed within the ice near to the ice/water interface have also been attributed to convective brine drainage from the ice (Lake and Lewis 1970). Also Bennington (1963), Lake and Lewis (1970), and Eide and Martin (1975) have described the characteristic brine drainage channels within the ice that are produced by this process, and Martin (1974) has examined the hydrodynamics of the circulation within individual channels. Dayton and Martin (1971) have observed, in natural see ice, brine draining from such channels at a rate of roughly 1ℓ per minute.

Hence, it is quite obvious that gravity drainage of brine from sea ice does occur. It is only a problem of establishing its importance relative to other postulated mechanisms.

The last desalination mechanism that has been considered by researchers is flushing. This process is actually a form of gravity drainage of brine above sea level. However, unlike the gravity drainage mechanism already discussed, flow is induced by flushing in response to the hydrostatic head which is produced when either snow or ice melts on the ice surface. The requirement of a melt induced hydrostatic head limits flushing to periods of melt and to the period when the ice above sea level (usually 20 to 40 cm in multiyear ice) is permeable, allowing meltwater percolation. It is very likely that flushing is the primary mechanism that controls the form of the steady-state salinity profile in multiyear ice (Untersteiner 1967, Cox and Weeks 1974).

This paper presents both experimental and theoretical information that increases our understanding of the desalination process, brine expulsion and gravity drainage, as well as initial solute entrapment.

EXPERIMENTAL DESIGN

The radioisotope ^{22}Na

^{22}Na is particularly useful in an experiment of this nature. Being an isotope of sodium, its chemical behavior is identical to that of ^{23}Na, the dominant cation in solution in natural sea water. ^{22}Na should therefore be partitioned in the same manner at the ice/water interface as ^{23}Na. The half-life of ^{22}Na is 2.60 years, corresponding to a specific activity of 6.28×10^3 curies per gram. Thus, the number of disintegrations per second is quite high and reasonable accuracy can be obtained during a short count interval. Its half-life is also sufficiently long so that only a slight correction has to be made for the amount of decay during the time of the experiment. The disintegration energy and decay scheme of the radioisotope are presented in Figure 2. It is evident that the emitted gamma rays are monoenergenic (1.276 MeV), that the photon yield per disintegration is essentially 100%, and that ^{22}Na decays to a stable daughter isotope. All these properties make the radioisotope a suitable tracer element.

When gamma radiation interacts with matter both absorptive and scattering processes are possible. The type of interaction is essentially a function of the gamma radiation energy and the nature of the material. For gamma rays having an energy of 1.276 MeV, as is the case for ^{22}Na, the major processes of interaction are the photoelectric effect, the Compton effect, and pair production. The most dominant of these is the Compton effect, which has interactions that are both absorptive and scattering. Pair production and the photoelectric effect may be regarded as absorptive processes.

Description of apparatus

The apparatus for this experiment consisted of a freezing chamber and a radioactive monitoring system which are schematically illustrated in Figure 3. The freezing chamber used to attain unidirectional freezing was an insulated Lucite cylinder cemented to a base with a copper coldplate (coolant chamber) at the top end. The cylinder had an inner diameter of 14 cm, a wall thickness of 0.5 cm, and was 69 cm in length. To ensure that no leakage would occur at the bottom of the cylinder, it was cemented to a solid 8-cm thick Lucite base. The thick base also provided a suitable means of securely attaching a pressure release tube, which prevented pressure buildup in the chamber due to the expansion associated with the water-ice phase change.

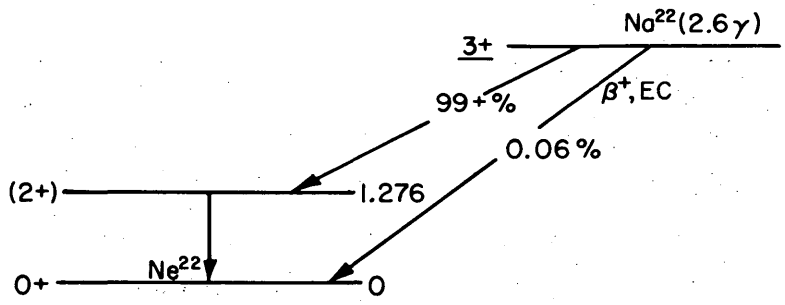

Figure 2. Disintegration energy and decay scheme of radioisotope ^{22}Na. β^+ and EC denote positive beta decay and electron capture.

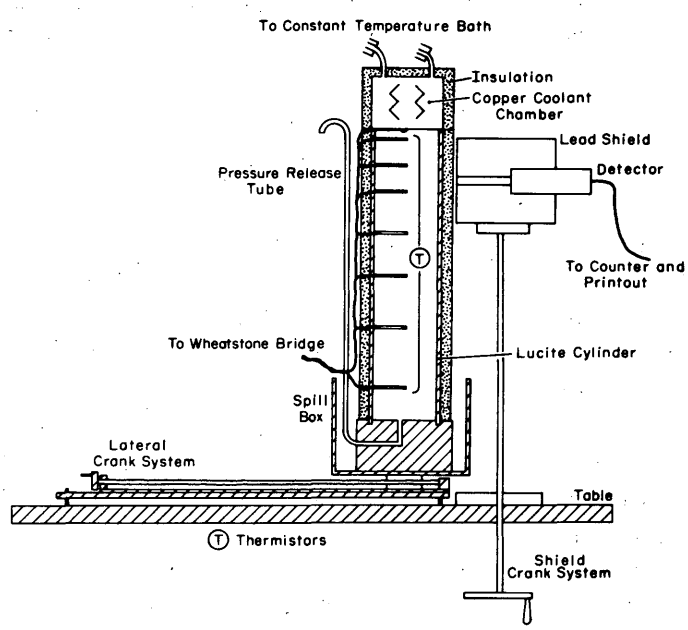

Figure 3. Schematic diagram of apparatus.

The copper coldplate had a 1ℓ capacity and protruded 1 cm into the Lucite cylinder. To obtain the desired temperature, ethylene glycol was continuously circulated through the coldplate from a constant temperature bath. The cold source for the bath was trichloroethane at −36°C tapped from the main coldroom brine system. The trichloroethane was circulated through a copper coil into the bath and then the ethylene glycol was heated to the required temperature within an accuracy of ±1°C.

The radioactive monitoring system consisted of a heavily shielded gamma ray scintillation detector and a Nuclear Chicago 8700 series counter with an automatic printout. Sufficient shielding was placed around the detector so that the transmission of the gamma rays through the lead was reduced to less than 0.1% of the original intensity (confirmed by experimentation). Since the transmission of gamma rays decreases exponentially, additional shielding would have had little effect

on the attenuation. A 2.86-cm ($1\frac{1}{8}$-in.) hole was drilled through the shield so that hollow lead plugs with desired coaxial window sizes could be inserted in front of the detector. Such a technique allowed any size window less than 2.86 cm to be used. Hence, the volume seen by the detector was adjustable and a solid lead plug could be placed in the hole to determine the background radiation. Both the shield and the encased detector were mounted on a crank system so that the activity could be measured at any specified position in the cylinder. The counter had an automatic timer and a count could be obtained for any preset time. At the end of the time interval, both the time interval and the count were recorded on a paper tape by the printout machine.

The dominant type of interaction of the ^{22}Na gamma rays with matter is the Compton effect. Because of the scattering nature of this effect, particular care was taken in the experimental design to minimize the degree of scattering. This was accomplished by placing the shield and detector as close to the freezing cylinder as possible in an attempt to obtain the best geometry. Since the background rate varied considerably along the axis of the cylinder, it was necessary to take both a background count and a window count at each interval. In order to exchange the plugs, the freezing chamber was mounted on a track so that it could be easily moved away from the shield by a crank and screw mechanism. The lateral movement was very slow and steady, in an effort not to disturb the state of the system.

EXPERIMENTAL PROCEDURE

At the beginning of each run, the freezing chamber was filled with a NaCl solution of known concentration that contained sufficient ^{22}Na to produce a total activity of 1 millicurie. The room temperature was then lowered to a specified value, slightly above the freezing point of the solution. By reducing the temperature gradient between the freezing chamber and the surroundings, the amount of heat gained by the system was reduced. Sufficient time was allowed for the solution to reach an equilibrium temperature.

Since radiation dosimetry is very sensitive to the geometry of the apparatus, tests were made to evaluate the end effects. It was found that the activity values for the upper 10 cm of the cylinder were too low and that appropriate corrections had to be made. (This is further described in Correction of Profiles.) At the same time a proportionality constant was evaluated relating the activity of the detected ^{22}Na to the salinity of the observed volume.

To initiate the freezing process, ethylene glycol was pumped from the constant temperature bath to the coldplate. The moment at which the initial ice skim formed was noted as time zero. Temperature and salinity profiles were then measured at regular intervals depending on the growth velocity of the interface and the rate of brine drainage. Ice thicknesses were also systematically recorded. For each salinity profile, measurements were taken every centimeter from the coldplate/ice interface to the base of the ice sheet. Each set of measurements consisted of a background count and a window count. Ten-minute count intervals proved to be the most efficient, in that even if the count interval were doubled, the increase in precision would be insignificant. The standard deviation of the salinity estimates based on this counting interval was less than 0.1‰. After an initial test run, two experimental runs were completed.

CORRECTION OF PROFILES

The salinity profiles that were obtained from the experimental runs represented averaged or smoothed salinity distributions that could not be used directly in an analysis. It was therefore necessary to devise a method of restoring the true salinity distributions.

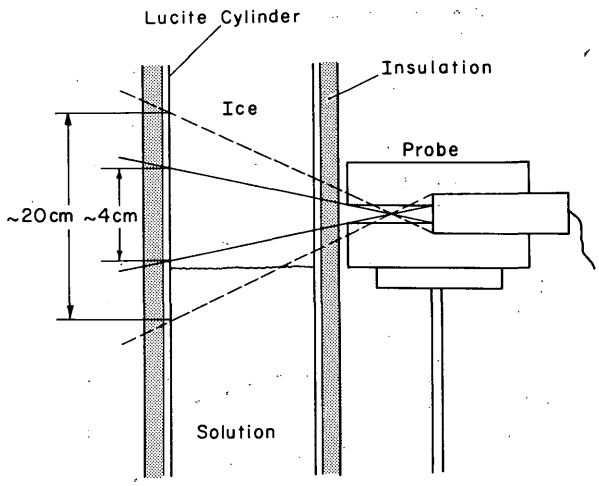

Figure 4. Cross section of apparatus illustrating portion of cylinder sampled by the probe. (Not drawn to scale.)

Assumptions

The length of time required to measure each complete salinity profile ranged from 1 to 16 hours depending on the ice thickness. During the counting interval, the amount of brine drainage was small, and therefore all the different levels composing a given profile are assumed in this report to be taken at the same time. It is also assumed that the ice thickness remained constant during the same period. The times and thicknesses assigned to the profile are those which occured when the detector reached the ice/solution boundary. The freezing chamber is assumed to be a closed system, in that the solution removed through the pressure release tube was not measured.

Decay correction

During each experimental run, the activity of the ^{22}Na decreases from its initial value due to radioactive decay. To compensate for this effect, the activity is recalculated using the exponential decay equation:

$$A_0 = \frac{A_t}{\exp(-0.693t/t_{½})} \tag{1}$$

where A_0 is the corrected activity, A_t is the activity at time t, and $t_{½}$ is the characteristic half-life of ^{22}Na (2.6 years).

Boundary correction

The experimental salinity value obtained at each level actually represents an average salinity value for the volume of ice or solution seen by the probe (Fig. 4). Rather than viewing an infinitesimally small portion of the cylinder, a relatively large conical volume is sampled. Two-dimensionally, this is the area between the solid lines. A substantial amount of radiation is also received from the particles between the dashed lines, since the lead shielding in their path is less than that required to eliminate their effect. The contribution from these particles decreases as they are farther removed from the solid lines. Thus, the vertical section of the cylinder seen by the probe is much larger than

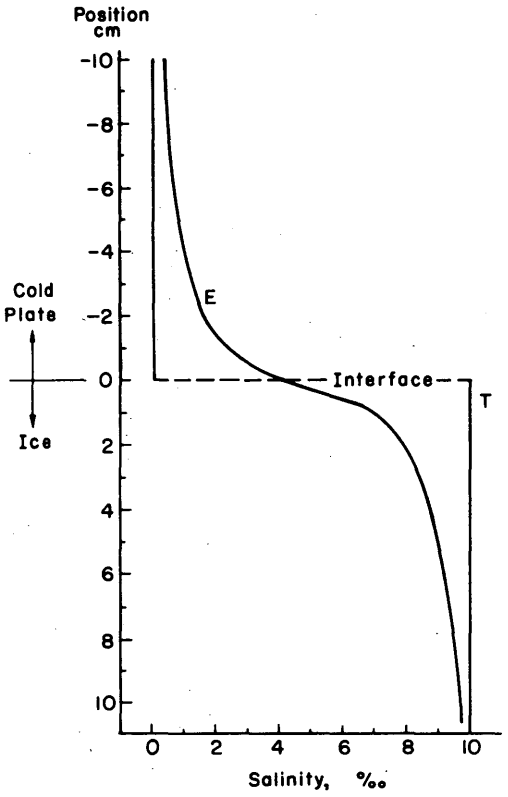

Figure 5. True (curve T) and experimental (curve E) salinity profiles.

the sampling interval (1 cm) and the experimental salinity profile represents an averaged rather than a true salinity distribution.

Such an averaged effect is most important at the upper and lower ice boundaries where there are large salinity changes. Consider the abrupt transition from 0 to 10‰ salinity at the coldplate/ice interface, as shown in Figure 5. The true salinity distribution resembles a step function (curve *T*), whereas the experimental salinity profile (curve *E*) shows a gradual transition. The measured salinity values of the upper portion of the ice are significantly lower than the true values. The problem is therefore to restore the experimental salinity profile to the true salinity distribution before averaging.

Physically, the true salinity profile can be considered as a space series which has subsequently been filtered or convolved with a smoothing function which consists of a series of fractional values, called weights. The weights determine in what proportion each value in the space series contributes to the estimate of the averaged or smoothed observation. The use of a smoothing function is demonstrated in Figure 6. The weights in the block are cumulatively cross-multiplied by the adjacent true values of the space series and the resulting product (experimental value) is entered opposite the space series value multiplied by the central weight. The smoothing function is then moved down one space increment (data interval) and the cross-multiplication is repeated to obtain a second smoothed value. This process is continued until the lowest weight in the smoothing function reaches the end of the series. The resulting product of this operation in this study is the experimental salinity profile.

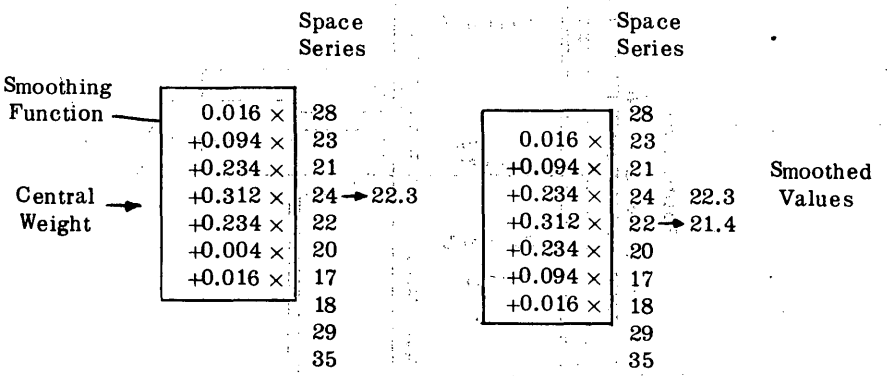

Figure 6. Smoothing a space series by means of a smoothing function (after Holloway 1958).

Applying this to the salinity profiles, the smoothed experimental salinity observation $S_e(x)$ corresponding to the true salinity value $S_t(x)$ in the space series is derived from the true values $S_t(x - n)$ through $S_t(x + m)$ by the following linear equation:

$$S_e(x) = \sum_{k=-n}^{m} w(k)S_t(x + k)$$

$$= w(-n)S_t(x - n) + \ldots + w(-1)S_t(x - 1) + w(0)S_t(x)$$

$$+ w(1)S_t(x + 1) + \ldots + w(m)S_t(x + m) \quad (2)$$

where $w(k)$ is a particular weight of $(n + m + 1)$ weights in the smoothing function.

If there is little noise in the data and the characteristics of the smoothing function are known, it is possible to restore a space series that has been previously smoothed. Possible techniques include transformations and inverse smoothing. However, these methods are not particularly useful here in that they result in the loss of too many end points in the final product. In the present analysis the salinity distribution beyond the upper boundary is known (since the salinity of the coldplate above the ice is zero). Also, the freezing chamber is a closed system where the total amount of ^{22}Na is initially specified. Making use of this information, it is possible to generate a series of independent linear equations having the form of eq 2 where the unknown $S_t(x)$ values can be solved.

First, however, it is necessary to obtain the weights of the smoothing function $w(k)$. The apparatus used to determine these weights (Fig. 7), consisted of two cylinders containing solutions of known activity separated by a sheet of Plexiglass with the activity of the lower solution always being greater. In the same manner as in the NaCl ice experiment, activity readings were taken at 1-cm intervals to obtained the smoothed activity distribution across the interface. This procedure was repeated several times using solutions of different activities. Then, if the activity or concentration of ^{22}Na in the upper cylinder is designated as C_1, and that in the lower cylinder as C_2, the concentration difference is $(C_2 - C_1)$. Using this as a relative scale, the results from the different runs were compared by the following formula:

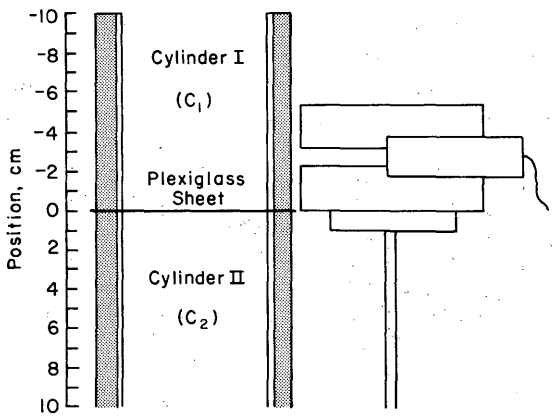

Figure 7. Apparatus used to determine smoothing function weights.

$$F(x) = C(x)/(C_2 - C_1) \tag{3}$$

where $F(x)$ is the fraction of the concentration difference and $C(x)$ is the concentration at a particular x position. The results are tabulated in Appendix A and illustrated graphically in Figure 8.

Given both the true and experimental salinity profiles, curves A and B respectively, a close approximation of the smoothing function can be calculated. The results are not exact in that the experimental data does contain some noise. Since both these profiles can be extrapolated indefinitely in either direction, it is possible to deconvolve the experimental profile by conventional techniques without any loss of end points. Consider a sequence Z obtained by the convolution of two sequences X and Y, where

$$X = [x(0), x(1), x(2), \ldots x(i)]$$

$$Y = [y(0), y(1), y(2), \ldots y(i)]$$

$$Z = [z(0), z(1), z(2), \ldots z(i)] \ .$$

If the X and Z sequences are known, Y can be calculated from the following algorithm

$$y(i) = \frac{z(i) - \sum_{j=0}^{i-1} y(j)x(i-j)}{x(0)} \tag{4}$$

where $y(0) = z(0)/x(0)$ (Healy 1969). The limits of summation must be restricted to include only non-zero values of X and Z. Choosing the proper limits of summation, and applying this equation to the profiles of Figure 8, the weights of the smoothing function are obtained. These are presented in Appendix A and plotted in Figure 9. Again it should be emphasized that these weights determine in what proportion each value in the true salinity distribution contributes to the averaged or smoothed observation. The distribution of the weights is asymmetrical because the experimental probe was not precisely leveled.

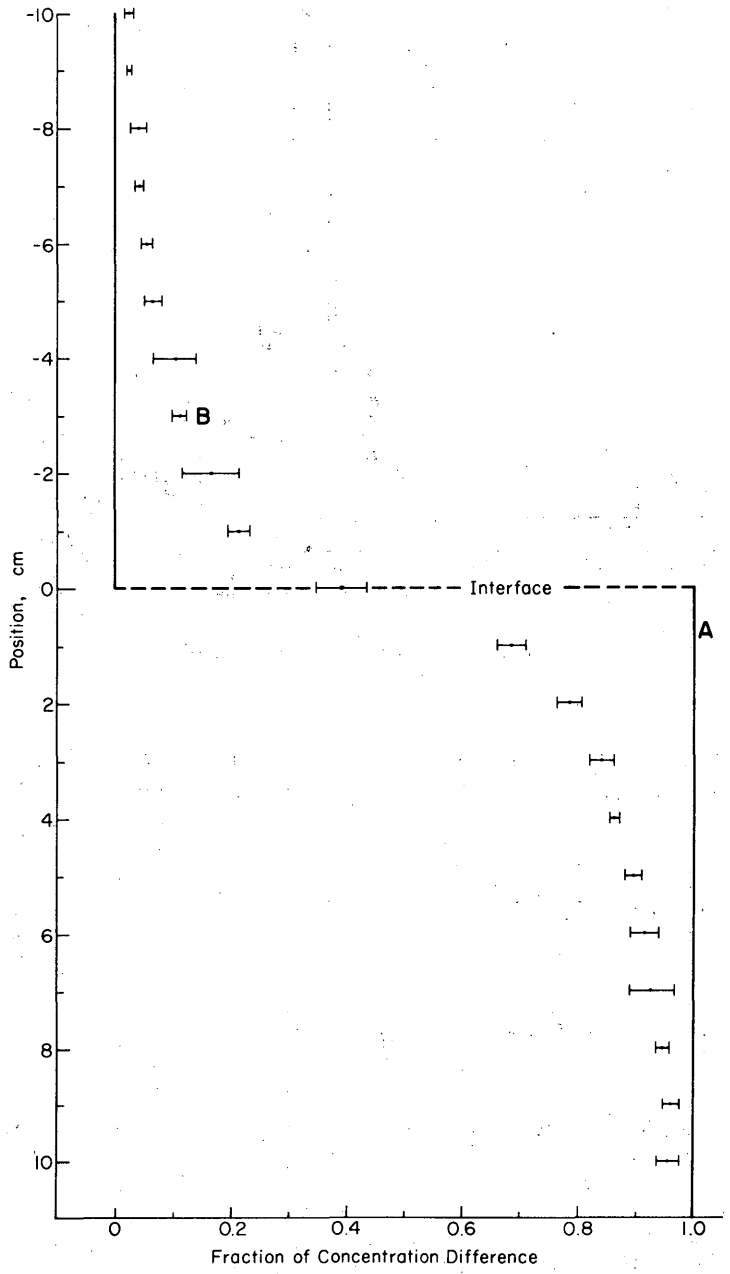

Figure 8. Fraction of concentration difference plotted as a function of position. Curves A and B are the true and experimental concentration distributions, respectively. The bars denote the standard deviation.

The properties of the smoothing function are best illustrated in terms of its frequency response and phase shift. Such an analysis is possible because the variations in the smoothing function and the space series can be produced by the superposition of sinusoidal waves of various amplitudes, frequencies, and phases. The frequency response of the smoothing function $R(f)$ is the ratio of the amplitude of a wave of a given frequency in the space series after smoothing to the original

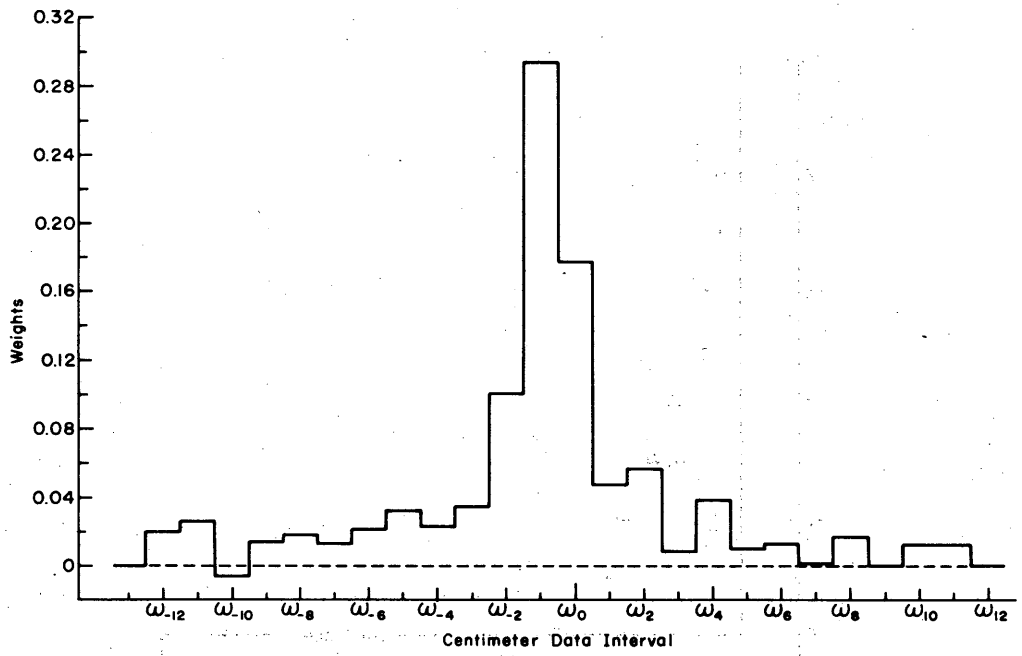

Figure 9. Smoothing function weights.

amplitude before smoothing. It is, therefore, a function of frequency and may be calculated by taking the inverse Fourier transform of the smoothing function (Holloway 1958):

$$R(f) = \int_{-\infty}^{\infty} w(x) \exp(2\pi i f x) dx$$

$$= \int_{-\infty}^{\infty} w(x) \cos(2\pi f x) dx + i \int_{-\infty}^{\infty} w(x) \sin(2\pi f x) dx \,. \tag{5}$$

For smoothing functions having $(n + m + 1)$ discrete weights, the frequency response is computed by (Holloway 1958) as

$$R(f) = \sum_{k=-n}^{m} w(k) \cos(2\pi f k) + i \sum_{k=-n}^{m} w(k) \sin(2\pi f k) \tag{6}$$

where the units of f are cycles per data interval. If the function $w(k)$ is odd, i.e., $w(-k) \neq w(k)$, then the terms containing the sines in the above equations are non-zero and $R(f)$ is an imaginary quantity. For such functions, the absolute value of $R(f)$, which is equal to the square root of the sum of the squares of the real and the imaginary parts, is calculated (Holloway 1958) by

$$R(f) = \left(\{\mathrm{Re}[R(f)]\}^2 + \{\mathrm{Im}[R(f)]\}^2 \right)^{1/2} . \tag{7}$$

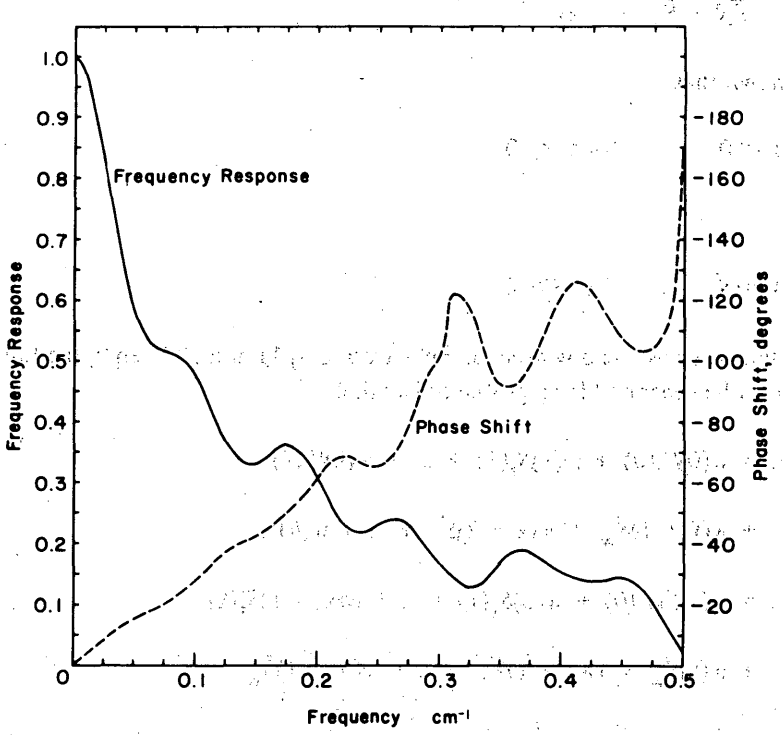

Figure 10. Frequency response and phase shift of smoothing function illustrated in Figure 9.

Odd smoothing functions also have a phase shift ϕ given by Holloway as

$$\phi = \tan^{-1} \{\mathrm{Im}[R(f)]/\mathrm{Re}[R(f)]\} . \tag{8}$$

For even symmetrical functions all the sine terms are zero and $R(f)$ is a real number. Also, since $\mathrm{Im}[R(f)]$ is zero, there is no phase shift.

The frequency response and phase shift of the smoothing function illustrated in Figure 9 are plotted in Figure 10. The attenuation is roughly proportional to the frequency up to 0.5 cm^{-1}. Above this frequency the attenuation is complete for all practical purposes.

Having determined the weights and properties of the smoothing function, the true salinity distribution can now be approximately restored. Let h be the height of the freezing chamber, ℓ the ice thickness including the skeleton layer, $\bar{S}_i$ the average ice salinity, $\bar{S}_w$ the average solution salinity, and S_0 the initial salinity of the solution before freezing. Extrapolating the weights of the smoothing function to minus infinity and to infinity in eq 2, eq 9 is obtained:

$$S_e(x) = \sum_{k=-\infty}^{\infty} w(k) S_t(x + k) . \tag{9}$$

Since the freezing chamber is a closed system, the total amount of ^{22}Na in the ice and solution remains constant giving

$$S_0 h = \bar{S}_i \ell + \bar{S}_w (h - \ell) . \tag{10}$$

It is also known that

$$S_t(x) = 0 \qquad \text{for } x < 0 \tag{11}$$

and

$$S_t(x) = \bar{S}_w \qquad \text{for } x > \ell \tag{12}$$

where x is taken as positive downwards. Substituting eq 11 and 12 in eq 9, the following set of equations may be generated for a profile of length ℓ:

$$\begin{aligned}
S_e(0) &= w(0)S_t(0) + w(1)S_t(1) + \ldots + w(\ell)S_t(\ell) \\
&\quad + w(\ell+1)\bar{S}_w + w(\ell+2)\bar{S}_w + \ldots + w(h)\bar{S}_w \\
S_e(1) &= w(-1)S_t(0) + w(0)S_t(1) + \ldots + w(\ell-1)S_t(\ell) \\
&\quad + w(\ell)\bar{S}_w + w(\ell+1)\bar{S}_w + \ldots + w(h-1)\bar{S}_w \\
&\vdots \\
S_e(\ell) &= w(-\ell)S_t(0) + w(-\ell+1)S_t(1) + \ldots + w(0)S_t(\ell) \\
&\quad + w(1)\bar{S}_w + w(2)\bar{S}_w + \ldots + w(h-\ell)\bar{S}_w \\
S_0 h &= S_t(0)/2 + S_t(1) + S_t(2) + \ldots + S_t(\ell)/2 + \bar{S}_w(h - \ell) .
\end{aligned} \tag{13}$$

Collecting terms containing $\bar{S}_w$ results in a set of $(\ell + 2)$ independent linear equations with $(\ell + 2)$ unknowns:

$$\begin{aligned}
S_e(0) &= w(0)S_t(0) + w(1)S_t(1) + \ldots + w(\ell)S_t(\ell) + \bar{S}_w \sum_{k=\ell+1}^{h} w(k) \\
S_e(1) &= w(-1)S_t(0) + w(0)S_t(1) + \ldots + w(\ell-1)S_t(\ell) + \bar{S}_w \sum_{k=\ell}^{h-1} w(k) \\
&\vdots \\
S_e(\ell) &= w(-\ell)S_t(0) + w(-\ell+1)S_t(1) + \ldots + w(0)S_t(\ell) + \bar{S}_w \sum_{k=1}^{h-\ell} w(k)
\end{aligned} \tag{14}$$

$$S_0 h = S_t(0)/2 + S_t(1) + \ldots + S_t(\ell)/2 + \bar{S}_w(h - \ell)$$

where $S_t(0), S_t(1), \ldots S_t(\ell)$ and $\bar{S}_w$ can be solved.

An example of an experimental salinity profile (R3-8) deconvolved in this manner is shown in Figure 11. The resulting curve consists of very high frequency components which have almost "drowned out" the true salinity distribution. The high frequency noise (experimental error and error introduced by assumptions) has been amplified in addition to the true high frequency fluctuations.

In deconvolving the experimental salinity profile, it is not the properties of the original smoothing function which are important, but rather the properties of the smoothing function's inverse. Deconvolution is actually a method of inverse smoothing. The frequency response of the inverse smoothing function, plotted in Figure 12, is obtained by taking the inverse of the frequency response of the smoothing function. Thus, the high frequency components of the experimental salinity profile are considerably more amplified than the lower frequency components.

To obtain a reasonable representation of the salinity distribution, it is necessary to attenuate the high frequency components of the deconvolved profile. This is performed by means of a Hamming smoothing filter having weights of 0.25, 0.5, and 0.25. The use of a three weight filtering function results in the loss of an end point at both ends of the space series. These points are therefore recalculated in terms of the remaining filtered deconvolved values using the equations in (14) where $S_t(0)$ and $S_t(\ell)$ are the only unknowns. Of the several possible solutions, the pair providing the best fit is chosen. The corrected salinity distribution for profile R3-8 is plotted in Figure 13.

The corrected salinity profile is then convolved or smoothed by the original smoothing function $w(k)$ and compared to the experimental salinity profile (Fig. 14). This procedure provides a means of testing the preceding deconvolution-filter technique and determines the best fitting end points. The difference between the two profiles is calculated. As can be seen in Figure 14, the corrected profile is a reasonable solution.

A flow diagram summarizing the sequence of steps involved in correcting the experimental salinity profiles is shown in Figure 15. A listing of the computer program "CORRECT" and a sample output is found in Appendix B. All the experimental and corrected salinity data for both runs are tabulated in Appendix C.

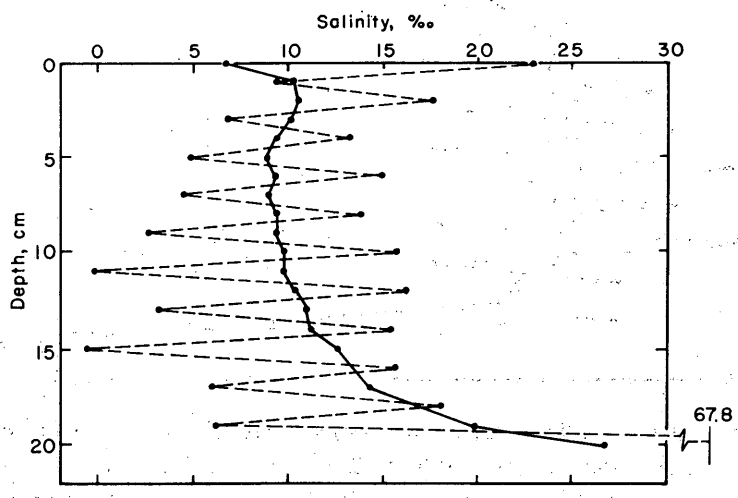

Figure 11. Deconvolution of experimental salinity profile. The solid curve is the experimental salinity profile (R3-8) and the dashed curve is the deconvolved experimental salinity profile.

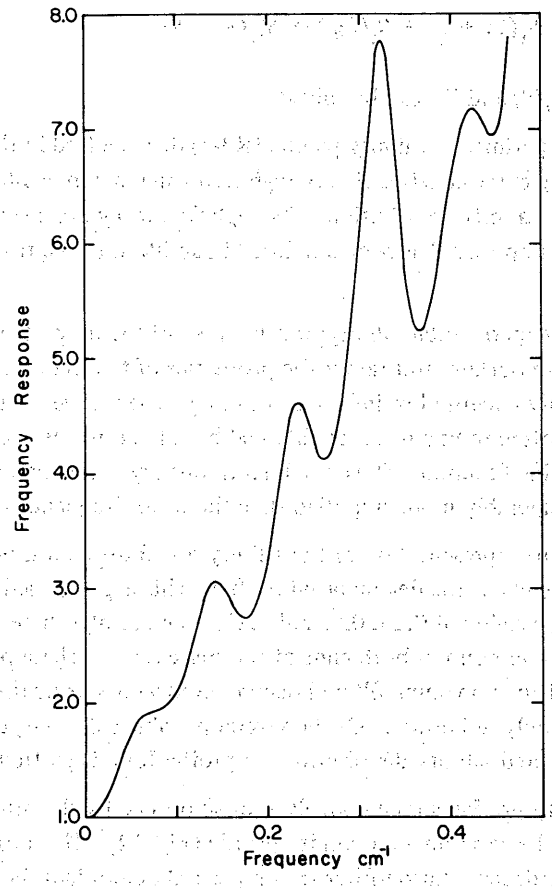

Figure 12. Frequency response of inverse smoothing function.

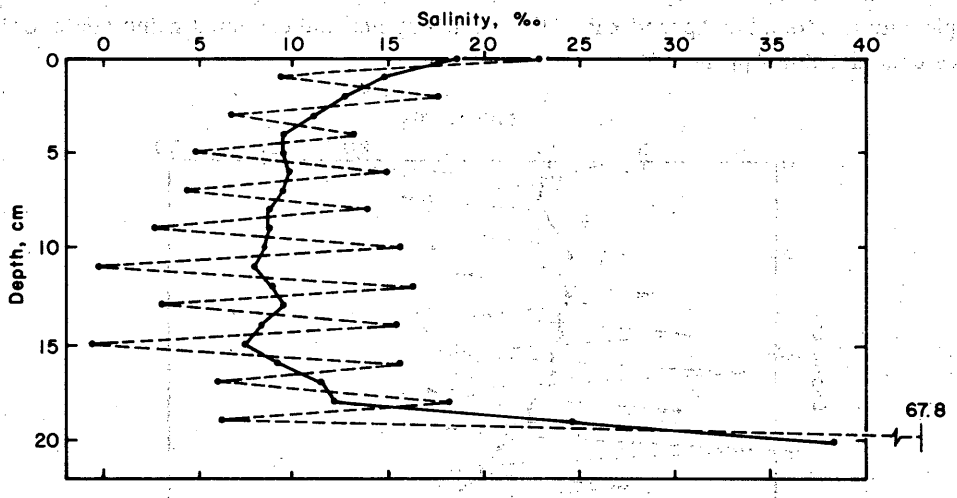

Figure 13. Corrected salinity distribution for profile R3-8. The dashed curve is the deconvolved experimental salinity profile and the solid curve is the filtered deconvolved profile, where the end points have been recalculated (according to the corrected salinity profile).

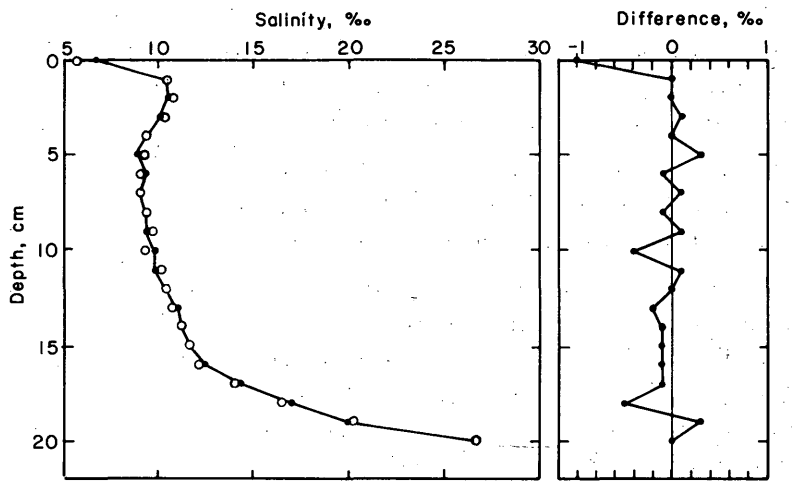

Figure 14. Comparison between the experimental salinity profile (solid curve) and convolved corrected profile (open circles). Difference plotted on the right.

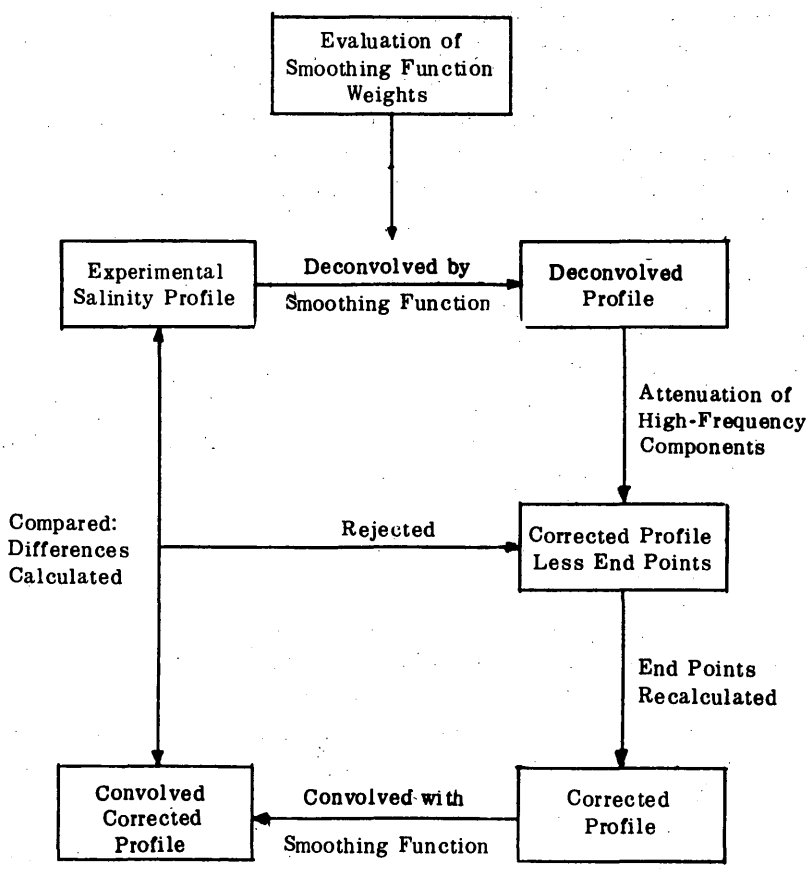

Figure 15. Flow diagram summarizing the sequence of steps involved in correcting the experimental salinity profiles.

Error analysis

The differences between the experimental and convolved corrected profiles indicate that the corrected profiles are not exact solutions. An attempt will now be made to account for these differences in terms of the possible types of errors that are introduced throughout all stages of the study.

All measured salinity values are subject to experimental error. The experimental error is a function of the number of counts obtained for each sample and is estimated at $0.3‰$. Relative to other methods of determining solution concentration, this is a respectable standard deviation.

In the correction procedure, error is initially introduced in the determination of the smoothing function weights. Although eq 4 is straightforward in principle, there are problems concerned with its application (Healy 1969). If the measured values of Z are noisy (i.e. if they contain experimental error) then the values of $y(i)$ obtained from eq 4 will be increasingly inaccurate as i increases. This is true because the errors accumulate in the summation of $y(j)x(i-j)$ in the equation. To avoid a large accumulation of errors, the experimental values are measured several times and an average value is used.

Both the experimental error and the error associated with the smoothing function weights contribute to the difference between the experimental and the convolved corrected profile. However, they do not explain the variation of the difference as a function of position within each profile. In general, the difference between the experimental and convolved corrected profiles is greatest in the vicinity of the boundaries and maximum at the lower boundary. Such a variation is produced during the deconvolution of the experimental salinity profile. The top and bottom boundaries of the true salinity distribution represent a high frequency portion of the curve, which is probably completely smoothed out by the probe. If the true salinity distribution is to be exactly restored, some residual amplitude must remain at each frequency in the experimental salinity profile. Thus, some information is most likely lost, and the difference between the experimental and convoluted corrected profiles is maximum in these regions.

The situation at the lower boundary is even further complicated. The assumption that the ice thickness remains constant during the profile counting interval breaks down during the early stages of growth, when the growth velocity is maximum. During this period, the ice may grow several centimeters and the relations presented in eq 14 no longer apply. As a consequence, the first two profiles in each run must be discarded. As the growth velocity decreases, the growth increment during the counting interval becomes smaller and the error decreases. The difference is also maximum at the lower boundary because, in deconvolving the experimental profile, the ice thickness must be rounded off to the nearest centimeter. This is required because the salinity measurements are only taken at 1-cm intervals. Thus, if the ice thickness does not coincide with the data spacing, the error at the lower boundary is further increased.

In deconvolving the experimental profile, it is assumed that the freezing chamber is a closed system. The fact that the calculated solution salinities are in good agreement with the experimentally determined values indicates that this assumption is reasonable (Fig. 16). In this figure the straight line represents the ideal one-to-one correspondence. As expected, during the latter part of each run, the calculated solution salinities are slightly greater. These minor variations should have little effect on the corrected salinity profiles.

The deconvolution-filter technique appears to work quite well. Besides correcting the experimental salinity profiles at the boundaries, the resolution of the profile in general is greatly increased.

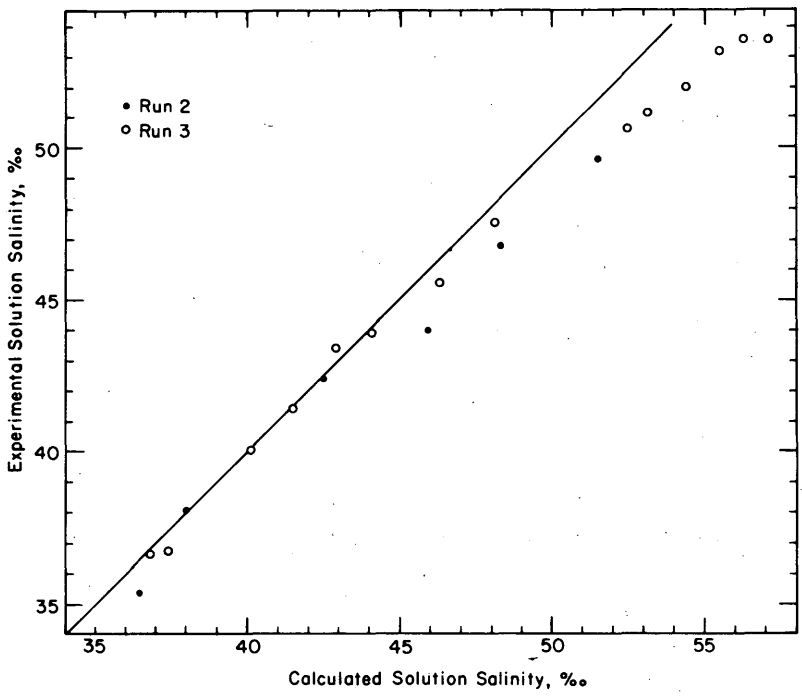

Figure 16. Experimental versus calculated solution salinities. The straight line represents a one-to-one correspondence.

RESULTS

Salinity data

Measurements of salinity were taken during two runs, Run 2 and Run 3. The initial salinity of the solution for the Run 2 was 34.7 $^{0}/_{00}$, close to that of sea water. The run was subdivided into two parts according to the temperature of the coldplate. These will be described as Phase I and Phase II. During Phase I the temperature of the coldplate was approximately $-20°$. This temperature was chosen in an attempt to simulate ambient air temperatures during the arctic fall, when freezing first begins and proceeds at a reasonable rate. In addition any lower temperature would have resulted in the precipitation of solid salts, since the eutectic point of the system NaCl-H_2O is at $-21.1°C$. Inasmuch as solid salt does not drain from the ice, this would have defeated the purpose of the experiment. Several salinity profiles taken during Phase I are illustrated in Figure 17.

After 300 hours the average salinity of the ice decreased at a constant rate and the salinity profiles did not exhibit any dramatic changes. Therefore, at 596 hours, the temperature of the coldplate was raised to $-5°C$ initiating Phase II. It would have been even more desirable to raise the temperature even closer to the melting point. However, since the freezing chamber was essentially a closed system, the salinity of the underlying solution was very high (66 $^{0}/_{00}$) and any further increase in the coldplate temperature would have resulted in considerable undesirable ablation at the ice/water interface. Profiles from Phase II are shown in Figure 18. The profile taken at 582 hours represents the salinity of the ice prior to warming and the remaining two profiles were measured once the new temperature gradient in the ice had stabilized.

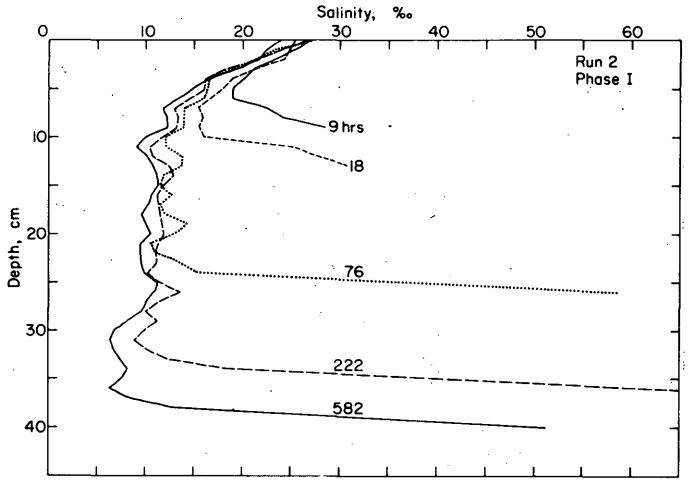

Figure 17. Corrected salinity profiles for Run 2, Phase I.

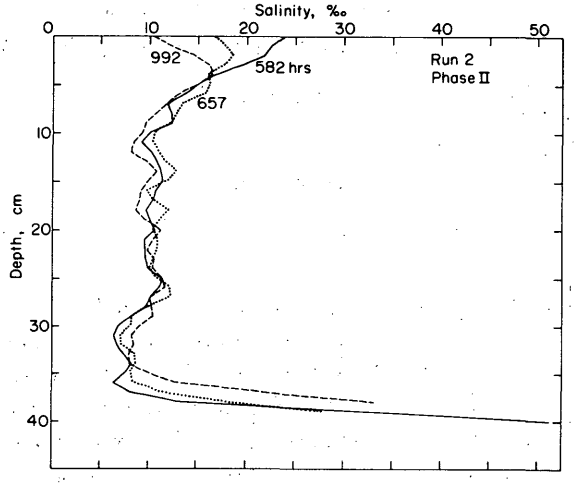

Figure 18. Corrected salinity profiles for Run 2, Phase II.

At 1009 hours (42 days) the temperature of the coldplate was lowered back to −20°C. Shortly thereafter, the circulation pump leading from the constant temperature bath to the coldplate failed. The run was then terminated after six weeks of operation.

The salinity of the initial solution for the Run 3 was also 34.7‰ so that the results could be compared to those of Run 2. However, the coldplate temperature was changed to −10°C. Several of the profiles from this run are presented in Figure 19. The average salinity of the ice, excluding the skeleton layer, is plotted against time for both runs in Figure 20. Here, the salinity of the skeleton layer is not included in calculating the average salinity of the ice, because it appears to be a distinct unit both structurally and compositionally. The brine pockets, which are of prime importance in this study, only begin to form at the top of the skeleton layer. The mechanisms controlling the salinity of this unit are also believed to differ from those controlling the salinity of the ice sheet proper.

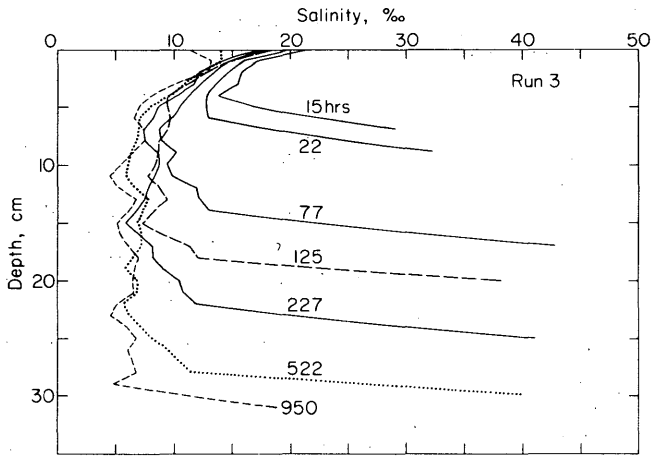

Figure 19. Corrected salinity profiles for Run 3.

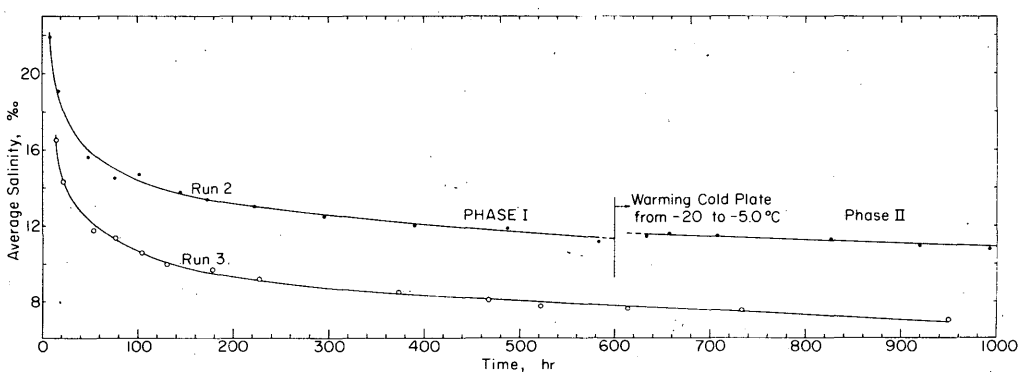

Figure 20. Average ice salinity (excluding skeleton layer) versus time for Runs 2 and 3.

Temperature data

Without a well-documented temperature history of the ice, it would be difficult to interpret the variation of the ice salinity with time, since the temperature must be known to determine the properties of the entrapped brine. These included such important variables as brine salinity, density, specific heat, and volume.

During each run, ice and solution temperatures were measured at least twice daily depending on the growth velocity of the interface. Thermistors were positioned at 0, 5.3, 11.2, 20.1, 33.8, 46.6, and 58.4 cm below the ice surface. The ice temperature profiles were determined by interpolating the readings taken at these positions to every centimeter. As an example, plots of several

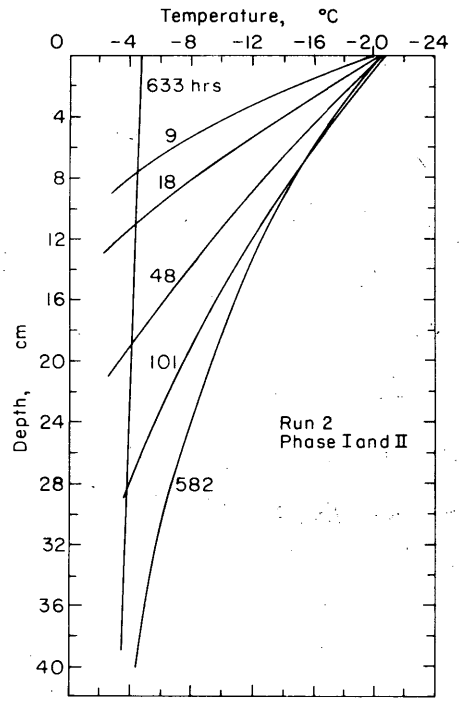

Figure 21. Temperature profiles obtained during both phases of Run 2.

temperature profiles taken during Run 2 are presented in Figure 21. All the profiles for both runs are tabulated in Appendix D.

Growth velocity

The growth velocity of the ice/water interface has proven to be a useful parameter in analyzing the variation of some sea ice properties such as the distribution coefficient (Weeks and Lofgren 1967) and the plate spacing (Lofgren and Weeks 1969). To obtain the growth velocity as a function of position, the thickness-time plots (Fig. 22) were approximated by equations using the method of least squares as described in Weeks and Lofgren (1967). However, unlike these authors, it was not possible to obtain good results using only a single polynominal for the whole growth period. In particular for growth velocities less than 10^{-5} cm/sec, the fourth order polynomial did not provide a good fit. Therefore it was necessary to divide the growth curves into segments and consider each separately. The time-thickness equations for both runs are presented in Appendix E. These equations were then differentiated to obtain the growth velocity at any position in the ice sheet. Because of difficulties in precisely measuring the location of the ice/water interface to less than ±0.5 cm, the estimated growth velocities show more scatter in the low velocity range.

DISCUSSION

The resemblance of the experimental salinity profiles (Fig. 17-19) to those of natural sea ice is very encouraging. The upper portion of the ice has a relatively high salinity and the salinity decreases with depth. Towards the bottom of the profile the salinity again increases. During the initial stage of ice growth, the growth velocity is quite high and considerable brine is trapped in the ice. As the thickness of the ice increases, the growth velocity decreases and less brine is taken into the ice structure. In the skeleton layer at the bottom of the ice, ice bridges have not formed between the individual ice platelets, and the structure is very open. The large amount of brine between the ice platelets in this layer results in the high salt content in this part of the ice sheet. The average thickness of this layer is about 3 cm, a value which agrees very well with skeleton layer thicknesses measured in natural sea ice (Weeks and Anderson 1958, Bennington 1963).

The effects of brine drainage are also clearly illustrated in Figures 17-19. Initially, the lower portion of the ice exhibits a rapid decrease in salinity and, as growth continues, the rate of brine drainage decreases. The salinity of the upper portion of the ice decreases at a slower rate. In contrast, field observations indicate that the salinity of the top layer in natural sea ice decreases at a faster rate. The reason for this difference is not well understood. In some situations it may be partly explained by the increase in permeability caused by the absorption of shortwave radiation.

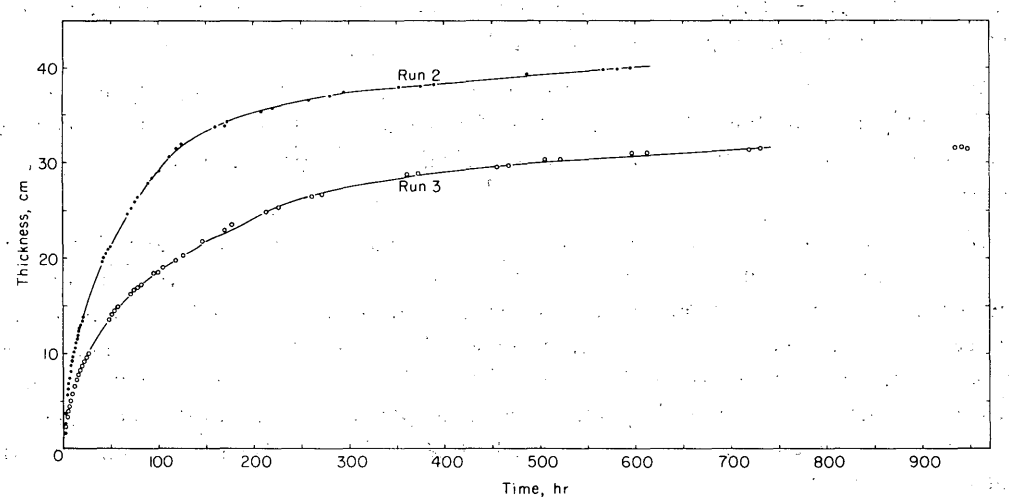

Figure 22. Ice thickness versus time plots for Runs 2 and 3. The solid curves represent equations fitted by the method of least squares.

The variation of the salinity profiles during the growth periods of Runs 2 and 3 can be explained by either brine expulsion or gravity drainage. In the brine expulsion model brine drainage results from the temporal variation of the temperature in the ice. As the thickness of the ice increases, the temperature of the ice at any given level decreases, producing a disequilibrium between the ice and the coexisting brine. To attain equilibrium, freezing takes place on the interior of the brine cavities so that the brine may achieve the more concentrated equilibrium value. This phase transformation results in a volume increase of approximately 10%, and brine is forced out of the cavities. According to this mechanism, the salinity variations should be most pronounced in the lower parts of the ice. The large temperature decrease in this zone during the earlier stages of growth should produce considerable brine expulsion. Closer to the coldplate, the amount of brine drainage should be less, since the ice is already close to its minimum temperature. The rate of brine drainage should also decrease as the ice becomes thicker (Cox and Weeks 1974). As the ice thickness increases, the growth velocity of the interface decreases, resulting in only small variations of the temperature gradient. All these features are clearly displayed in Figures 17-19, suggesting that brine expulsion is a possible desalination mechanism during the period of ice growth.

The variations in the salinity profiles can also be explained by a gravity drainage process where, according to phase relations, the denser brine in the colder portions of the ice moves downward through the ice sheet under its own weight. The rate of gravity drainage should be strongly dependent on both the ice permeability and temperature gradient; that is, as the permeability or temperature gradient increases, the rate of gravity drainage should increase. During the early period of ice growth, the temperature gradients are greater and, as a consequence, more gravity drainage should occur. As the ice sheet increases in thickness, the temperature gradient becomes smaller and should result in less drainage. The amount of gravity drainage should also be greater in the lower portion of the ice where the ice is more permeable. Thus, the variation in salinity in Figures 17-19 can also be explained by gravity drainage. The problem is therefore to determine the relative importance of brine expulsion and gravity drainage during ice growth.

In both Runs 2 and 3 the decrease in the average salinity of the ice was slower after 200 hours (Fig. 20). Since the temperature gradient was smaller than before and there was little change in

the temperature gradient at each level, these lower brine drainage rates can be attributed to a decreased rate of gravity drainage and/or brine expulsion.

After the coldplate temperature was raised to $-5^{\circ}C$ there was a substantial decrease in the salinity of the upper portion of the ice (Fig. 18). This variation of the salinity profile can only be explained by a gravity drainage process, since no cooling of the ice occurred after the temperature change.

After warming there was only a minor change in the average ice salinity (Fig. 20). The decrease in salinity of the upper half of the ice was compensated by an increase in the lower half (Fig. 18). The increase in salinity in the lower portion of the ice sheet can be explained by the warming of this ice when the coldplate temperature was increased. For the brine to remain in equilibrium with the warmer ice, it was necessary for the ice around the brine cavities to melt. Since the density of the ice is less than that of water, the phase change resulted in upward flow of the underlying solution to compensate for the volume difference. The salinity at the bottom also increased due to gravity drainage from above.

Further examination of these profiles indicates that the permeability of the ice is an important parameter in gravity drainage. The rate of brine drainage in the upper part of the ice during Run 3 was somewhat greater than during Run 2. Because the growth velocity was lower, this cannot be explained by increased brine expulsion. The only logical explanation is that more gravity drainage has occurred in the ice of Run 3. In Run 2 the upper portion of the ice was very close to its eutectic temperature and, relative to Run 3, the brine volume was much smaller. The brine pockets in the ice of Run 2 were then smaller resulting in a lower permeability. In Run 3 the higher ice temperature resulted in large brine pockets and a greater permeability, permitting more gravity drainage. The importance of the ice permeability is also demonstrated in Figure 18. Although the brine in the upper part of the ice was much denser than the brine at lower levels, gravity drainage was inhibited until the warming phase was initiated. As a result of warming, the brine pockets became larger, increasing the permeability. The denser brine was then free to move more rapidly to lower levels.

To determine the relative importance of brine expulsion and gravity drainage during the period of ice growth, a theoretical brine expulsion model is derived and then compared to the experimental data. However, the model does require a knowledge of the brine and ice properties. These are described in the next section.

BRINE AND ICE PROPERTIES

If any theoretical analysis of experimentally grown NaCl ice is performed, a knowledge of the properties of the ice and coexisting brine is required. This section presents a compilation of such data. The brine properties include: salinity S_b, density ρ_b, relative volume v_b, viscosity μ_b, specific heat Cp_b, and thermal conductivity k_b, while the ice properties include: density ρ_i, specific heat Cp_i, and thermal conductivity k_i. Accurate least squares equations have been determined for some of the brine properties. Table I gives the least squares coefficients, the correlation coefficients, and the standard errors of the estimates for curves that are fitted to data on the temperature dependent variations in the above parameters.

Brine salinity

According to the phase relations illustrated in Figure 23, at each temperature the brine has a unique composition. If the temperature of the coexisting ice is known, the brine salinity may be determined. The liquidus curve in the phase diagram can be described by the equation:

Table I. Least squares coefficients α, correlation coefficient, and standard error of the estimate for brine property curve fits which are discussed in text.

Brine property	α_1	α_2	α_3	α_4	*Correlation coefficient*	*Standard error*
Salinity S_b	−17.5730	−0.381246	-3.28366×10^{-3}		0.999927	0.433824
Viscosity μ_b	1.78823	-5.94609×10^{-2}	7.94871×10^{-3}	-9.46621×10^{-5}	0.999998	6.45424×10^{-3}
Thermal conductivity k_b	1.35285×10^{-3}	7.36164×10^{-6}	4.39196×10^{-8}		0.999991	1.99516×10^{-7}
Specific heat Cp_b	1.00584	2.66162×10^{-2}	1.22405×10^{-3}	2.23428×10^{-5}	0.999806	1.82467×10^{-3}
Latent heat of freezing Li_b	−79.6313	−1.18425	-7.13999×10^{-3}		0.999981	4.47471×10^{-2}

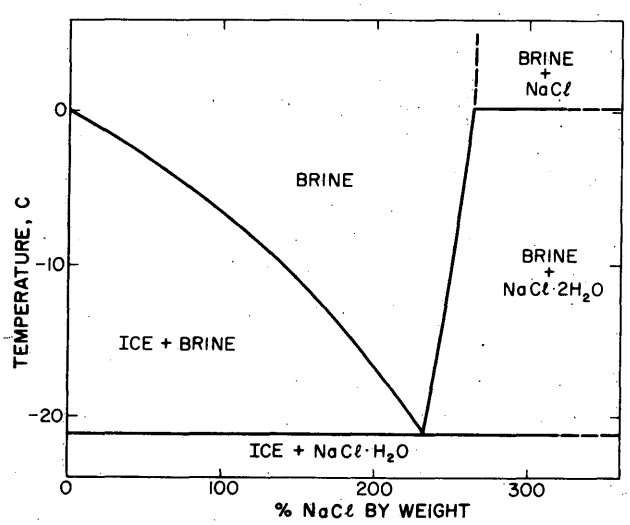

Figure 23. Low temperature portion of the system NaCl – H_2O (Weeks 1968).

$$S_b = \alpha_1 T + \alpha_2 T^2 + \alpha_3 T^3 \tag{15}$$

where S_b is the brine salinity in $^0/_{00}$ and T is the ice temperature in °C. The experimental data used were those compiled by Wolf and Brown (1965).

Brine density

Unfortunately, there are not enough data available to give an accurate estimate of the brine density in equilibrium with ice. Most of the analyses of the variation of brine density with temperature and

composition were terminated at, or near, 0°C. Thus, at temperatures below 0°C only an approximation may be obtained.

Zubov (1945) presented the following argument. At temperatures above 0°C, the variation of the density with concentration is approximately equal to 0.0008 g/cm^3 per $^0/_{00}$ from 0 to 260$^0/_{00}$. It is also known that the density of supercooled water is approximately equal to 1 g/cm^3. Thus, the variation of the brine may be expressed as

$$\rho_b = 1.0000 + 0.0008 S_b \tag{16}$$

where ρ_b is the brine density in g/cm^3 and S_b is the brine salinity in $^0/_{00}$.

Brine volume

Weeks (1962) has calculated the brine volume for NaCl ice from the experimentally determined properties of the ice and brine that coexist at the different temperatures between 0°C and the eutectic temperature (-21.2°C). The relation used was

$$v_b = 1000\left(\frac{S_i/\rho_b S_b}{S_i/\rho_b S_b + (1 - S_i/S_b)/\rho_i}\right) \tag{17}$$

where v_b is the brine content by volume in $^0/_{00}$, S_i is the bulk ice salinity in $^0/_{00}$, S_b is the brine salinity in $^0/_{00}$, ρ_i is the pure ice density in g/cm^3, and ρ_b is the brine density in g/cm^3. A tabulation of the results is given in Weeks (1961, App. A).

Brine latent heat of freezing

The latent heat of freezing of pure ice from a saline solution Li_b is equal to

$$Li_b(S_b, T) = H_f(T) + \bar{L}_w(S_b) \tag{18}$$

where $H_f(T)$ is the latent heat of the freezing of pure water at temperature T, and $\bar{L}_w(S_b)$ is the relative partial molal enthalpy of water in a NaCl solution or a brine of salinity S_b (Anderson 1966). $\bar{L}_w$ accounts for the effects of the dissolved salts during the freezing process.

Values of the latent heat of the freezing of pure, supercooled water converting isothermally (reversibly) to ice, are given by Dorsey (1940). These values are listed in Table II. A least squares polynominal curve fit of this data yields

$$H_f = -79.7443 - 1.2896T - 0.0092T^2 \tag{19}$$

where H_f is in cal/g and T is measured in °C. The correlation coefficient is 0.9999 and the standard error of the estimate is 0.0196. A comparison between the tabulated values and the least squares curve is shown in Figure 24.

The relative partial molal enthalpy of water in NaCl solutions has been determined by Randall and Bisson (1920) and their results appear in Table III. Note that the enthalpy values are given in cal/mole (of water). This data may also be well approximated by a least squares curve giving

$$\bar{L}_w = 0.5520 + 0.0334 S_b + 0.0008 S_b^2 \tag{20}$$

Table II. Values of the latent heat of the freezing of pure supercooled water at various temperatures (Dorsey 1940).

Temperature T (°C)	*Latent heat H_f (cal/g)*
0	−79.7
− 5	−73.6
−10	−67.8
−15	−62.4
−20	−57.6
−22	−55.9

Table III. Relative partial molal enthalpy of water in sodium chloride solutions at various salinities (Randall and Bisson 1920).

Salinity S_b (‰)	*Relative enthalpy $\bar{L}_w$ (cal/mole)*
0	0
16.2	0.2
21.6	0.3
32.1	0.9
46.2	2.4
68.9	4.0
90.4	7.3
124.5	11.0
162.5	15.9
201.2	20.0
270.0	21.4
324.2	15.6
356.5	11.5

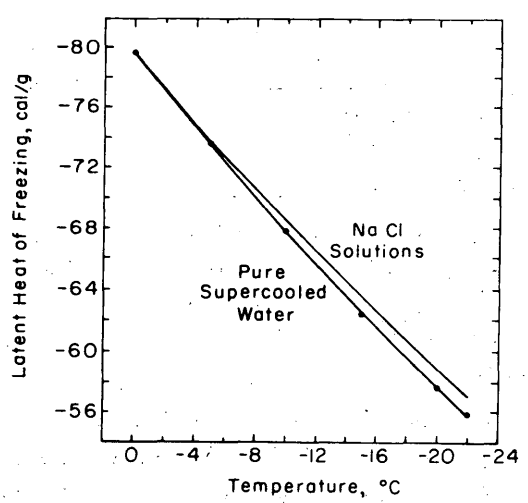

Figure 24. Latent heat of the freezing of pure water H_f and NaCl brine in equilibrium with ice Li_b as functions of temperature. Curves determined by method of least squares.

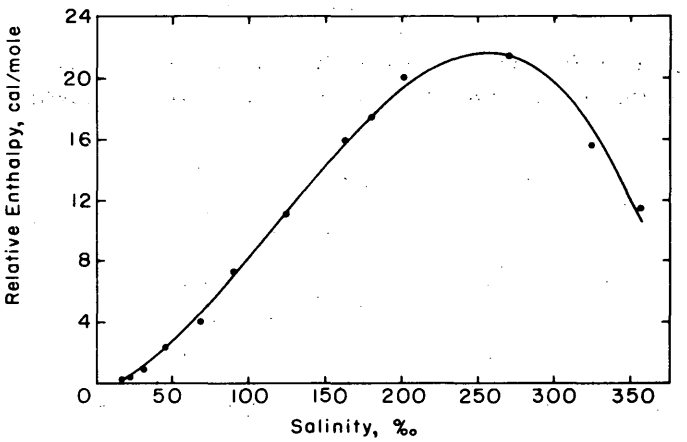

Figure 25. Variation of the relative partial molal enthalphy of water $\bar{L}_w$ with salinity. Curve determined by method of least squares.

where $\bar{L}_w$ is the relative partial enthalpy in cal/mole and S_b is the salinity in $^0/_{00}$. The correlation coefficient is 0.9974 and the standard error of the estimate is 0.6612. The experimental values and the fitted curve are plotted in Figure 25. To obtain $\bar{L}_w$ in cal/g the right hand side of eq 20 is divided by 18:

$$\bar{L}_w = \frac{1}{18}(0.5520 + 0.0334S_b + 0.0008S_b^2). \tag{21}$$

Since the concentration of brine in equilibrium with ice is determined by the ice temperature, it is possible to express $\bar{L}_w$ as a function of T. Hence, substituting eq 15 into eq 21, and substituting the result with eq 19 into eq 18, the latent heat of freezing of brine in equilibrium with ice is obtained. The resulting curve is illustrated in Figure 24. This curve may be approximated by

$$Li_b = \alpha_1 + \alpha_2 T + \alpha_3 T^2 \tag{22}$$

where Li_b is in cal/g and T is in °C. Assuming that the Li_b curve in Figure 24 is exact, the correlation coefficient and standard error are calculated.

Brine viscosity, specific heat, and thermal conductivity

The remaining brine property relations to be derived, including viscosity, specific heat, and thermal conductivity, are based on data cited in Kaufmann (1960). These properties were tabulated at different concentrations and temperatures. However, since the concentration of the brine is specified by the ice temperature, the properties of the brine in equilibrium with the ice may be given in terms of only the ice temperature.

The viscosity, specific heat, and thermal conductivity of NaCl brine in equilibrium with ice at different temperatures are tabulated in Tables IV-VI. These values were graphically interpolated from Kaufmann's tables. Least squares polynomial curve fits of this data yield

$$\mu_b = a_1 + a_2T + a_3T^2 + a_4T^3 \quad (23)$$

$$Cp_b = a_1 + a_2T + a_3T^2 + a_4T^3 \quad (24)$$

and

$$k_b = a_1 + a_2T + a_3T^2 \quad (25)$$

where μ_b = the brine viscosity in centipoise (cp)
Cp_b = the brine specific heat in cal/g °C
k_b = the brine thermal conductivity in cal/cm s °C
T = the ice temperature in °C.

The plotted values and the least squares curves are presented in Figures 26-28.

Table IV: Viscosity of NaCl brine in equilibrium with ice at various temperatures.

Temperature T (°C)	*Viscosity μ_b (cp)*
0	1.798
−5	2.293
−10	3.277
−15	4.785
−20	6.915

Table V. Specific heat of NaCl brine in equilibrium with ice at various temperatures.

Temperature, T (°C)	*Specific heat, Cp_b (cal/g °C)*
0	1.007
−3.3	0.928
−5.2	0.897
−7.2	0.870
−9.5	0.846
−11.9	0.826
−14.6	0.807
−17.8	0.793
−21.1	0.780

Table VI. Thermal conductivity of NaCl brine in equilibrium with ice at various temperatures.

Temperature T (°C)	*Thermal conductivity k_b (cal/cm s °C)*
0	1.353×10^{-3}
−3.0	1.331×10^{-3}
−6.6	1.306×10^{-3}
−10.9	1.278×10^{-3}
−16.4	1.244×10^{-3}
−21.1	1.217×10^{-3}

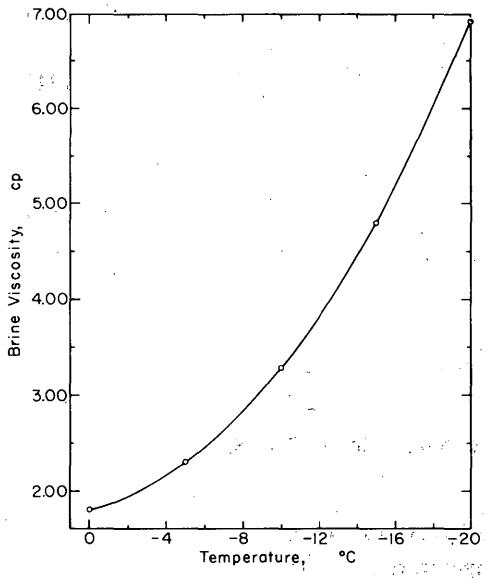

Figure 26. Variation of the brine viscosity μ_b with temperature. Curve determined by method of least squares.

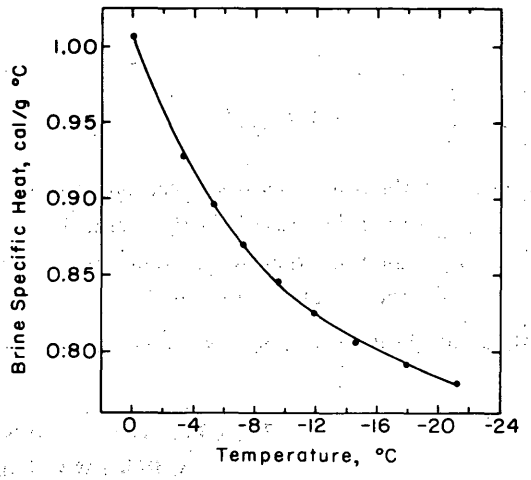

Figure 27. Variation of brine specific heat Cp_b with temperature. Curve determined by method of least squares.

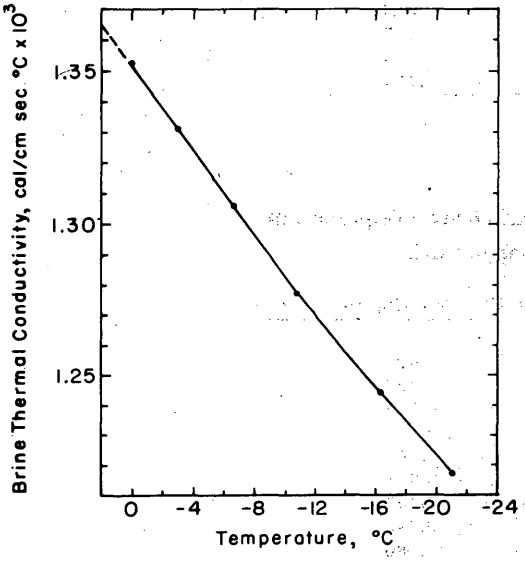

Figure 28. Variation of brine thermal conductivity k_b with temperature. Curve determined by method of least squares.

Ice properties

The ice density, specific heat, and thermal conductivity as a function of temperature were obtained from Pounder (1965). For the ice density ρ_i in g/cm^3:

$$\rho_i = 0.917 - 1.403 \times 10^{-4} T . \quad (26)$$

For the ice specific heat Cp_i in cal/g °C:

$$Cp_i = 0.506 + 1.863 \times 10^{-3} T. \quad (27)$$

And for the ice thermal conductivity k_i in cal/cm s °C

$$k_i = 5.35 \times 10^{-3} - 2.568 \times 10^{-5} T \quad (28)$$

where T is the ice temperature in °C.

Having obtained expressions for the ice and brine properties, a theoretical brine expulsion model may now be derived and compared to the experimental data.

THEORETICAL BRINE EXPULSION MODEL

To determine the relative importance of brine expulsion and gravity drainage, a one-dimensional brine expulsion model is formulated. A thermal energy equation and two continuity equations are derived by performing energy and mass balances over a control volume of NaCl ice. This results in

three equations and three unknowns which in principle can be solved. However, to provide a more useful working relationship the model is simplified. The result is then compared to the experimental data in the next section.

Continuity equations

A salt conservation equation and a brine conservation equation are derived by writing mass balances over a stationary volume element, the control volume, through which the brine is flowing such that (Bird, Stewart and Lightfoot 1960):

$$\begin{pmatrix}\text{rate of}\\ \text{mass}\\ \text{accumulation}\end{pmatrix} = \begin{pmatrix}\text{rate of}\\ \text{mass}\\ \text{in}\end{pmatrix} - \begin{pmatrix}\text{rate of}\\ \text{mass}\\ \text{out}\end{pmatrix} + \begin{pmatrix}\text{rate of mass}\\ \text{production by}\\ \text{internal processes}\end{pmatrix}. \tag{29}$$

Let ρ'_α be the mass of species α per unit volume of ice and brine (m_α/U), ρ''_α the mass of species α per unit volume of brine (m_α/U_b), ρ_α the density of species α, and n the porosity or relative brine volume (U_b/U). Let I_α be the rate of mass production of species α per unit volume (U) by internal processes (such as chemical reactions, phase changes, etc.) and $\overline{V}_\alpha$ the average instantaneous velocity of species α. The subscripts s, w, b and i are used to denote salt, water, brine, and ice respectively. Velocity fluctuations (hydrodynamic dispersion or mechanical diffusion) in the brine are neglected.

Using the notation in the previous paragraph, the mass average velocity of the fluid $\overline{V}^*$ is defined as (Bear 1972):

$$\overline{V}^* = \sum_\alpha \rho''_\alpha \overline{V}_\alpha/\rho \tag{30}$$

where ρ ($= \rho''$) is the total fluid density equal to

$$\rho = \sum_\alpha \rho''_\alpha. \tag{31}$$

For salt and water, eq 30 becomes

$$\overline{V}^* = (\rho''_s \overline{V}_s + \rho''_w \overline{V}_w)/\rho_b \tag{32}$$

and it is evident that $\overline{V}^*$ is equal to $\overline{V}_b$.

The diffusive mass flux of species α with respect to the mass average velocity $\overline{J}^*_\alpha$ is (Bear 1972):

$$\overline{J}^*_\alpha = \rho_\alpha(\overline{V}_\alpha - \overline{V}^*) = -\rho D_{sw} \nabla w_\alpha \tag{33}$$

where D_{sw} is the binary diffusivity of salt in water and w_α is the mass fraction; that is

$$w_\alpha = \rho''_\alpha/\rho. \tag{34}$$

Having defined the required variables, from eq 29 the mass conservation of salt may be written as

$$\frac{\partial \rho'_s}{\partial t} = -\frac{\partial(\rho'_s \overline{V}_s)}{\partial z} = -\frac{\partial(n\rho''_s \overline{V}_s)}{\partial z} \tag{35}$$

where $\rho'_s = n\rho''_s$ and $I_s = 0$. Substitution of eq 33 into eq 35 gives

$$\frac{\partial \rho_s'}{\partial t} = -\frac{\partial (n\rho_s'' \overline{V}^*)}{\partial z} + \frac{\partial}{\partial z}\left[n\rho_b D_{sw} \frac{\partial}{\partial z}\left(\frac{m_s}{m_b}\right)\right]. \tag{36}$$

However,

$$\rho_s' = \frac{m_s}{U} = \frac{m_b S_b}{U} = \frac{U_b \rho_b S_b}{U} = n\rho_b S_b \tag{37}$$

where S_b is the brine salinity equal to

$$S_b = m_s/m_b \tag{38}$$

and

$$n\rho_s'' \overline{V}^* = \rho_s' \overline{V}^* = n\rho_b S_b \overline{V}^* = n\rho_b S_b V \tag{39}$$

where $V = \overline{V}^*$. Thus, in the most convenient form the salt conservation equation becomes

$$\frac{\partial (n\rho_b S_b)}{\partial t} = -\frac{\partial (n\rho_b S_b V)}{\partial z} + \frac{\partial}{\partial z}\left[n\rho_b D_{sw}\left(\frac{\partial S_b}{\partial z}\right)\right] \tag{40}$$

where the rate of change of salt in the control volume is equal to the net accumulation by bulk fluid flow and by diffusion.

To derive the brine conservation equation, or the mass conservation of all the species, the conservation of water and ice must also be considered. For water

$$\frac{\partial \rho_w'}{\partial t} = -\frac{\partial (\rho_w' \overline{V}_w)}{\partial z} + I_w \tag{41}$$

and for ice

$$\frac{\partial \rho_i'}{\partial t} = I_i \tag{42}$$

where the ice velocity $\overline{V}_i$ is assumed to be zero. Summing eq 35, 41 and 42, the total mass conservation equation is

$$\frac{\partial (\rho_s' + \rho_w' + \rho_i')}{\partial t} = -\frac{\partial (\rho_s' \overline{V}_s + \rho_w' \overline{V}_w)}{\partial z} \tag{43}$$

where

$$\sum_\alpha I_\alpha = 0. \tag{44}$$

Since

$$\rho_s' + \rho_w' + \rho_i' = \frac{m_s}{U} + \frac{m_w}{U} + \frac{m_i}{U}$$

$$= \frac{m_b}{U} + \frac{m_i}{U}$$

$$= \frac{U_b \rho_b}{U} + \frac{U_i \rho_i}{U}$$

$$= n\rho_b + (1 - n)\rho_i \tag{45}$$

and

$$\rho_s' \overline{V}_s + \rho_w' \overline{V}_w = n\rho_b V \tag{46}$$

eq 43 becomes

$$\frac{\partial[n(\rho_b - \rho_i) + \rho_i]}{\partial t} = -\frac{\partial(n\rho_b V)}{\partial z} . \tag{47}$$

Since ρ_i, ρ_b and S_b are only functions of temperature T we have two equations and three unknowns. To obtain the third equation an energy balance over the control volume is performed. A momentum balance, or equation of motion, is not considered since it would introduce an additional unknown term, the pressure gradient.

Thermal energy equation

The thermal energy equation is derived in the same manner as the continuity equations, by considering a balance of internal energy E in a control volume. If we assume that the brine is incompressible, the internal energy increase per unit volume by compression is zero. Also, since the brine velocity is very low, the internal energy increase per unit volume by viscous dissipation is negligible. This term is only important for high flow rates. Neglecting these two terms and assuming that the brine and the ice are at the same temperature, the energy equation for the ice and brine is

$$\begin{pmatrix} \text{rate of} \\ \text{accumulation} \\ \text{of internal} \\ \text{energy} \end{pmatrix} = \begin{pmatrix} \text{net rate of} \\ \text{heat addition} \\ \text{by} \\ \text{convection} \end{pmatrix} + \begin{pmatrix} \text{net rate of} \\ \text{heat addition} \\ \text{by} \\ \text{conduction} \end{pmatrix} . \tag{48}$$

Equation 48 represents the sum of the rates of internal energy accumulation of both the brine and the ice, and no source terms appear. This is analogous to

$$\sum_{\alpha} I_\alpha = 0 \tag{49}$$

in the derivation of the brine continuity equation.

Designating q as the conductive heat flux and performing similar operations used to obtain the continuity equations, eq 48 yields

$$\frac{\partial(n\rho_b E_b)}{\partial t} + \frac{\partial[(1-n)\rho_i E_i]}{\partial t} = -\frac{\partial(n\rho_b E_b V)}{\partial z} - \frac{\partial(nq_b)}{\partial z} - \frac{\partial[(1-n)q_i]}{\partial z} . \tag{50}$$

The conductive heat flux q is equal to

$$q = -k\frac{\partial T}{\partial z} \tag{51}$$

where k is the thermal conductivity of the medium. The variation of the internal energy E with temperature is

$$\frac{\partial E}{\partial T} = Cp \tag{52}$$

where Cp is the specific heat of the substance. And the difference between the energy of the brine and the ice is equal to the latent heat of fusion L:

$$E_b - E_i = L. \tag{53}$$

Before substituting these equations into the energy equation, it will be further assumed that the ice density remains constant. The brine conservation equation then reduces to

$$\frac{\partial(n\rho_b)}{\partial t} + \frac{\partial(n\rho_b V)}{\partial z} = \rho_i \frac{\partial n}{\partial t} . \tag{54}$$

Substituting eq 51-53 into eq 50, differentiating, and making use of eq 54, gives the internal energy equation in its most convenient form:

$$\rho_i \frac{L\partial n}{\partial t} + [n\rho_b Cp_b + (1-n)\rho_i Cp_i]\frac{\partial T}{\partial t} + n\rho_b Cp_b V\frac{\partial T}{\partial z}$$

$$-\left[(k_b - k_i)\frac{\partial n}{\partial z} + \frac{n\partial k_b}{\partial z} + (1-n)\frac{\partial k_i}{\partial z}\right]\frac{\partial T}{\partial z} - [nk_b + (1-n)k_i]\frac{\partial^2 T}{\partial z^2} = 0. \tag{55}$$

We thus have developed three equations (salt and brine conservation and thermal energy) with three unknowns (n, V and T). Since the brine is in equilibrium with the adjacent ice, all the brine properties (excluding volume) are only functions of temperature. The assumptions made during the derivation of the equations are reasonable and include:

1) NaCl ice is saturated
2) pure ice velocity is zero
3) density of pure ice is constant
4) internal energy increase due to compression is zero
5) internal energy increase due to viscous dissipation is zero
6) ice and brine are at the same temperature.

Hence, given the appropriate boundary and initial conditions, the migration of brine through NaCl ice due to brine expulsion can be predicted.

Simplified brine expulsion equations

If the rate of change of temperature at each position is known, the variation of the salinity due to brine expulsion may be obtained using only the continuity equations. Neglecting diffusion and assuming that the ice density remains constant, the continuity equations become

$$\frac{\partial(n\rho_b S_b)}{\partial t} + \frac{\partial(n\rho_b S_b V)}{\partial z} = 0 \tag{56}$$

and

$$\frac{\partial(n\rho_b)}{\partial t} + \frac{\partial(n\rho_b V)}{\partial z} = \rho_i \frac{\partial n}{\partial t} . \tag{57}$$

Eliminating $\partial V/\partial z$ from eq 56 and 57 and collecting terms gives

$$S_b \rho_i \frac{\partial n}{\partial t} + n\rho_b \left(\frac{\partial S_b}{\partial t} + V \frac{\partial S_b}{\partial z} \right) = 0. \tag{58}$$

Since S_b is only a function of temperature

$$\frac{\partial S_b}{\partial t} = \frac{dS_b}{dT} \frac{\partial T}{\partial t} \tag{59}$$

and

$$\frac{\partial S_b}{\partial z} = \frac{dS_b}{dT} \frac{\partial T}{\partial z} . \tag{60}$$

Substituting eq 59 and 60 into eq 58 and solving for $\partial n/\partial t$ results in

$$\frac{\partial n}{\partial t} = -\frac{n\rho_b}{S_b \rho_i} \frac{dS_b}{dT} \left(\frac{\partial T}{\partial t} + V \frac{\partial T}{\partial z} \right). \tag{61}$$

From eq 57 the brine velocity gradient may also be obtained

$$\frac{\partial V}{\partial z} = \frac{(\rho_i - \rho_b)}{n\rho_b} \frac{\partial n}{\partial t} - \frac{1}{\rho_b} \frac{d\rho_b}{dT} \frac{\partial T}{\partial t} - \frac{V}{\rho_b} \frac{d\rho_b}{dT} \frac{\partial T}{\partial z} - \frac{V}{n} \frac{\partial n}{\partial z} . \tag{62}$$

If the velocity of the brine at the upper interface is zero, as in the brine drainage experiments, we thus have at $z = 0$:

$$\left. \frac{\partial n}{\partial t} \right|_{z=0} = \left(-\frac{n\rho_b}{S_b \rho_i} \frac{dS_b}{dT} \frac{\partial T}{\partial t} \right)_{z=0} \tag{63}$$

and

$$\left.\frac{\partial V}{\partial z}\right|_{z=0} = \left[\frac{(\rho_i - \rho_b)}{n\rho_b}\frac{\partial n}{\partial t} - \frac{1}{\rho_b}\frac{d\rho_b}{dT}\frac{\partial T}{\partial t}\right]_{z=0}. \tag{64}$$

Hence, given

$$\frac{\partial T}{\partial t} = f(z,t) \tag{65}$$

eq 61-64 were solved using a finite differences technique where

$$n_{(z,t+\Delta t)} = n_{(z,t)} + \left(\frac{\Delta n}{\Delta t}\right)_{(z,t)} \Delta t \tag{66}$$

$$V_{(z+\Delta z,t)} = V_{(z,t)} \left(\frac{\Delta V}{\Delta z}\right)_{(z,t)} \Delta z \tag{67}$$

and

$$T_{(z,t+\Delta t)} = T_{(z,t)} + \left(\frac{\Delta T}{\Delta t}\right)_{(z,t)} \Delta t \tag{68}$$

for small Δz and Δt.

From eq 61-68 the change in salinity due to brine expulsion alone was calculated (e.g. gravity drainage, salt diffusion, and flushing are not taken into consideration). A comparison is next made with the experimental results.

BRINE EXPULSION IN NaCl ICE

Results

Given the salinity and temperature profiles at time t_1, the temperature profile at time t_2, and assuming that the temperature varies linearly with time at each position, the change in salinity of the initial profile due to brine expulsion was calculated using the simplified brine expulsion equations. The results were then compared to the experimental salinity profile at time t_2 to determine the relative importance of brine expulsion and gravity drainage during the analyzed time interval.

This procedure was applied to several of the profiles of Runs 2 and 3. The time period between two analyzed profiles was large enough such that perturbations in the salinity profile caused by fluctuations in the coldplate temperature and other irregular processes were minimized. The position increment Δz in the finite-differences equations was set equal to 0.1 cm and the time increment Δt was varied between one and five minutes depending on the length of the time interval. Smaller values of Δz and Δt produced little change in the results. Since the rate of change of temperature was assumed to be constant, the calculated change in porosity represents an average value over the time period. From the final brine volume calculated using the model and the ice temperature, the change in salinity due to brine expulsion was obtained.

Figure 29 contains the results for the time period between profiles R2-3 and R2-6. The solid curves are the initial and final experimental salinity profiles and the broken curves were calculated using the model. The dotted curve was obtained by setting the brine velocity equal to zero

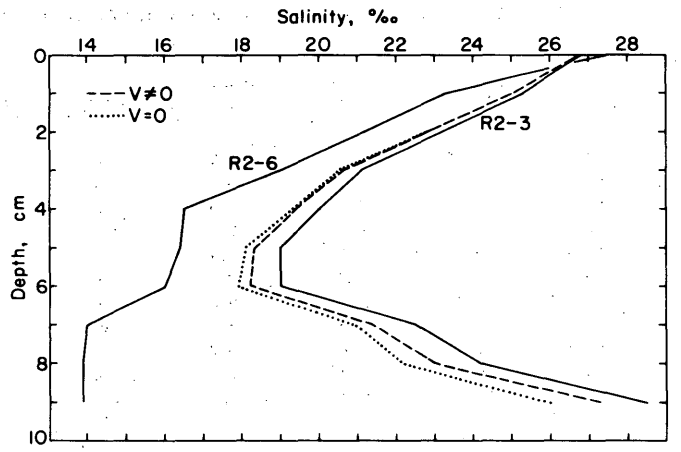

Figure 29. Comparison between experimental salinity curves and theoretical salinity curves determined from the brine expulsion model. R2-3 and R2-6 are the initial and final experimental curves, respectively. The remaining curves were calculated from the model. The dashed curve considers the effect of the brine velocity; whereas the dotted curve assumes that this velocity is zero throughout the ice sheet.

throughout the ice sheet, whereas the dashed curve was calculated by solving for this variable. The approximation of setting V equal to zero was felt to be justified inasmuch as the term $[V(\partial T/\partial z)]$ in eq 61 is commonly two orders of magnitude smaller than $(\partial T/\partial t)$.

The percentage of the salinity change which can be attributed to brine expulsion may be written as

$$\%\,\text{expulsion} = 100 \times \frac{S_c - S_1}{S_2 - S_1} \tag{69}$$

where S_1 and S_2 are the initial and final experimental salinity values, respectively, and S_c is the calculated salinity value at the final time using the expulsion model where $v \neq 0$. For example, if S_c is equal to S_2, then the entire salinity change can be explained by brine expulsion. This parameter has been tabulated in Table VII for the time intervals between various profiles of Runs 2 and 3. The asterisks denote an increase in the ice temperature over the time interval. These values are thus usually negative. A negative value is also obtained if salinity increased in the experimental values during the time period. In such cases the denominator in eq 69 is positive.

Discussion

The plotted results in Figure 29 and the tabulated data in Table VII indicate that brine expulsion played a small role in desalination during the periods of ice growth of Runs 2 and 3. However, the change in salinity was significant and cannot be neglected, especially during the periods of rapid ice growth where the rate of change of temperature at each level was high (< 200 hours). Since salt diffusion is negligible and flushing was not possible under these experimental conditions, the bulk of the salinity change must have been due to gravity drainage.

Table VII. Percent of salinity change which can be attributed to brine expulsion between various salinity profiles. The asterisks denote warming during the analyzed interval.

Position (cm)	*R2-3→ R2-6*	*R2-6→ R2-10*	*R2-10→ R2-13*	*R3-4→ R3-6*	*R3-6→ R3-10*	*R3-10→ R3-13*
0	−12.1	−2.1*	−1.9*	1.4	0	0.8
1	11.8	0	−5.2*	6.6	1.1	−3.4
2	17.8	−15.2*	−2.6*	7.8	2.6	–
3	22.4	3.2	4.2*	10.2	10.5	3.7
4	16.4	10.8	1.9*	12.5	5.5	1.7
5	24.7	11.0	−1.5*	9.9	3.4	1.0
6	26.4	2.8	−1.7*	9.0	4.5	0.6
7	12.5	4.2	7.3*	5.1	6.1	2.5
8	11.5	11.4	−1.1*	3.9	6.7	2.7
9	8.1	10.6	−0.9*	1.9	8.6	2.0
10		19.1	−0.7*		17.3	1.2
11		5.0	0.2*		10.7	1.6
12		3.7	1.7		4.9	10.4
13		10.9	0.6		5.3	39.1
14		−10.3	0.7		4.7	–
15		−43.8	−1.6		3.1	−3.5
16		10.9	4.7		2.1	7.7
17		77.8	0.8		0.2	3.5
18		34.7	2.4			6.0
19		9.6	8.6			4.1
20		22.3	2.0			2.9
21		−21.1	3.7			3.2
22		–	4.1			2.0
23		13.1	4.7			1.6
24		7.2	−4.5			1.0
25		3.4	11.5			0.2
26		0.2	1.9			
27		–				
28		−65.0				
29		2.4				
30		3.0				
31		10.8				
32		3.8				
33		2.7				
34		1.8				
35		0.7				
36		<0.1				

The brine expulsion equations of the previous section can be further simplified if the brine velocity is neglected. However, as illustrated in Figure 29, this results in brine expulsion salinity values which are too low. In the lower portion of the ice, the predicted change in salinity was almost doubled. The effect of the brine velocity was therefore considered in all calculations.

From a modeling and prediction standpoint it is unfortunate that brine expulsion is not the dominant brine drainage mechanism during the early period of ice growth. Unlike gravity drainage, brine expulsion is independent of the initial ice permeability. Therefore, a detailed knowledge of the ice microstructure is not required in a brine expulsion model. Even if the brine pockets were unconnected, the high pressures generated by the brine-ice phase change would rupture the ice, allowing the passage of the expelled brine (Knight 1962). In contrast, the ice microstructure must be known in a theoretical gravity drainage model where the permeability is an important parameter in the equation of motion. Unfortunately, the understanding of the microstructure is very limited.

In summary, comparison between the theoretical brine expulsion model and the experimental data has revealed that brine expulsion cannot explain the observed changes in ice salinity. The magnitude of the change in salinity due to brine expulsion was too small. Rather than brine expulsion, gravity drainage was therefore the dominant desalination mechanism. This process is examined further in the next section.

Table VIII. Average rate of change of salinity with time due to gravity drainage for the time interval between profiles R2-3 and R2-6.

Position Z (cm)	$dS/dt \times 10^6$ (‰/sec)	*Average brine volume* v_b (‰)	*Average temperature gradient* $\partial T/\partial z$ (°C/cm)
0	3.25	95.1	1.85
1	−7.31	90.0	1.7
2	−6.82	89.5	1.6
3	−6.76	88.5	1.45
4	−12.13	89.8	1.3
5	−8.11	97.5	1.3
6	−9.16	113.0	1.15
7	−30.85	149.7	1.1
8	−37.77	203.8	1.05
9	−55.60	337.5	1.05

GRAVITY DRAINAGE IN NaCl ICE

The residual or unexplained salinity between the calculated salinity determined by the brine expulsion model and the final experimental salinity is attributed to gravity drainage. Given the change in salinity due to gravity drainage and the elapsed time between the two experimental profiles, the average rate of change of salinity due to gravity drainage over the time period can be determined.

This has been done for the profiles contained in Table VII. As an example, the results for the time interval between profiles R2-3 and R2-6 are listed in Table VIII. The average brine volume and the average temperature gradient for the time interval are also tabulated. The rate of gravity drainage was significantly greater in the lower part of the ice. Since the brine volume was much larger in this zone, the higher drainage rates were probably due to the greater permeability of the ice which would facilitate convective overturn of the brine with the underlying less saline solution. Oscillations of outflowing brine and the subsequent inflow of the underlying solution have been observed by Eide and Martin (1975) in brine channels in the lower portion of salt ice. Using a thermistor chain embedded in growing sea ice, Lake and Lewis (1970) observed regular variations of the temperature in the ice near the ice/water interface and also attributed the results to convective processes. Since the period of these oscillations is of the order of one hour (Eide and Martin 1975), it is not surprising that the gravity drainage rates are greater in this part of the ice.

In Table VIII any relationship between the gravity drainage rate and the temperature gradient is not obvious. If a relationship is present, it is obscured by the large variation in brine volume. Because of the dependency of the brine density on the temperature (eq 15 and 16), one would expect the rate of gravity drainage to increase at any given permeability as the temperature gradient increases.

To determine whether or not a strong relationship exists between the gravity drainage rate and the temperature gradient, the rate of change of salinity due to gravity drainage has been plotted against the brine volume for different temperature gradients. It would have been more desirable to plot the rate of change of salinity against the ice permeability. However, since the details of the ice microstructure are not known, this was not possible. Figure 30 contains all the data up to 700‰ brine volume and Figure 31 illustrates the data in more detail at lower brine volumes. Because of the limited range of the data only three temperature gradient intervals were considered.

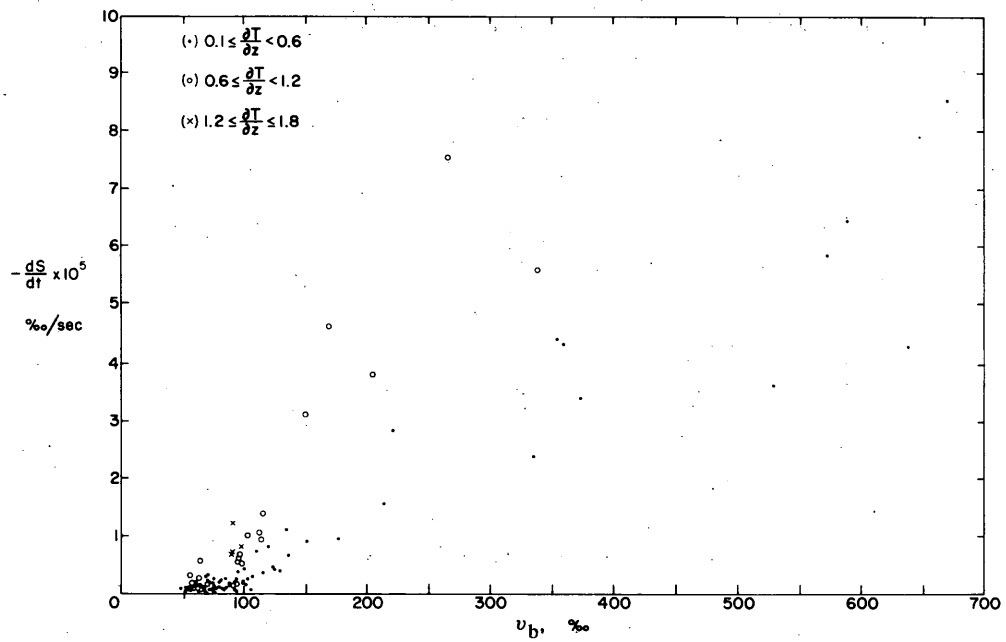

Figure 30. Plot of rate of change of salinity due to gravity drainage dS/dT against brine volume v_b for different temperature gradients $\partial T/\partial z$ (°C/cm).

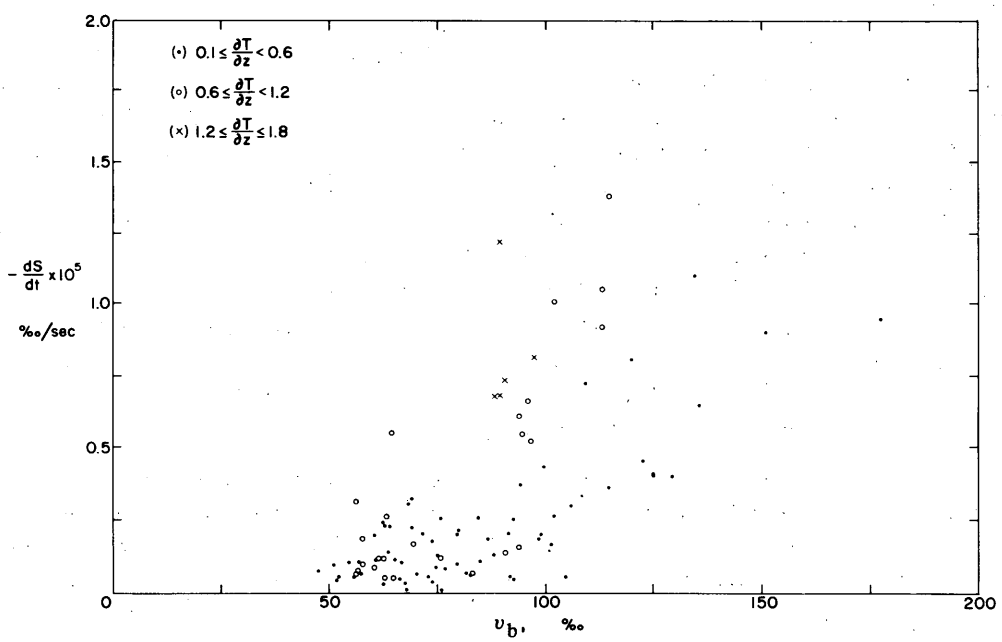

Figure 31. Detailed plot of the rate of change of salinity due to gravity drainage dS/dT against brine volume v_b (at low brine volumes) for different temperature gradients $\partial T/\partial z$ (°C/cm).

In Figures 30 and 31 the dependency of the rate of gravity drainage on the brine volume and temperature gradient is clearly shown. As either the brine volume or temperature gradient increases, the rate of change of salinity due to gravity drainage increases. If such a relationship were not found, the choice of gravity drainage as the dominant brine drainage mechanism would be questionable.

APPLICATION OF RESULTS TO NATURAL SEA ICE

All the results of the previous sections can be applied to sea ice above $-8.2°C$. Below this temperature the precipitation of solid salts must be taken into consideration and additional source terms would appear in the continuity equations if a brine expulsion model were derived.

Based on the experimental results, gravity drainage is the dominant desalination mechanism in young sea ice. During the first several hours of the ice growth brine expulsion is important and may account for up to 50% of the salinity change in the upper half of the ice. However, as the ice approaches 25 cm in thickness, brine expulsion becomes a minor desalination process. Since the rate of gravity drainage is dependent on the temperature gradient, the rate of brine drainage decreases as the ice sheet becomes thicker. As the salt drains from the ice, the ice permeability decreases due to the presence of smaller volumes of brine. This also tends to decrease the rate of gravity drainage with time. It is also possible that at these low brine volumes, long brine drainage tubes might separate into "chains" of individual disconnected brine pockets. At such a time, brine expulsion would again be expected to become important in a relative sense.

EFFECTIVE DISTRIBUTION COEFFICIENT

Prediction of the salinity profile of an ice sheet at any given time requires a knowledge of the amount of salt that is initially incorporated into the ice and the amount of brine drainage which has subsequently occurred. Before brine drainage in sea ice can be systematically analyzed, a reliable expression giving the amount of salt which is initially entrapped in the ice must be obtained.

The effective distribution coefficient k_{eff} is a measure of the amount of impurity that is incorporated into a solid during growth, since it is the ratio of the amount of impurity in the solid to that present in the liquid beyond the high concentration boundary layer. For NaCl ice and sea ice k_{eff} is equal to

$$k_{\text{eff}} = \frac{S_i'}{S_w} \tag{70}$$

where S_i' is the initial ice salinity and S_w is the bulk salinity of the underlying solution. Both quantities are measured in $^0/_{00}$. Relations between this parameter and the growth conditions have been examined and, unlike previous investigations, brine drainage was taken into consideration.

Previous work

For NaCl ice and sea ice, previous investigators have found that k_{eff} increases with an increase in the growth velocity v and with an increase in the impurity content in the melt (Adams et al. 1963, Weeks and Lofgren 1967, Kvajic and Brajovic 1970). The effective distribution coefficient has also been related to the temperature gradient at the growing interface (Fertuck et al. 1972).

Unfortunately, these investigators neglected the effects of brine drainage. It was clearly shown in the previous sections that, as the ice sheet is growing, both brine expulsion and gravity drainage result in a decrease in the ice salinity from its initial value. In previous experiments, salinity values were determined for different sections of the ice sheet after it had reached a particular thickness. The growth velocity and solution salinity corresponding to the time each section of ice was grown were then calculated to obtain k_{eff} versus v values. However, all salinity values, except those just above the skeleton layer, are a function of both the initial ice salinity and the amount of brine drainage. This resulted in the k_{eff} determinations of past investigators being too low. Their data also contain much scatter.

Experimental procedure and results

During the measurement of each salinity profile for Runs 2 and 3, the ice salinity just above the skeleton layer and the average solution salinity were obtained. The ice above the skeleton layer was chosen because, being newly formed ice, it had not as yet undergone any appreciable brine drainage. The thickness of the skeleton layer was about 3 cm throughout each run and this value was assumed to be a constant. At very high growth velocities, greater than approximately 10^{-4} cm/sec, it was difficult to measure the ice salinity just above the skeleton layer because of the rapid movement of the ice/water interface (20 min is required for each salinity determination). However, the salinity of the upper portion of the ice was later measured and it was assumed that no brine drainage had occurred in this part of the ice. This is not unreasonable since later profiles showed little brine drainage in this zone. The low ice temperature and small temperature change near the coldplate resulted in little gravity drainage or brine expulsion. Solution salinities corresponding to the time when each of these upper sections was grown were calculated. Growth velocities for all k_{eff} values were then determined from the ice thickness-time curves. Since the skeleton layer thickness was assumed to be constant, the growth velocity at the bridging layer at the upper boundary of the skeleton layer v^* was equal to the growth velocity at the interface v. The distribution coefficient and velocity data are tabulated in Appendix F.

The equation which is generally used to calculate the salinity of a growing ice sheet is the BPS (Burton, Prim and Slichter) equation (Burton et al. 1953) as used by Weeks and Lofgren (1967):

$$k_{eff} = \frac{k^*}{k^* + (1 - k^*)\exp(-v\delta/D)} \tag{71}$$

where k^* is considered to be the value of k_{eff} at $v = 0$ (provided a cellular interface were to remain stable), v is the growth velocity at the interface, δ is the thickness of the boundary layer and D is the diffusion coefficient of salt in water. By plotting $\ln(1/k_{eff} - 1)$ values against v, both δ and k^* were determined by a least squares linear curve fit. They obtained $k^* = 0.26$ and $\delta/D = 5090$ s/cm.

The results from Runs 2 and 3 were analyzed in the same manner and a plot of $\ln(1/k_{eff} - 1)$ vs v^* values is shown in Figure 32. The velocity at the bridging layer v^* is used rather than the velocity at the ice/water interface, because it is a measure of the rate at which the ice platelets are necking to form brine cavities. For velocities less than 2.0×10^{-5} cm/s, the distribution of the points deviated from linearity. Therefore, when k^* and δ/D were determined, values at low growth velocities were not considered. A least squares linear curve fit gave $k^* = 0.26$ and $\delta/D = 7243$ s/cm. The correlation coefficient and the standard error of the estimate are 0.9912 and 0.0746 respectively. Hence, at growth velocities greater than 2.0×10^{-5} cm/s k_{eff} may be calculated from

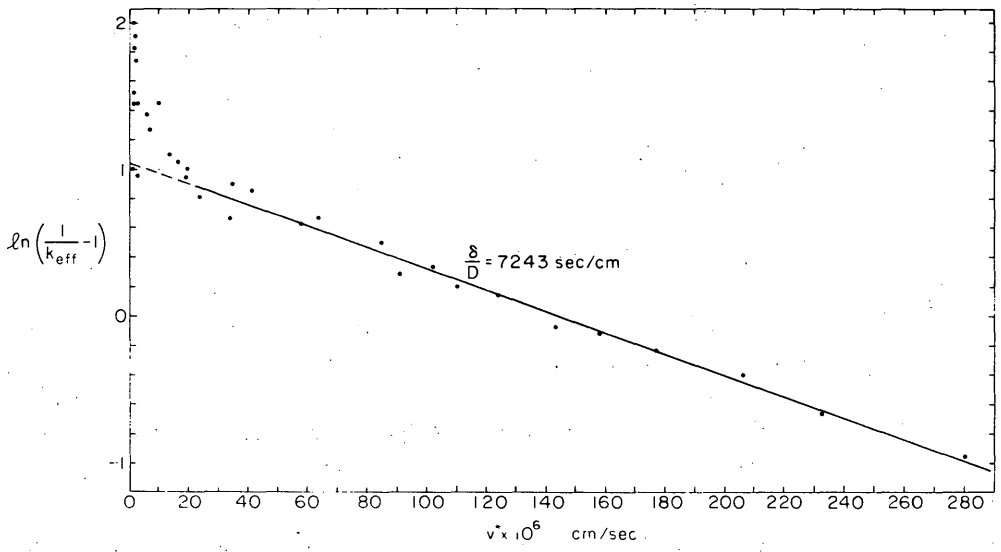

Figure 32. Plot of $ln(1/k_{eff} - 1)$ versus v^*. The value of δ/D is obtained by a least squares linear curve fit.

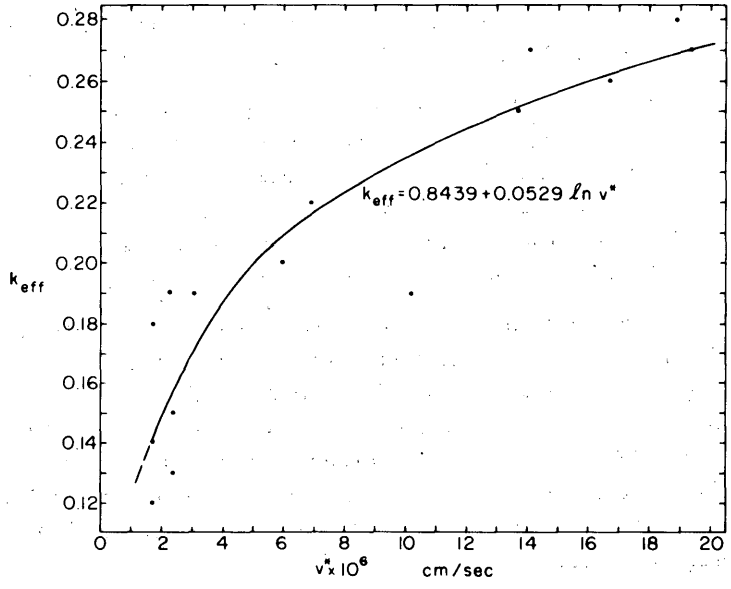

Figure 33. Plot of k_{eff} versus v^* at low growth velocities. The fitted curve was determined by least squares method.

$$k_{eff} = \frac{0.26}{0.26 + (1 - 0.26)\exp(-7243v^*)} \tag{72}$$

where v^* is the growth velocity at the bridging layer in cm/s. Compared to the results of Weeks and Lofgren (1967) these data show much less scatter. The k_{eff} values are also higher since brine drainage was not a problem.

At growth velocities less than 2.0×10^{-5} cm/s, the k_{eff} values decrease rapidly with further decrease in v^* (Fig. 33). The change in slope is probably due to a change in the morphology of the ice/water interface. By the method of least squares, a fitted curve was obtained for this data. Thus, at low growth velocities less than 2.0×10^{-5} cm/s, k_{eff} may be estimated by

$$k_{eff} = 0.8439 + 0.0529 \ln v^*. \tag{73}$$

The correlation coefficient is 0.9415 and the standard error of the estimate is 0.0225.

CONCLUSIONS

To obtain a better understanding of the desalination of natural sea ice, an experimental technique was developed to measure sequential salinity profiles of a growing sodium chloride ice sheet. Using radioactive ^{22}Na as a tracer, it was possible to determine both the concentration and movement of the brine within the ice without destroying the sample. A detailed temperature and growth history of the ice was also maintained so that the variation of the salinity profiles could be properly interpreted.

Since the experimental salinity profile represented a smoothed, rather than a true, salinity distribution, a deconvolution method was devised to restore the true salinity profile. This was achieved without any significant loss of end points.

In all respects, the salinity profiles are similar to those of natural sea ice. They have a characteristic C-shape, and clearly exhibit the effects of brine drainage.

Not knowing the rates of brine expulsion or gravity drainage, the variation of the salinity profiles during the period of ice growth could be explained by either process. To determine the relative importance of the desalination mechanisms, a theoretical brine expulsion model was derived and compared to the experimental data. As input for the model, equations describing the variation of some properties of NaCl brine with temperature were developed. These included the brine salinity, viscosity, specific heat, thermal conductivity, and latent heat of freezing.

In deriving the theoretical brine expulsion model, mass and energy balances were made over a control volume of NaCl ice. When a simplified form of the model is compared to the experimental results, it suggests that brine expulsion is the dominant brine drainage mechanism only during the first several hours of ice growth. For the remainder of the period of ice growth that was studied (up to six weeks), gravity drainage appeared to be the dominant mechanism. The rate of gravity drainage was found to be dependent on the brine volume and the temperature gradient in the ice. As either the brine volume or temperature gradient was increased, the rate of change of salinity due to gravity drainage increased.

The equation commonly used to calculate the effective distribution coefficient (Weeks and Lofgren 1967) was modified, and improved constants were determined based on the experimental data. An expression was also derived to give the distribution coefficient at very low growth velocities. In this equation, brine drainage was taken into consideration.

LITERATURE CITED

Adams, C.M., D.M. French and W.D. Kingery (1963) Field solidification and desalination of sea ice. In *Ice and snow: Properties, processes and applications* (W.D. Kingery, Ed.). Cambridge, Mass.: The MIT Press, p. 277-288.

Anderson, D.M. (1966) Heat of freezing and melting of sea ice. U.S. Army Cold Regions Research and Engineering Laboratory (USA CRREL) Research Report 202, 15 p. AD 640 151.

Assur, A. (1958) Composition of sea ice and its tensile strength. In *Arctic sea ice*. National Academy of Sciences, National Research Council Publication 598, p. 106-138.

Bear, J. (1972) *Dynamics of fluids in porous media.* New York: Elsevier Publishing Co. Inc.

Bennington, K.O. (1963) Some crystal growth features of sea ice. *Journal of Glaciology*, vol. 4, no. 36, p. 669-688.

Bird, R.B., W.E. Stewart and E.N. Lightfoot (1960) *Transport phenomena.* New York: John Wiley and Sons, Inc.

Burton, J.A., R.C. Prim and W.P. Slichter (1953) The distribution of solute in crystals grown from the melt, Part I, Theoretical. *Journal of Chemical Physics*, vol. 21, p. 1987-1991.

Cox, G.F.N. and W.F. Weeks (1974) Salinity variations in sea ice. *Journal of Glaciology*, vol. 13, no. 67, p. 109-120.

Dayton, P.K. and S. Martin (1971) Observations of ice stalactites in McMurdo Sound, Antarctica. *Journal of Geophysical Research*, vol. 76, no. 6, p. 1595-1599.

Dorsey, N.E. (1940) *Properties of the ordinary water substance.* New York: Reinhold Publishing Corporation.

Eide, I.E. and S. Martin (1975) The formation of brine drainage features in young sea ice. *Journal of Glaciology*, vol. 14, no. 70, p. 137-154.

Fertuck, L., J.W. Spyker and W.H.W. Husband (1972) Computing salinity profiles in ice. *Canadian Journal of Physics*, vol. 50, no. 3, p. 264-267.

Harrison, J.D. (1965) Measurements of brine pocket migration in ice. *Journal of Applied Physics*, vol. 36, no. 12, p. 3811-3815.

Healy, T.J. (1969) Convolution revisited. Institute of Electrical and Electronics Engineers (IEEE) *Spectrum*, April, p. 87-93.

Hoekstra, P. and P. Cappillino (1971) Dielectric properties of sea and sodium chloride ice at UHF and microwave frequencies. *Journal of Geophysical Research*, vol. 76, no. 20, p. 4922-4931.

Hoekstra, P., T. Ostercamp and W.F. Weeks (1965) The migration of liquid inclusions in single ice crystals. *Journal of Geophysical Research*, vol. 70, no. 20, p. 5035-5041.

Holloway, J.L. Jr. (1958) Smoothing and filtering of time series and space fields. In *Advances in geophysics* (H.E. Landsberg and J. Van Mieghem, Eds.). New York: Academic Press, vol. IV, p. 351-388.

Kaufmann, D.W. (1960) Physical properties of sodium chloride in crystal, liquid, gas, and aqueous solution states. In *Sodium chloride* (D.W. Kaufmann, Ed.). New York: Reinhold Publishing Corporation, p. 587-626.

Kingery, W.D. and W.H. Goodnow (1963) Brine migration in salt ice. In *Ice and snow: Properties, processes and applications* (W.D. Kingery, Ed.). Cambridge, Mass.: The MIT Press, p. 237-247.

Knight, C.A. (1962) Polygonization of aged sea ice. *Journal of Geology*, vol. 70, no. 2, p. 240-246.

Kvajic, G. and V. Brajovic (1970) Segregation of $(^{134}Cs)^{+}$ impurity during the growth of polycrystalline ice. *Canadian Journal of Physics*, vol. 48, no. 23, p. 2877-2887.

Lake, R.A. and E.S. Lewis (1970) Salt rejection by sea ice during growth. *Journal of Geophysical Research*, vol. 75, no. 3, p. 583-597.

Lofgren, G. and W.F. Weeks (1969) Effect of growth parameters on the substructure spacing in NaCl ice crystals. *Journal of Glaciology*, vol. 8, no. 52, p. 153-164.

Malmgren, F. (1927) On the properties of sea ice. *Norwegian North Pole expedition with the "Maud", 1918-1925*, vol. 25, no. 5.

Martin, S. (1974) Ice stalactites: comparison of a laminar flow theory with experiment. *Journal of Fluid Mechanics*, vol. 63, part 1, p. 51-79.

Pounder, E.R. (1965) *The physics of ice.* New York: Pergamon Press.

Randall, M. and C.S. Bisson (1920) The heat of solution and the partial molal heat content of the constituents in aqueous solutions of sodium chloride. *Journal of the American Chemical Society*, vol. 42, no. 3, p. 347-367.

Schwarzacher, W. (1959) Pack-ice studies in the Arctic Ocean. *Journal of Geophysical Research*, vol. 64, no. 12, p. 2257-2367.

Untersteiner, N. (1967) Natural desalination and equilibrium salinity profile of old sea ice. In *Physics of Snow and Ice: International Conference on Low Temperature Science (1966), Proceedings* (H. Oura, Ed.). Sapporo: Institute of Low Temperature Science, Hokkaido University, vol. 1, part 1, p. 569-577.

Weeks, W.F. (1961) Studies of salt ice. I: The tensile strength of NaCl ice. USA CRREL Research Report 80. AD 277540.

Weeks, W.F. (1962) Tensile strength of NaCl ice. *Journal of Glaciology*, vol. 4, no. 31, p. 25-52.

Weeks, W.F. (1968) Understanding the variations of the physical properties of sea ice. In *SCAR/SCOR/IAPO/IUPS Symposium on Antarctic Oceanography (Santiago, Chile, 1966)*. Cambridge, England: Scott Polar Research Institute, p. 173-190.

Weeks, W.F. and D.L. Anderson (1958) An experimental study on the strength of young sea ice. *Transactions of the American Geophysical Union*, vol. 39, no. 4, p. 641-647.

Weeks, W.F. and A. Assur (1967) The mechanical properties of sea ice. USA CRREL Cold Regions Science and Engineering Series Monograph II-C3, 80 p. AD 662 716.

Weeks, W.F. and A. Assur (1969) Fracture of lake and sea ice. USA CRREL Research Report 269, 79 p. AD 697 750.

Weeks, W.F. and O.S. Lee (1958) Observations on the physical properties of sea ice at Hopedale, Labrador. *Arctic*, vol. 11, no. 3, p. 134-155.

Weeks, W.F. and O.S. Lee (1962) The salinity distribution in young sea ice. *Arctic*, vol. 15, no. 2, p. 92-108.

Weeks, W.F. and G. Lofgren (1967) The effective solute distribution coefficient during the freezing of NaCl solutions. In *Physics of Snow and Ice: International Conference on Low Temperature Science (1966), Proceedings* (H. Oura, Ed.). Sapporo: Institute of Low Temperature Science, Hokkaido University, vol. 1, part 1, p. 579-597.

Whitman, W.G. (1926) Elimination of salt from seawater ice. *American Journal of Science*, vol. 211, p. 126-132.

Wolf, A.V. and M.G. Brown (1965) Concentrative properties of aqueous solutions: conversion tables. In *Handbook of Chemistry and Physics* (R.C. Weast, Ed.), 46th edition, p. D-127 - D-166.

Zubov, N.N. (1945) *L'dy arktiki (Arctic ice)*. Moscow: Izdatel'stvo Glavsevmorputi. Translation, U.S. Naval Electronics Laboratory, 1963.

"POSITION" is the position of the probe, F(x) is the fraction of the concentration difference, "STD. DEV." is the standard deviation, and w(k) are the smoothing function weights.

POSITION	F(x)	STD. DEV.	
$-\infty$	0	-	
.	.	.	
.	.	.	
-12	0	-	
-11	0.012	-	
-10	0.024	0.008	
-9	0.024	0.003	
-8	0.041	0.014	
-7	0.042	0.007	
-6	0.055	0.009	
-5	0.065	0.015	
-4	0.103	0.038	
-3	0.111	0.012	Cylinder I
-2	0.167	0.049	↑
-1	0.214	0.018	----------
0	0.391	0.043	↓
1	0.685	0.025	
2	0.785	0.022	
3	0.839	0.022	Cylinder II
4	0.862	0.008	
5	0.894	0.015	
6	0.915	0.024	
7	0.928	0.039	
8	0.946	0.012	
9	0.960	0.014	
10	0.954	0.019	
11	0.980	-	
12	1.000	-	
.	.	.	
.	.	.	
∞	1.000	-	

SMOOTHING FUNCTION WEIGHTS	
$w(-\infty)$	0.000
.	.
.	.
w(-13)	0.000
w(-12)	0.020
w(-11)	0.026
w(-10)	-0.006
w(-9)	0.014
w(-8)	0.018
w(-7)	0.013
w(-6)	0.021
w(-5)	0.032
w(-4)	0.023
w(-3)	0.054
w(-2)	0.100
w(-1)	0.294
w(0)	0.177
w(1)	0.047
w(2)	0.056
w(3)	0.008
w(4)	0.038
w(5)	0.010
w(6)	0.013
w(7)	0.001
w(8)	0.017
w(9)	0.000
w(10)	0.012
w(11)	0.012
w(12)	0.000
w(13)	0.000
.	.
.	.
$w(\infty)$	0.000

Listing of BASIC program "CORRECT" and sample output using data for salinity profile R3-8.

```
100'  THIS PROGRAM DECONVOLUTES SMOOTH EXPERIMENTAL SALINITY PROFILES.
110'
120'  THE WEIGHTS OF THE ORIGINAL SMOOTHING FUNCTION, THE EXPERIMENTAL
130'  SALINITY PROFILE, ITS LENGTH, AND THE APPROXIMATE THICKNESS
140'  OF THE SKELETON LAYER MUST BE KNOWN.
150'
160'  FILES "FIL-1" AND "WEIGHTS" ARE USED DURING EXECUTION.
170'
180'      *      *      *      *      *      *      *      *      *      *
190'
1000 DIM A(50,50), B(50), E(50), D(50), S(3), W(101)
1010 DIM F(100), H(4), P(3)
1020 FILE#1:"WEIGHTS"
1030 FOR I = 1 TO 101
1040     READ#1:W(I)
1050     IF W(I) <> 0 THEN 1070
1060     LET W(I) = 0.000000001
1070 NEXT I
1080 PRINT "ENTER THE NAME OF THE RANF CONTAINING THE EXPERIMENTAL"
1090 PRINT "SALINITY PROFILE";
1100 INPUT A$
1110 PRINT
1120 PRINT "ENTER THE LENGTH OF THE PROFILE (BOTTOM)";
1130 INPUT L
1140 PRINT
1150 PRINT "ENTER THICKNESS OF SKELETON LAYER";
1160 INPUT L1
1170 PRINT
1180 FILE#2:A$
1190 FOR I = 1 TO L+1
1200     READ#2:E(I)
1210 NEXT I
1220'
1230'  RADIOACTIVE DECAY CORRECTION
1240 PRINT "ENTER TIME OF PROFILE (HOURS)";
1250 INPUT Z
1260 PRINT
1270 FOR I = 1 TO L+1
1280     LET E(I) = E(I)/EXP(-0.693*Z/22776)
1290 NEXT I
1300 PRINT
1310'
1320'  DETERMINATION OF COEFFICIENTS FOR SIMULTANEOUS EQUATIONS
1330 FOR I = 1 TO L+1
1340     FOR J = 1 TO L+1
1350         LET A(I,J) = W(51+J-I)
1360     NEXT J
1370 NEXT I
1380 FOR J = 2 TO L
1390     LET A(L+2,J) = 1
1400 NEXT J
1410 LET A(L+2,1) = A(L+2,L+1) = 0.5
1420 LET A(L+2,L+2) = 69 - L
1430 FOR I = 1 TO L+1
1440     LET V = 0.000000001
1450     FOR K = 53+L-I TO 62
1460         LET V = V + W(K)
1470     NEXT K
1480     LET A(I,L+2) = V
1490     LET B(I) = E(I)
1500 NEXT I
1510 LET B(L+2) = 34.7*69
1520 LET N = L+2
2000'
2010'  SOLUTION OF SIMULTANEOUS EQUATIONS BY CROUT ALGORITHM
2020'  START THE ELIMINATIONS
2030 FOR I = 1 TO N
2040     LET X = -1
2050     FOR K = I TO N
2060         IF ABS(A(K,I)) <= X THEN 2090
2070         LET Q = K
2080         LET X = ABS(A(K,I))
2090     NEXT K
2100     IF X > 0 THEN 2130
2110     PRINT "MATRIX OF COEFFICIENTS IS SINGULAR!!!!!!!!!"
2120     STOP
2130'    INTERCHANGE IF NEEDED
2140     IF I = Q THEN 2230
2150     FOR J = 1 TO N
2160         LET T = A(I,J)
2170         LET A(I,J) = A(Q,J)
2180         LET A(Q,J) = T
2190     NEXT J
2200     LET T = B(I)
2210     LET B(I) = B(Q)
2220     LET B(Q) = T
2230'    ELIMINATE ON THAT ONE ROW
2240     FOR J = 1 TO N
2250         IF I < J THEN 2280
2260         LET M1 = J - 1
2270         GOTO 2290
2280         LET M1 = I -1
2290         LET S = 0
2300         FOR K = 1 TO M1
2310             LET S = S + A(I,K)*A(K,J)
```

```
2320          NEXT K
2330          LET A(I,J) = A(I,J) + S
2340          IF I >= J THEN 2360
2350          LET A(I,J) = -A(I,J)/A(I,I)
2360      NEXT J
2370 NEXT I
2380 '  LEFT HAND SIDE IS REDUCED---------START ON RIGHT
2390 FOR I = 1 TO N
2400      LET S = 0
2410      FOR K = 1 TO I-1
2420          LET S = S + A(I,K)*B(K)
2430      NEXT K
2440      LET B(I) = -(B(I) + S)/A(I,I)
2450 NEXT I
2460 FOR I = N TO 1 STEP -1
2470      LET S = 0
2480      FOR K = I+1 TO N
2490          LET S = S + A(I,K)*B(K)
2500      NEXT K
2510      LET B(I) = -B(I) + S
2520 NEXT I
2530 LET A1 = B(1)/2
2540 LET A2 = B(L+1)/2
2550 LET A3 = 0
2560 FOR I = 2 TO L
2570      LET A3 = A3 + B(I)
2580 NEXT I
2590 LET A4 = (A1 + A2 + A3)/L
2600 LET C1 = B(L+2)
2610 '
3000 PRINT "DATA FOR PROFILE ";A$
3010 PRINT
3020 PRINT "AVERAGE ICE SALINITY IS ";INT(A4*10+.5)/10;
3030 PRINT TAB(48);"(INCL. SKELETON LAYER)"
3040 PRINT "AVERAGE SOLUTION SALINITY IS ";INT(C1*10+.5)/10;
3050 PRINT TAB(48);"(INCL. SKELETON LAYER)"
3060 PRINT
3070 FOR I = 0 TO L
3080      LET B(I) = B(I+1)
3090      LET E(I) = E(I+1)
3100 NEXT I
3110 '
3120 '  SMOOTHING DECONVOLUTED PROFILE USING HANNING FILTER.
3130 FILE#3:"FIL-1"
3140 FOR I = 0 TO 2
3150      READ#3:S(I)
3160 NEXT I
3170 FOR I = 1 TO L-1
3180      LET S = 0
3190      FOR K = -1 TO 1
3200          LET S = S + S(K+1)*B(I+K)
3210      NEXT K
3220      LET D(I) = S
3230 NEXT I
3240 PRINT "POSITION","DCV.  PROF.","FILT. DCV. PROF."
3250 PRINT TAB(3);0;TAB(17);INT(B(0)*10+.5)/10
3260 FOR I = 1 TO L-1
3270      PRINT TAB(3);I;TAB(17);INT(B(I)*10+.5)/10;TAB(35);
3280      PRINT INT(D(I)*10+.5)/10
3290 NEXT I
3300 PRINT TAB(3);L;TAB(17);INT(B(L)*10+.5)/10
4000 '
4010 '  RECALCULATING LOST END POINTS.
4020 LET D(0) = D(1)
4030 LET D(L) = D(L-1)
4040 FOR J = 0 TO 3
4050      LET S1 = 0
4060      FOR I = 1 TO L
4070          LET S1 = S1 + W(51+I-J)*D(I)
4080      NEXT I
4090      LET S2 = 0
4100      FOR I = L+1 TO 11+J
4110          LET S2 = S2 + W(51+I-J)
4120      NEXT I
4130      LET S2 = S2*C1
4140      LET H(J) = (E(J)-S1-S2)/W(51-J)
4150 NEXT J
4160 PRINT
4170 PRINT "BASED ON THE FILTERED DECONVOLUTED PROFILE, THE TOP"
4180 PRINT "SALINITIES ARE:"
4190 LET S3 = 0
4200 FOR I = 0 TO 3
4210      PRINT INT(H(I)*10+.5)/10,
4220      LET S3 = S3 + H(I)
4230 NEXT I
4240 PRINT
4250 LET H(4) = S3/4
4260 PRINT "HAVING AN AVERAGE OF ";INT(H(4)*10+.5)/10
4270 PRINT
4280 FOR J = 0 TO 2
4290      LET S1 = 0
4300      FOR I = 0 TO L-1
4310          LET S1 = S1 + W(51-L+I+J)*D(I)
4320      NEXT I
4330      LET S2 = 0
4340      FOR I = 52 TO 62-J
4350          LET S2 = S2 + W(I+J)
4360      NEXT I
4370      LET S2 = S2*C1
4380      LET P(J) = (E(L-J)-S1-S2)/W(51+J)
4390 NEXT J
4400 PRINT "BASED ON THE FILTERED DECONVOLUTED PROFILE, THE BOTTOM"
```

```
4410 PRINT "SALINITIES ARE:"
4420 LET S3 = 0
4430 FOR I = 0 TO 2
4440      PRINT INT(P(I)*10+.5)/10,
4450      LET S3 = S3 + P(I)
4460 NEXT I
4470 PRINT
4480 LET P(3) = S3/3
4490 PRINT "HAVING AN AVERAGE OF ";INT(P(3)*10+.5)/10
5000'
5010'  CONVOLUTING DECONVOLUTED PROFILES USING COMBINATIONS OF
5020'  RECALCULATED END POINTS. DIFFERENCE BETWEEN EXPT. PROFILE
5030'  AND CONVOLUTED DECONVOLUTED PROFILE COMPUTED.
5040 PRINT
5050 FOR I = 0 TO 11
5060      LET F(I) = 0
5070 NEXT I
5080 FOR I = 12 TO 12+L
5090      LET F(I) = D(I-12)
5100 NEXT I
5110 FOR I = 13+L TO 23+L
5120      LET F(I) = C1
5130 NEXT I
5140 PRINT "DO YOU WISH AN ANALYSIS OF THE END POINTS";
5150 INPUT Q$
5160 PRINT
5170 IF Q$ = "NO" THEN 6000
5180 PRINT "TOP SAL.","BOT. SAL.","SUM DIFF.","SUM ABS. DIFF."
5190 FOR U = 0 TO 4
5200      LET F(12) = H(U)
5210      FOR V = 0 TO 3
5220           LET F(12+L) = P(V)
5230           LET S1 = S2 = 0
5240           FOR I = 12 TO 12+L
5250                LET S = 0
5260                FOR K = -12 TO 11
5270                     LET S = S + W(K+51)*F(I+K)
5280                NEXT K
5290                LET S = S - E(I-12)
5300                LET S1 = S1 + S
5310                LET S2 = S2 + ABS(S)
5320           NEXT I
5330           PRINT F(12),F(12+L),S1,S2
5340      NEXT V
5350 NEXT U
5360 PRINT
6000'
6010'  PRINT OUT OF INDIVIDUAL CASES.
6020 PRINT "ENTER TOP AND BOTTOM SALINITIES RESP.";
6030 INPUT F(12), F(12+L)
6040 PRINT
6050 PRINT "-----------------------------------------------------------------"
6060 PRINT
6070 PRINT "PROFILE ";A$
6080 PRINT
6090 PRINT "POSITION","CORR. PROF.","EXPT. PROF.","CNV. CORR.",
6100 PRINT "DIFFERENCE"
6110 LET S1 = S2 = S3 = S4 = 0
6120 FOR I = 12 TO 12+L
6130      LET S = 0
6140      FOR K = -12 TO 11
6150           LET S = S + W(K+51)*F(I+K)
6160      NEXT K
6170      LET S3 = S - E(I-12)
6180      LET S1 = S1 + S3
6190      LET S2 = S2 + ABS(S3)
6200      PRINT TAB(3);I-12;TAB(17);INT(F(I)*10+.5)/10;TAB(32);
6210      PRINT INT(E(I-12)*10+.5)/10;TAB(47);INT(S*10+.5)/10;TAB(63);
6220      PRINT INT(S3*10+.5)/10
6230      LET S4 = S4 + F(I)
6240 NEXT I
6250 LET S5 = S4
6260 FOR I = 0 TO L1-1
6270      LET S5 = S5 - F(12+L-I)
6280 NEXT I
6290 LET S5 = S5 - F(12)/2 - F(12+L-L1)/2
6300 LET S4 = S4 - F(12)/2 - F(12+L)/2
6310 PRINT
6320 PRINT "RECALCULATED AVERAGE ICE SALINITY IS ";INT(S4/L*10+.5)/10;
6330 PRINT TAB(48);"(INCL. SKELETON LAYER)"
6340 PRINT "RECALCULATED AVERAGE ICE SALINITY IS ";
6350 PRINT INT(S5/(L-L1)*10+.5)/10;
6360 PRINT TAB(48);"(EXCL. SKELETON LAYER)"
6370 LET C2 = (34.7*69-S4)/(69-L)
6380 PRINT "RECALCULATED AVERAGE SOLUTION SALINITY IS ";
6390 PRINT INT(C2*10+.5)/10
6400 PRINT
6410 IF L1 < 3 THEN 6450
6420 LET K = INT(F(12+L-L1)/C2*100+.5)/100
6430 PRINT "DISTRIBUTION COEFFICIENT IS ";K
6440 PRINT
6450 PRINT "SUM OF THE DIFFERENCES IS ";S1;
6460 PRINT TAB(48);"(INCL. SKELETON LAYER)"
6470 PRINT "SUM OF THE ABS. DIFFERENCES IS ";S2;
6480 PRINT TAB(48);"(INCL. SKELETON LAYER)"
6490 PRINT
6500 PRINT "-----------------------------------------------------------------"
6510 PRINT
6520 PRINT "DO YOU WISH TO USE ANY OTHER END POINTS";
6530 INPUT F$
6540 PRINT
6550 IF F$ = "YES" THEN 6020
```

6560 END

CORRECT 02/12/73 15:27
ENTER THE NAME OF THE RANF CONTAINING THE EXPERIMENTAL SALINITY PROFILE? R3-8

ENTER THE LENGTH OF THE PROFILE BOTTOM? 20

ENTER THICKNESS OF SKELETON LAYER? 3

ENTER TIME OF PROFILE (HOURS)? 125

DATA FOR PROFILE R3-8

AVERAGE ICE SALINITY IS 11.5 (INCL. SKELETON LAYER)
AVERAGE SOLUTION SALINITY IS 44.2 (INCL. SKELETON LAYER)

POSITION	DCV. PROF.	FILT. DCV. PROF.
0	22.9	
1	9.4	14.8
2	17.6	12.8
3	6.8	11.1
4	13.2	9.5
5	4.9	9.5
6	14.9	9.8
7	4.5	9.5
8	13.9	8.8
9	2.7	8.8
10	15.7	8.5
11	-0.2	7.9
12	16.3	8.9
13	3.2	9.5
14	15.4	8.3
15	-0.6	7.4
16	15.7	9.2
17	6	11.5
18	18.1	12.2
19	6.3	24.6
20	67.8	

BASED ON THE FILTERED DECONVOLUTED PROFILE, THE TOP SALINITIES ARE:
24 18.6 18.4 17.6
HAVING AN AVERAGE OF 19.6

BASED ON THE FILTERED DECONVOLUTED PROFILE, THE BOTTOM SALINITIES ARE:
38.4 32.7 46.5
HAVING AN AVERAGE OF 39.2

DO YOU WISH AN ANALYSIS OF THE END POINTS? YES

TOP SAL.	BOT. SAL.	SUM DIFF.	SUM ABS. DIFF.
24.0315	38.3849	2.52097	5.41672
24.0315	32.7123	0.302949	6.83122
24.0315	46.4579	5.6775	6.86142
24.0315	39.185	2.83381	5.50873
18.6415	38.3849	-1.71556	3.5882
18.6415	32.7123	-3.93358	5.13684
18.6415	46.4579	1.44097	4.95144
18.6415	39.185	-1.40273	3.65301
18.3618	38.3849	-1.93542	3.67435
18.3618	32.7123	-4.15344	5.22299
18.3618	46.4579	1.22111	5.0264
18.3618	39.185	-1.62258	3.73916
17.5516	38.3849	-2.57224	4.08594
17.5516	32.7123	-4.79026	5.63458
17.5516	46.4579	0.584288	5.40558
17.5516	39.185	-2.25941	4.15075
19.6466	38.3849	-0.925564	3.86962
19.6466	32.7123	-3.14358	5.41827
19.6466	46.4579	2.23097	5.27307
19.6466	39.185	-0.612726	3.93443

ENTER TOP AND BOTTOM SALINITIES RESP.? 18.6,38.4

PROFILE R3-8

POSITION	CORR. PROF.	EXPT. PROF.	CNV. CORR.	DIFFERENCE
0	18.6	6.7	5.7	-1
1	14.8	10.3	10.3	0
2	12.8	10.5	10.6	0
3	11.1	10.1	10.2	0.1
4	9.5	9.4	9.4	0
5	9.5	8.9	9.2	0.3
6	9.8	9.3	9.2	-0.1
7	9.5	9	9.1	0.1
8	8.8	9.4	9.3	-0.1
9	8.8	9.4	9.5	0.1
10	8.5	9.8	9.3	-0.4
11	7.9	9.8	9.9	0.1
12	8.9	10.4	10.4	0
13	9.5	11	10.8	-0.2
14	8.3	11.2	11.2	-0.1
15	7.4	11.6	11.6	-0.1
16	9.2	12.4	12.3	-0.1
17	11.5	14.3	14.2	-0.1
18	12.2	17	16.5	-0.5

Appendix B (cont'd)

19	24.6	19.9	20.1	0.3
20	38.4	26.7	26.7	0

RECALCULATED AVERAGE ICE SALINITY IS 11.6 (INCL. SKELETON LAYER)
RECALCULATED AVERAGE ICE SALINITY IS 10 (EXCL. SKELETON LAYER)
RECALCULATED AVERAGE SOLUTION SALINITY IS 44.1

DISTRIBUTION COEFFICIENT IS 0.26

SUM OF THE DIFFERENCES IS -1.7423 (INCL. SKELETON LAYER)
SUM OF THE ABS. DIFFERENCES IS 3.6022 (INCL. SKELETON LAYER)

DO YOU WISH TO USE ANY OTHER END POINTS? NO

3.251 SEC. 51 I/O

APPENDIX C: TABULATION OF SALINITY DATA

Partial output from program "CORRECT" for the salinity profiles of run 2 (R2-) and run 3 (R3-). "POSITION" is the position of the probe below the cold-plate/ice interface; "CORR. PROF." is the corrected salinity profile; "EXPT. PROF." is the experimental salinity profile (corrected for radioactive decay); "CNV. CORR." is the corrected salinity profile convoluted with the smoothing function; and "DIFFERENCE" is the difference between the convoluted corrected salinity profile and the experimental salinity profile. Skeleton layer thicknesses other than 3 cm. are specified. Partition coefficients for salinity profiles measured during warming phases are not calculated (R2-15 to R2-20).

PROFILE R2-3 (9 hours)

POSITION	CORR. PROF.	EXPT. PROF.	CNV. CORR.	DIFFERENCE
0	26.8	12	9.9	-2.1
1	25.3	17.3	17.4	0.1
2	23.2	19.7	19.3	-0.4
3	21.1	19.6	19.7	0.1
4	20	19.2	19.4	0.2
5	19	19.6	19.9	0.3
6	19	19.8	20.4	0.6
7	22.5	21.1	21.5	0.4
8	24.2	22.5	23.7	1.2
9	28.5	25.9	25.9	0

RECALCULATED AVERAGE ICE SALINITY IS 22.5 (INCL. SKELETON LAYER)
RECALCULATED AVERAGE ICE SALINITY IS 21.9 (EXCL. SKELETON LAYER)
RECALCULATED AVERAGE SOLUTION SALINITY IS 36.5

DISTRIBUTION COEFFICIENT IS 0.52

SUM OF THE DIFFERENCES IS 0.362145 (INCL. SKELETON LAYER)
SUM OF THE ABS. DIFFERENCES IS 5.39124 (INCL. SKELETON LAYER)

PROFILE R2-4 (18 hours)

POSITION	CORR. PROF.	EXPT. PROF.	CNV. CORR.	DIFFERENCE
0	25.4	11.1	9.1	-2
1	24.8	16.3	16.3	0
2	24.2	18.7	18.3	-0.4
3	21.3	18.6	19	0.4
4	18.9	18.5	18.2	-0.3
5	18	17.3	17.9	0.6
6	16.8	17.6	17.7	0.1
7	15.5	17.6	17.6	0

PROFILE R2-4 (cont'd)

POSITION	CORR. PROF.	EXPT. PROF.	CNV. CORR.	DIFFERENCE
8	15.9	17.2	17.7	0.5
9	15.5	17.8	18.5	0.7
10	16	18.3	19	0.7
11	24.9	20.3	21.5	1.2
12	27.5	24.3	25.5	1.2
13	30.7	28	28	0

RECALCULATED AVERAGE ICE SALINITY IS 20.6 (INCL. SKELETON LAYER)
RECALCULATED AVERAGE ICE SALINITY IS 19.2 (EXCL. SKELETON LAYER)
RECALCULATED AVERAGE SOLUTION SALINITY IS 38

DISTRIBUTION COEFFICIENT IS 0.42

SUM OF THE DIFFERENCES IS 2.5754 (INCL. SKELETON LAYER)
SUM OF THE ABS. DIFFERENCES IS 8.09056 (INCL. SKELETON LAYER)

PROFILE R2-5 (48 hours)

POSITION	CORR. PROF.	EXPT. PROF.	CNV. CORR.	DIFFERENCE
0	28.6	11.3	9.1	-2.2
1	23.1	16.3	16.3	0
2	22.3	16.9	17.1	0.2
3	20.7	17.5	17.3	-0.3
4	17.6	16.4	16.4	0
5	15.9	15.7	15.6	-0.1
6	15.3	14.6	14.9	0.3
7	13.6	14.5	14.3	-0.2
8	12.7	13.8	13.9	0.1
9	13.9	13.5	13.8	0.3
10	12.8	13.8	13.6	-0.2
11	11.5	13.8	14.1	0.3
12	13.2	14	14.4	0.4
13	13.4	14.8	14.8	0
14	12.4	14.7	15	0.3
15	12.7	15.1	15.2	0.1
16	13.5	15.2	15.7	0.5
17	14.1	16.2	16.8	0.6
18	15	17.5	18.2	0.6
19	21.5	19.4	20.4	0.9
20	26.6	22.2	24.2	1.9
21	35.5	28.3	28.3	0

RECALCULATED AVERAGE ICE SALINITY IS 16.8 (INCL. SKELETON LAYER)
RECALCULATED AVERAGE ICE SALINITY IS 15.6 (EXCL. SKELETON LAYER)
RECALCULATED AVERAGE SOLUTION SALINITY IS 42.5

DISTRIBUTION COEFFICIENT IS 0.35

PROFILE R2-5 (cont'd)

SUM OF THE DIFFERENCES IS 3.44367 (INCL. SKELETON LAYER)
SUM OF THE ABS. DIFFERENCES IS 9.64721 (INCL. SKELETON LAYER)

PROFILE R2-6 (76 hours)

POSITION	CORR. PROF.	EXPT. PROF.	CNV. CORR.	DIFFERENCE
0	27.5	10.7	8.8	-1.9
1	23.3	15.9	15.9	0
2	21.2	17	16.8	-0.3
3	19	16.4	16.6	0.2
4	16.5	15.9	15.6	-0.3
5	16.4	14.7	15.2	0.4
6	16	15.2	14.9	-0.3
7	14	14.4	14.5	0
8	13.9	14	14.1	0
9	13.9	13.7	13.8	0.1
10	12	13.3	13	-0.3
11	12.1	12.8	13.1	0.3
12	13.8	13.6	13.5	-0.1
13	13.7	13.5	13.6	0.1
14	11.8	13.7	13.6	-0.2
15	11.5	13.3	13.4	0.1
16	12.7	13.8	13.4	-0.4
17	11.5	13.8	13.7	-0.1
18	12	14.1	13.9	-0.2
19	14.3	14.3	14.3	0
20	13	15.6	15.2	-0.4
21	10.5	15.9	15.6	-0.3
22	11.1	16.3	16.1	-0.3
23	13.6	17.7	17.4	-0.4
24	15.3	20.5	20.6	0
25	35.5	26.1	25.2	-0.9
26	58.5	33.8	34.8	1

RECALCULATED AVERAGE ICE SALINITY IS 16.2 (INCL. SKELETON LAYER)
RECALCULATED AVERAGE ICE SALINITY IS 14.5 (EXCL. SKELETON LAYER)
RECALCULATED AVERAGE SOLUTION SALINITY IS 45.9

DISTRIBUTION COEFFICIENT IS 0.3

SUM OF THE DIFFERENCES IS -4.04249 (INCL. SKELETON LAYER)
SUM OF THE ABS. DIFFERENCES IS 8.6236 (INCL. SKELETON LAYER)

PROFILE R2-7 (101 hours)

POSITION	CORR. PROF.	EXPT. PROF.	CNV. CORR.	DIFFERENCE
0	29.2	10.5	9.2	-1.3
1	24.4	16.6	16.6	0
2	21.3	17.3	17.2	0
3	18.5	16.8	16.8	0
4	17.1	15.4	15.6	0.2
5	16.5	15.3	15.3	0
6	15.2	14.9	14.9	-0.1
7	13.3	14	14.1	0.1
8	12.6	13.6	13.6	-0.1
9	13.4	12.8	13.3	0.5
10	12.5	13.4	12.8	-0.6
11	11.7	12.7	13.1	0.3
12	12.4	13.2	13.2	0
13	13.3	13.1	13.2	0.1
14	13.4	13.4	13.3	-0.1
15	12.3	13.2	13.1	-0.1
16	12.1	12.6	12.9	0.3
17	12.9	13.1	13	-0.1
18	12.5	13.1	13.2	0.1
19	11.8	12.8	13.5	0.6
20	12.8	13.6	13.7	0
21	12.7	13.9	14.2	0.3
22	11.1	14.2	14.4	0.2
23	12	14.3	14.9	0.5
24	15.4	15.6	16.1	0.5
25	17.3	17.5	18.3	0.9
26	16.2	20	20.2	0.2
27	22.9	20.7	22.2	1.6
28	29	23.9	26.4	2.5
29	39	31.2	31.2	0

RECALCULATED AVERAGE ICE SALINITY IS 15.9 (INCL. SKELETON LAYER)
RECALCULATED AVERAGE ICE SALINITY IS 14.7 (EXCL. SKELETON LAYER)
RECALCULATED AVERAGE SOLUTION SALINITY IS 48.3

DISTRIBUTION COEFFICIENT IS 0.34

SUM OF THE DIFFERENCES IS 6.3654 (INCL. SKELETON LAYER)
SUM OF THE ABS. DIFFERENCES IS 11.3789 (INCL. SKELETON LAYER)

PROFILE R2-8 (124 hours)

POSITION	CORR. PROF.	EXPT. PROF.	CNV. CORR.	DIFFERENCE
0	28.5	10.3	8.9	-1.4
1	23.5	16.1	16.1	0
2	20.5	16.7	16.6	0
3	17.8	16.1	16.2	0.1

PROFILE R2-8 (cont'd)

POSITION	CORR. PROF.	EXPT. PROF.	CNV. CORR.	DIFFERENCE
4	16	15.1	15	0
5	16.1	14.5	14.7	0.3
6	15	14.7	14.4	-0.2
7	13	13.8	13.7	0
8	12.9	13	13.3	0.2
9	12.4	13.1	13	-0.1
10	11.1	12	12.2	0.1
11	11.3	12.4	12.4	0
12	12.3	12.6	12.8	0.1
13	12.9	12.8	12.8	0
14	12.8	13	12.9	-0.1
15	13	12.8	12.8	0
16	12.9	12.6	12.7	0.1
17	12.1	12.8	12.6	-0.2
18	12.2	12.1	12.3	0.2
19	12.8	12.2	12.3	0.1
20	11.6	12.6	12.6	-0.1
21	10.6	12.7	12.6	-0.1
22	11.1	12.7	12.6	-0.2
23	10.9	12.9	13	0
24	11.8	13.8	13.5	-0.2
25	14.5	14.4	14.4	0.1
26	14.1	16.1	15.7	-0.4
27	12.1	16.8	16.5	-0.3
28	12.4	17.4	17.1	-0.3
29	14	18.8	18.6	-0.2
30	17.4	21.3	21.5	0.2
31	35.8	27	26.6	-0.4
32	52.7	35.3	35.3	0

RECALCULATED AVERAGE ICE SALINITY IS 15.2 (INCL. SKELETON LAYER)
RECALCULATED AVERAGE ICE SALINITY IS 13.8 (EXCL. SKELETON LAYER)
RECALCULATED AVERAGE SOLUTION SALINITY IS 51.5

DISTRIBUTION COEFFICIENT IS 0.27

SUM OF THE DIFFERENCES IS -2.78042 (INCL. SKELETON LAYER)
SUM OF THE ABS. DIFFERENCES IS 5.80766 (INCL. SKELETON LAYER)

PROFILE R2-9 (173 hours)

POSITION	CORR. PROF.	EXPT. PROF.	CNV. CORR.	DIFFERENCE
0	27.9	10.6	8.9	-1.7
1	23.5	16	16	0
2	21.4	16.9	16.8	-0.1
3	18.9	16.6	16.6	0
4	16.3	15.5	15.5	0

PROFILE R2-9 (cont'd)

POSITION	CORR. PROF.	EXPT. PROF.	CNV. CORR.	DIFFERENCE
5	15.3	14.8	14.8	0.1
6	15.1	14.2	14.4	0.2
7	13.5	14.2	13.9	-0.3
8	13.3	13.4	13.5	0.2
9	13.9	13.2	13.4	0.2
10	11.6	13.4	12.8	-0.6
11	11.2	12.2	12.6	0.5
12	12.4	12.9	12.8	-0.1
13	12.6	12.8	12.8	0.1
14	12.5	12.9	12.7	-0.1
15	11.8	12.5	12.5	0
16	11.5	12.1	12.2	0.1
17	11.9	12.1	12	-0.1
18	12.2	11.9	12	0.1
19	11.6	12.1	11.9	-0.1
20	12.3	11.8	11.9	0.1
21	12.7	12	12	0
22	10.2	12.2	12	-0.2
23	9.9	11.8	11.9	0.1
24	11.7	12.6	12.2	-0.4
25	11.8	13.1	13	-0.1
26	13.5	13.9	13.7	-0.2
27	13.9	14.9	14.3	-0.6
28	10.3	14.7	14.5	-0.2
29	8.7	14.6	14.5	-0.1
30	10.3	15.4	15	-0.4
31	10.3	17.3	16.6	-0.7
32	10.6	19	19	0
33	32.7	24.3	23.9	-0.4
34	54.2	34	34.2	0.2

RECALCULATED AVERAGE ICE SALINITY IS 14.4 (INCL. SKELETON LAYER)
RECALCULATED AVERAGE ICE SALINITY IS 13.4 (EXCL. SKELETON LAYER)
RECALCULATED AVERAGE SOLUTION SALINITY IS 54.4

DISTRIBUTION COEFFICIENT IS 0.19

SUM OF THE DIFFERENCES IS -4.40966 (INCL. SKELETON LAYER)
SUM OF THE ABS. DIFFERENCES IS 8.08697 (INCL. SKELETON LAYER)

PROFILE R2-10 (222 hours)

POSITION	CORR. PROF.	EXPT. PROF.	CNV. CORR.	DIFFERENCE
0	26.7	10.2	8.7	-1.5
1	23.7	15.6	15.6	0
2	21.3	16.9	16.7	-0.3
3	18.1	16.4	16.4	0

PROFILE R2-10 (cont'd)

POSITION	CORR. PROF.	EXPT. PROF.	CNV. CORR.	DIFFERENCE
4	16.2	15.1	15.2	0.1
5	16.1	14.6	14.8	0.2
6	14.6	14.6	14.4	-0.2
7	13	13.6	13.6	0
8	13.4	13	13.2	0.3
9	13.2	13.4	13.2	-0.2
10	11.6	12.4	12.4	0
11	10.4	12.4	12.3	-0.1
12	10.8	12	12.2	0.3
13	12.5	12.1	12.2	0.1
14	12.9	12.7	12.5	-0.2
15	11.8	12.5	12.4	-0.1
16	11.2	11.9	12	0.1
17	11.3	11.6	11.7	0.1
18	11.5	11.6	11.6	0
19	11.8	11.6	11.6	0
20	11.9	11.6	11.6	0.1
21	11.3	11.8	11.6	-0.2
22	11.1	11.3	11.4	0.1
23	11.2	11.2	11.3	0.1
24	10.2	11.6	11.6	0.1
25	11.5	12.2	12.2	0
26	13.7	13.1	12.9	-0.2
27	11.4	14.1	13.5	-0.6
28	10.1	13.2	13.4	0.2
29	11.3	13.4	13.3	-0.1
30	9.9	14.1	14	-0.1
31	8.9	14.9	14.8	-0.1
32	10.3	16.1	16	-0.1
33	12.5	18.3	18.1	-0.2
34	18.6	21.6	22.2	0.6
35	42.6	29.1	29	-0.1
36	64.7	40.3	40.3	0

RECALCULATED AVERAGE ICE SALINITY IS 14.7 (INCL. SKELETON LAYER)
RECALCULATED AVERAGE ICE SALINITY IS 13 (EXCL. SKELETON LAYER)
RECALCULATED AVERAGE SOLUTION SALINITY IS 56.6

DISTRIBUTION COEFFICIENT IS 0.22

SUM OF THE DIFFERENCES IS -2.26751 (INCL. SKELETON LAYER)
SUM OF THE ABS. DIFFERENCES IS 6.50689 (INCL. SKELETON LAYER)

PROFILE R2-11 (295 hours)

POSITION	CORR. PROF.	EXPT. PROF.	CNV. CORR.	DIFFERENCE
0	28.2	9.9	8.8	-1
1	23.3	15.9	15.9	0
2	20.5	16.5	16.6	0
3	18.5	16	16.2	0.2
4	16.7	15.3	15.3	-0.1
5	15.7	14.7	14.9	0.1
6	15.3	14.4	14.4	-0.1
7	13.6	13.7	13.8	0
8	11.9	13.4	13.2	-0.3
9	12.3	12	12.6	0.6
10	11.3	12.3	11.9	-0.4
11	9.9	11.9	12	0.1
12	10.8	11.7	12	0.3
13	12	12	12	0
14	12.5	12.2	12.2	0
15	12.4	12.4	12.2	-0.2
16	11.9	11.9	12	0.1
17	11.3	11.8	11.7	-0.1
18	11	11.4	11.4	0
19	10.5	11	11	0.1
20	9.6	10.8	10.7	-0.1
21	10.5	10.4	10.6	0.2
22	11.5	10.9	10.8	-0.1
23	11.3	11.2	11.1	-0.1
24	11.4	11.1	11.3	0.2
25	12.2	11.8	11.6	-0.2
26	12.1	11.8	12	0.2
27	10.4	12.2	12.3	0
28	9.7	11.7	12	0.3
29	9.4	11.8	12	0.2
30	8.7	11.8	12.2	0.4
31	8.5	12.5	12.6	0.1
32	8.9	12.8	13.4	0.5
33	10.1	14.2	15	0.7
34	11.6	16.4	17.2	0.8
35	20.2	19.6	20.7	1.1
36	30.6	24.2	26.7	2.5
37	45.5	34	34	0

RECALCULATED AVERAGE ICE SALINITY IS 13.7 (INCL. SKELETON LAYER)
RECALCULATED AVERAGE ICE SALINITY IS 12.5 (EXCL. SKELETON LAYER)
RECALCULATED AVERAGE SOLUTION SALINITY IS 59

DISTRIBUTION COEFFICIENT IS 0.2

SUM OF THE DIFFERENCES IS 6.16971 (INCL. SKELETON LAYER)
SUM OF THE ABS. DIFFERENCES IS 11.2074 (INCL. SKELETON LAYER)

PROFILE R2-12 (390 hours)

POSITION	CORR. PROF.	EXPT. PROF.	CNV. CORR.	DIFFERENCE
0	27.7	9.8	8.8	-1
1	24.1	15.9	15.9	0
2	20.9	17.1	16.8	-0.3
3	18.7	16	16.3	0.3
4	16.1	15.4	15.2	-0.2
5	13.9	14.4	14.4	0.1
6	14.6	13.4	13.8	0.4
7	14.2	13.8	13.5	-0.3
8	12.4	13.4	13.2	-0.1
9	12.3	12.4	12.7	0.3
10	11.9	12	12	-0.1
11	10.4	12.3	12.1	-0.2
12	10.7	11.6	12	0.4
13	11.6	11.9	11.8	-0.1
14	11.9	11.7	11.9	0.1
15	11.4	12	11.7	-0.3
16	10.7	11.1	11.3	0.2
17	10.6	11	11	0
18	10.8	10.9	10.9	0
19	10.3	10.7	10.7	0
20	9.8	10.5	10.5	0
21	10.8	10.2	10.4	0.2
22	11.2	10.8	10.7	-0.2
23	10.8	10.7	10.8	0
24	11.2	10.7	10.7	0
25	11.7	10.7	10.8	0.1
26	10.8	10.9	11	0
27	10.3	11.2	11	-0.3
28	10.2	11.1	11	-0.1
29	7.6	11.3	11	-0.4
30	6.3	10.3	10.4	0.1
31	7.4	10.4	10.4	0
32	7.5	11	11	0
33	8.2	12.3	12.3	0
34	9.6	14.4	13.7	-0.6
35	9.5	16	15.8	-0.1
36	9.4	18.3	18	-0.3
37	26.9	22.4	22.9	0.5
38	45.9	32.1	32.1	0

RECALCULATED AVERAGE ICE SALINITY IS 12.7 (INCL. SKELETON LAYER)
RECALCULATED AVERAGE ICE SALINITY IS 12 (EXCL. SKELETON LAYER)
RECALCULATED AVERAGE SOLUTION SALINITY IS 61.6

DISTRIBUTION COEFFICIENT IS 0.15

SUM OF THE DIFFERENCES IS -2.10938 (INCL. SKELETON LAYER)
SUM OF THE ABS. DIFFERENCES IS 7.46814 (INCL. SKELETON LAYER)

PROFILE R2-13 (487 hours)

POSITION	CORR. PROF.	EXPT. PROF.	CNV. CORR.	DIFFERENCE
0	25.4	9.5	8.3	-1.2
1	23.1	15	15	0
2	20.2	16.6	16.1	-0.5
3	18.7	15.5	15.9	0.4
4	17.4	15.4	15.2	-0.2
5	15	14.9	14.7	-0.2
6	13.7	13.6	13.9	0.3
7	13.1	13.2	13.1	-0.1
8	12.7	12.8	12.8	0.1
9	12.2	12.6	12.6	0
10	10.7	11.8	11.7	-0.1
11	9.7	11.6	11.6	0
12	10.4	11.4	11.6	0.2
13	11.4	11.5	11.5	0.1
14	11.8	11.8	11.7	-0.1
15	12.2	11.7	11.7	0.1
16	10.9	11.8	11.5	-0.2
17	9.4	11	11	0
18	10.5	10.1	10.5	0.4
19	11.4	10.9	10.7	-0.1
20	10.7	11.1	10.9	-0.2
21	10.4	10.6	10.7	0.1
22	10.3	10.5	10.5	0
23	10.5	10.4	10.4	0.1
24	11.1	10.6	10.5	0
25	11	10.7	10.6	0
26	10.8	10.7	10.7	0.1
27	11.4	10.9	10.9	0
28	10.2	11.1	11	-0.1
29	7.7	10.3	10.8	0.6
30	7.9	10.4	10.5	0.2
31	8.3	10.5	10.8	0.3
32	7.7	11	11.3	0.3
33	8.1	11.7	11.9	0.3
34	9.4	12.6	13	0.4
35	10	13.9	14.9	0.9
36	9.3	16.2	16.8	0.6
37	17.7	18.3	19.8	1.6
38	29.5	22.9	26.1	3.2
39	46.9	34.3	34.3	0

RECALCULATED AVERAGE ICE SALINITY IS 12.9 (INCL. SKELETON LAYER)
RECALCULATED AVERAGE ICE SALINITY IS 11.9 (EXCL. SKELETON LAYER)
RECALCULATED AVERAGE SOLUTION SALINITY IS 63.1

DISTRIBUTION COEFFICIENT IS 0.15

SUM OF THE DIFFERENCES IS 7.00508 (INCL. SKELETON LAYER)

PROFILE R2-13 (cont'd)

SUM OF THE ABS. DIFFERENCES IS 13.0802 (INCL. SKELETON LAYER)

PROFILE R2-14 (582 hours)

POSITION	CORR. PROF.	EXPT. PROF.	CNV. CORR.	DIFFERENCE
0	23.9	9.5	8.1	-1.4
1	22.5	14.6	14.6	0
2	21.7	16.4	16	-0.4
3	19.4	16.3	16.2	-0.1
4	16.6	15.5	15.3	-0.2
5	14.9	14.4	14.4	0.1
6	13.5	13.5	13.6	0.1
7	11.9	12.9	12.8	-0.2
8	12.3	11.9	12.3	0.4
9	12.3	12.4	12.2	-0.2
10	10	11.5	11.4	-0.1
11	9.2	11.1	11.1	0
12	10.3	10.8	11.1	0.3
13	10.9	11.4	11.2	-0.2
14	11.3	11.2	11.3	0.1
15	11.4	11.4	11.3	-0.1
16	10.7	11.1	11	-0.1
17	10.4	10.6	10.7	0.2
18	9.7	10.7	10.4	-0.3
19	10.2	9.7	10.1	0.5
20	10.7	10.5	10.3	-0.2
21	9.6	10.4	10.2	-0.2
22	9.7	9.6	9.9	0.3
23	9.7	10	9.8	-0.1
24	10	9.9	9.9	0
25	11.5	9.9	10.1	0.2
26	11.1	10.8	10.4	-0.4
27	10.2	10.1	10.2	0.1
28	9.8	9.9	10.1	0.2
29	8.3	10.4	10	-0.4
30	6.9	10.1	9.7	-0.4
31	6.5	9.5	9.6	0.2
32	6.8	10	9.8	-0.2
33	7.5	10.7	10.5	-0.2
34	8.3	11.1	11.3	0.2
35	7.6	13	12.6	-0.5
36	6.4	14.1	13.6	-0.6
37	8.5	15.7	15.6	-0.1
38	13.3	18.7	19	0.2
39	33.2	26.4	25.7	-0.7
40	51.3	35.9	35.9	0

RECALCULATED AVERAGE ICE SALINITY IS 12.3 (INCL. SKELETON LAYER)

PROFILE R2-14 (cont'd)

RECALCULATED AVERAGE ICE SALINITY IS 11.2 (EXCL. SKELETON LAYER)
RECALCULATED AVERAGE SOLUTION SALINITY IS 65.6

DISTRIBUTION COEFFICIENT IS 0.13

SUM OF THE DIFFERENCES IS -4.03169 (INCL. SKELETON LAYER)
SUM OF THE ABS. DIFFERENCES IS 10.1285 (INCL. SKELETON LAYER)

PROFILE R2-15 (633 hours, skeleton layer 2 cm)

POSITION	CORR. PROF.	EXPT. PROF.	CNV. CORR.	DIFFERENCE
0	23	8.6	7.7	-0.9
1	20.2	13.8	13.8	0
2	19.3	14.9	14.9	0
3	18.4	15.1	15.1	0
4	15.9	14.8	14.6	-0.2
5	14.2	14	14	0
6	14.2	13.2	13.4	0.3
7	13.4	13.4	13.1	-0.3
8	12.5	12.7	12.9	0.1
9	12.5	12.5	12.6	0
10	11.5	11.9	11.9	0
11	10.4	12	11.9	-0.1
12	11.4	11.6	11.9	0.3
13	12.4	11.9	12	0
14	11.4	12.3	12	-0.3
15	10.9	11.4	11.6	0.2
16	10.9	11.2	11.2	0
17	10.6	11.1	11.1	-0.1
18	11.2	10.8	11	0.2
19	10.9	11.1	10.9	-0.2
20	10.3	10.6	10.7	0.1
21	10.4	10.5	10.5	0
22	10	10.4	10.3	-0.1
23	9.4	10.1	10.1	0
24	10.1	9.9	10.1	0.2
25	11.4	10.5	10.3	-0.2
26	12	10.4	10.6	0.2
27	11.2	11.2	10.8	-0.5
28	9.7	10.2	10.5	0.3
29	8.3	10.6	10.3	-0.3
30	7.5	9.8	10.2	0.4
31	7	10.3	10	-0.3
32	7.4	9.9	10.4	0.5
33	8.2	11	10.8	-0.2
34	8.1	11.7	11.8	0.1
35	8.2	12.6	12.7	0.1
36	7.1	14.4	14.6	0.2

PROFILE R2-15 (cont'd)

POSITION	CORR. PROF.	EXPT. PROF.	CNV. CORR.	DIFFERENCE
37	8	15.6	15.8	0.2
38	16.8	18.6	20.1	1.5
39	29.2	26.5	26.5	0

RECALCULATED AVERAGE ICE SALINITY IS 11.8 (INCL. SKELETON LAYER)
RECALCULATED AVERAGE ICE SALINITY IS 11.5 (EXCL. SKELETON LAYER)
RECALCULATED AVERAGE SOLUTION SALINITY IS 64.5

SUM OF THE DIFFERENCES IS 1.6001 (INCL. SKELETON LAYER)
SUM OF THE ABS. DIFFERENCES IS 8.69069 (INCL. SKELETON LAYER)

PROFILE R2-16 (657 hours, skeleton layer 2 cm)

POSITION	CORR. PROF.	EXPT. PROF.	CNV. CORR.	DIFFERENCE
0	16.6	7	6.4	-0.6
1	17.7	11.4	11.4	0
2	18.6	13.7	13.4	-0.3
3	17.7	14.4	14.3	0
4	16	14.6	14.2	-0.4
5	16.2	13.7	14.1	0.4
6	15.7	14.3	14	-0.3
7	13.4	13.8	13.6	-0.2
8	12.8	12.7	12.9	0.3
9	12.2	12.5	12.5	-0.1
10	10.5	11.9	11.8	-0.1
11	10.3	11.3	11.5	0.2
12	11	11.5	11.6	0.1
13	11.6	11.8	11.8	-0.1
14	12.8	11.9	12	0.1
15	11.9	12.3	12	-0.3
16	9.8	11.5	11.6	0
17	10.5	10.8	11	0.2
18	12	11	11.1	0.1
19	11.1	11.6	11.3	-0.4
20	10.5	10.8	11	0.2
21	10.9	10.8	10.8	0
22	10.9	10.7	10.8	0.1
23	10.5	10.9	10.7	-0.2
24	10.1	10.4	10.5	0.1
25	10.8	10.4	10.5	0.1
26	12.2	10.8	10.8	0
27	12.3	11.2	11.1	-0.1
28	10	11.1	10.9	-0.2
29	8.3	10.4	10.7	0.3
30	8.2	10.4	10.5	0.1
31	7.2	10.3	10.3	0
32	7.2	10.4	10.7	0.3

PROFILE R2-16 (cont'd)

POSITION	CORR. PROF.	EXPT. PROF.	CNV. CORR.	DIFFERENCE
33	8.6	10.9	11.1	0.2
34	8.7	12.2	12.2	0
35	8.2	13	13.2	0.3
36	8.4	14.4	15	0.6
37	11.3	16.4	16.7	0.3
38	17.4	19.5	21.2	1.7
39	27.8	26.8	26.8	0

RECALCULATED AVERAGE ICE SALINITY IS 12 (INCL. SKELETON LAYER)
RECALCULATED AVERAGE ICE SALINITY IS 11.6 (EXCL. SKELETON LAYER)
RECALCULATED AVERAGE SOLUTION SALINITY IS 64.3

SUM OF THE DIFFERENCES IS 2.58684 (INCL. SKELETON LAYER)
SUM OF THE ABS. DIFFERENCES IS 8.97921 (INCL. SKELETON LAYER)

PROFILE R2-17 (707 hours, skeleton layer 2 cm)

POSITION	CORR. PROF.	EXPT. PROF.	CNV. CORR.	DIFFERENCE
0	13	5.8	5.6	-0.3
1	15.2	9.8	9.8	0
2	17	12.1	12	-0.1
3	17	13.6	13.3	-0.3
4	16.6	13.6	13.6	0.1
5	15.8	14	13.8	-0.2
6	14.9	13.5	13.6	0.1
7	13.9	13.3	13.2	-0.1
8	12.5	12.8	12.7	-0.1
9	11.6	12.1	12.2	0.1
10	10.9	11.5	11.5	0
11	10.9	11.4	11.4	0
12	11.1	11.3	11.5	0.2
13	10.5	11.8	11.5	-0.3
14	11	11	11.3	0.3
15	11.8	11.4	11.4	-0.1
16	10.5	11.6	11.4	-0.3
17	9.7	10.7	10.9	0.2
18	10.4	10.5	10.6	0.1
19	10.9	10.7	10.7	0
20	11.1	10.9	10.9	-0.1
21	11.3	10.8	10.9	0.1
22	10.4	11	10.9	-0.2
23	10.1	10.5	10.6	0.1
24	11.5	10.4	10.7	0.2
25	11.8	11.2	11	-0.2
26	11.9	11.1	11.2	0.1
27	12.1	11.2	11.3	0.1
28	10.7	11.5	11.2	-0.4

PROFILE R2-17 (cont'd)

POSITION	CORR. PROF.	EXPT. PROF.	CNV. CORR.	DIFFERENCE
29	9.7	10.8	11.1	0.3
30	8.4	11.3	11.1	-0.3
31	7.1	10.4	10.6	0.2
32	8	10.8	11	0.2
33	8.5	11.5	11.5	-0.1
34	7.7	12.3	12.3	0.1
35	8.3	13.1	13.2	0.1
36	10.5	15.2	15.6	0.4
37	13	17.8	17.7	-0.1
38	19.2	21.6	22.2	0.7
39	27.5	27.6	27.6	0

RECALCULATED AVERAGE ICE SALINITY IS 11.9 (INCL. SKELETON LAYER)
RECALCULATED AVERAGE ICE SALINITY IS 11.5 (EXCL. SKELETON LAYER)
RECALCULATED AVERAGE SOLUTION SALINITY IS 64.4

SUM OF THE DIFFERENCES IS 0.55398 (INCL. SKELETON LAYER)
SUM OF THE ABS. DIFFERENCES IS 6.40241 (INCL. SKELETON LAYER)

PROFILE R2-18 (826 hours, skeleton layer 2 cm)

POSITION	CORR. PROF.	EXPT. PROF.	CNV. CORR.	DIFFERENCE
0	12.1	5.5	5.3	-0.2
1	14.8	9.3	9.3	0
2	15.8	11.8	11.5	-0.3
3	16.3	12.7	12.6	-0.1
4	17.4	13.1	13.3	0.1
5	16.1	14.3	13.7	-0.6
6	14.2	13	13.3	0.2
7	12.7	12.7	12.5	-0.2
8	10.8	11.7	11.7	0
9	9.9	10.9	11	0.2
10	9.6	10.5	10.4	0
11	10.3	10.3	10.5	0.2
12	10.5	10.9	10.8	-0.1
13	9.9	10.9	10.7	-0.2
14	10.6	10.3	10.6	0.3
15	10.8	11	10.7	-0.3
16	9.3	10.6	10.5	-0.1
17	8.5	9.9	10	0
18	9.8	9.4	9.8	0.3
19	10.4	10.3	10	-0.2
20	10.3	10.2	10.2	0.1
21	10.7	10.3	10.3	0
22	10.5	10.5	10.4	-0.1
23	10.2	10.5	10.4	0
			10.4	0.1

PROFILE R2-18 (cont'd)

POSITION	CORR. PROF.	EXPT. PROF.	CNV. CORR.	DIFFERENCE
25	11.7	10.6	10.7	0.1
26	12.9	11.2	11.2	0
27	11.7	11.9	11.5	-0.4
28	10.4	11	11.2	0.2
29	9.5	11.6	11.2	-0.4
30	8.7	11	11.3	0.3
31	8.2	11.4	11.1	-0.3
32	8.1	11.6	11.7	0.1
33	9.1	12	12.1	0.1
34	9.9	13.4	13.4	0
35	10.9	15.2	14.7	-0.5
36	13.2	17	17.3	0.3
37	14.4	20	19.5	-0.5
38	21.8	23.8	23.8	0
39	29.9	29.2	29.2	0

RECALCULATED AVERAGE ICE SALINITY IS 11.8 (INCL. SKELETON LAYER)
RECALCULATED AVERAGE ICE SALINITY IS 11.3 (EXCL. SKELETON LAYER)
RECALCULATED AVERAGE SOLUTION SALINITY IS °64.4

SUM OF THE DIFFERENCES IS -1.82648 (INCL. SKELETON LAYER)
SUM OF THE ABS. DIFFERENCES IS 7.30654 (INCL. SKELETON LAYER)

PROFILE R2-19 (919 hours, skeleton layer 1 cm)

POSITION	CORR. PROF.	EXPT. PROF.	CNV. CORR.	DIFFERENCE
0	12.2	4.8	5.1	0.2
1	13.5	8.9	9	0
2	14.7	10.8	10.8	0
3	15.9	11.9	12	0
4	16	12.9	12.7	-0.2
5	15.5	13.1	13	-0.1
6	14.6	12.9	12.8	-0.1
7	12.3	12.3	12.2	-0.1
8	10.4	11.3	11.4	0
9	10.1	10.4	10.6	0.2
10	8.8	10.2	10	-0.2
11	7.5	9.5	9.6	0.2
12	8.7	9.4	9.5	0.2
13	10.5	9.8	9.9	0.1
14	10.4	10.7	10.4	-0.3
15	10.2	10.4	10.4	0.1
16	10.1	10.3	10.3	0
17	9.4	10.3	10.2	-0.1
18	9.7	9.8	10	0.2
19	9.9	10.1	9.9	-0.2
20	10.1	9.8	10	0.2

PROFILE R2-19 (cont'd)

POSITION	CORR. PROF.	EXPT. PROF.	CNV. CORR.	DIFFERENCE
21	10.5	10.4	10.2	-0.2
22	10.5	10.2	10.3	0.1
23	10.5	10.3	10.3	0
24	10.9	10.5	10.5	0
25	11.7	10.8	10.8	0
26	12.2	11	11.2	0.2
27	10.9	11.8	11.4	-0.4
28	10.5	11.3	11.5	0.2
29	10.2	11.6	11.7	0.1
30	8.4	11.9	11.5	-0.4
31	8.7	11	11.7	0.7
32	9.1	12.3	12	-0.4
33	8.1	12.5	12.8	0.2
34	8	13.7	13.5	-0.1
35	9	15	15.5	0.5
36	12.3	17.5	17.6	0.2
37	22.1	21.8	22.6	0.8
38	34.1	29.3	29.3	0

RECALCULATED AVERAGE ICE SALINITY IS 11.4 (INCL. SKELETON LAYER)
RECALCULATED AVERAGE ICE SALINITY IS 11 (EXCL. SKELETON LAYER)
RECALCULATED AVERAGE SOLUTION SALINITY IS 63.2

SUM OF THE DIFFERENCES IS 1.62663 (INCL. SKELETON LAYER)
SUM OF THE ABS. DIFFERENCES IS 7.35139 (INCL. SKELETON LAYER)

PROFILE R2-20 (992 hours, skeleton layer 1 cm)

POSITION	CORR. PROF.	EXPT. PROF.	CNV. CORR.	DIFFERENCE
0	10.4	5.1	4.7	-0.3
1	12.1	8	8.1	0.1
2	14.6	10.1	10.1	0
3	16.2	12	11.7	-0.2
4	16.4	12.7	12.6	-0.1
5	15	13.1	12.8	-0.3
6	12.9	12.4	12.3	0
7	11.7	11.4	11.5	0.1
8	10.6	10.9	10.9	0
9	9.6	10.5	10.5	-0.1
10	9.3	9.7	9.9	0.2
11	8.4	9.9	9.7	-0.2
12	8.2	9.4	9.6	0.2
13	9.9	9.5	9.6	0.2
14	10.8	10.2	10.1	-0.1
15	9.9	10.6	10.4	-0.3
16	9.2	10	10	0.1
17	9.1	9.6	9.7	0.1

PROFILE R2-20 (cont'd)

POSITION	CORR. PROF.	EXPT. PROF.	CNV. CORR.	DIFFERENCE
18	8.7	9.7	9.6	-0.1
19	9.7	9.4	9.6	0.2
20	11.3	9.9	10	0.1
21	10.5	10.7	10.4	-0.3
22	9.9	10.2	10.2	0
23	10.6	9.8	10.1	0.3
24	10.4	10.6	10.3	-0.3
25	11.4	10.2	10.5	0.3
26	11.7	11.1	10.9	-0.2
27	10.2	11.2	11.1	-0.2
28	10.3	11.1	11.2	0.1
29	10.5	11.6	11.6	-0.1
30	9.1	11.7	11.6	-0.2
31	8.3	11.9	11.9	0
32	8.5	11.7	11.9	0.1
33	8	12.7	12.7	0
34	8.1	13.7	13.5	-0.2
35	10.1	15.4	15.7	0.3
36	13	18	18	0
37	22.5	22.7	22.9	0.3
38	33.1	29.4	29.4	0

RECALCULATED AVERAGE ICE SALINITY IS 11.3 (INCL. SKELETON LAYER)
RECALCULATED AVERAGE ICE SALINITY IS 10.8 (EXCL. SKELETON LAYER)
RECALCULATED AVERAGE SOLUTION SALINITY IS 63.4

SUM OF THE DIFFERENCES IS -0.487756 (INCL. SKELETON LAYER)
SUM OF THE ABS. DIFFERENCES IS 5.88187 (INCL. SKELETON LAYER)

PROFILE R3-3 (15 hours)

POSITION	CORR. PROF.	EXPT. PROF.	CNV. CORR.	DIFFERENCE
0	21.7	9.1	8.2	-0.9
1	17.1	13.8	13.9	0.1
2	15.8	14.5	14.8	0.3
3	15.5	14.9	15.5	0.6
4	13.8	16.1	16.1	-0.1
5	16.8	16.3	17.3	1
6	22.3	18.8	20	1.1
7	29.1	23.4	23.5	0.1

RECALCULATED AVERAGE ICE SALINITY IS 18.1 (INCL. SKELETON LAYER)
RECALCULATED AVERAGE ICE SALINITY IS 16.5 (EXCL. SKELETON LAYER)
RECALCULATED AVERAGE SOLUTION SALINITY IS 36.6

DISTRIBUTION COEFFICIENT IS 0.38

SUM OF THE DIFFERENCES IS 2.14312 (INCL. SKELETON LAYER)
SUM OF THE ABS. DIFFERENCES IS 4.15298 (INCL. SKELETON LAYER)

PROFILE R3-4 (22 hours)

POSITION	CORR. PROF.	EXPT. PROF.	CNV. CORR.	DIFFERENCE
0	20.2	9.2	7.4	-1.8
1	16	12.5	12.6	0.1
2	14.6	13.1	13.3	0.2
3	13.5	13.7	13.7	0
4	12.8	13.5	13.8	0.3
5	12.7	14.2	14.6	0.4
6	12.9	15.2	15.6	0.4
7	18.3	16.6	17.5	0.8
8	24.4	19.8	21	1.2
9	32.3	25.1	25.2	0.1

RECALCULATED AVERAGE ICE SALINITY IS 16.8 (INCL. SKELETON LAYER)
RECALCULATED AVERAGE ICE SALINITY IS 14.3 (EXCL. SKELETON LAYER)
RECALCULATED AVERAGE SOLUTION SALINITY IS 37.4

DISTRIBUTION COEFFICIENT IS 0.34

SUM OF THE DIFFERENCES IS 1.72216 (INCL. SKELETON LAYER)
SUM OF THE ABS. DIFFERENCES IS 5.41702 (INCL. SKELETON LAYER)

PROFILE R3-5 (54 hours)

POSITION	CORR. PROF.	EXPT. PROF.	CNV. CORR.	DIFFERENCE
0	22.9	7.9	6.8	-1.1
1	16.6	11.1	12.1	1

PROFILE R3-5 (cont'd)

POSITION	CORR. PROF.	EXPT. PROF.	CNV. CORR.	DIFFERENCE
2	13	11.9	11.9	0
3	11.1	11.1	11.4	0.3
4	11.6	11	10.9	-0.1
5	10.4	11.4	11.3	-0.1
6	9.4	11.2	11.2	-0.1
7	10.1	11.2	11.2	0
8	10.2	11.8	11.8	0
9	9.7	12.6	12.6	0
10	10	13.5	12.9	-0.7
11	11.7	14.5	14.7	0.1
12	12.1	17.3	16.8	-0.5
13	24	19.9	19.8	-0.2
14	36	25.5	25.5	0

RECALCULATED AVERAGE ICE SALINITY IS 13.5 (INCL. SKELETON LAYER)
RECALCULATED AVERAGE ICE SALINITY IS 11.8 (EXCL. SKELETON LAYER)
RECALCULATED AVERAGE SOLUTION SALINITY IS 40.1

DISTRIBUTION COEFFICIENT IS 0.29

SUM OF THE DIFFERENCES IS -1.48754 (INCL. SKELETON LAYER)
SUM OF THE ABS. DIFFERENCES IS 4.29228 (INCL. SKELETON LAYER)

PROFILE R3-6 (77 hours)

POSITION	CORR. PROF.	EXPT. PROF.	CNV. CORR.	DIFFERENCE
0	18.1	7.5	5.8	-1.7
1	14.9	10.4	10.4	0
2	13.3	11.1	10.9	-0.2
3	12.3	10.6	10.8	0.2
4	11.3	10.5	10.5	0
5	10.5	10.7	10.5	-0.2
6	9.9	10.2	10.5	0.3
7	8.7	10.3	10.5	0.2
8	8.9	10.4	10.5	0.1
9	10.2	10.6	11.1	0.5
10	9.4	11.5	11.4	-0.1
11	9.9	12.2	12.5	0.2
12	11.9	13.3	13.7	0.4
13	12.1	14.9	15.3	0.4
14	13	15.8	16.6	0.8
15	21.6	18.5	19.6	1.1
16	30.9	22.6	24.4	1.8
17	42.9	30.2	30.2	0

RECALCULATED AVERAGE ICE SALINITY IS 14.1 (INCL. SKELETON LAYER)
RECALCULATED AVERAGE ICE SALINITY IS 11.4 (EXCL. SKELETON LAYER)

PROFILE R3-6 (cont'd)

RECALCULATED AVERAGE SOLUTION SALINITY IS 41.4

DISTRIBUTION COEFFICIENT IS 0.31

SUM OF THE DIFFERENCES IS 3.66474 (INCL. SKELETON LAYER)
SUM OF THE ABS. DIFFERENCES IS 8.13762 (INCL. SKELETON LAYER)

PROFILE R3-7 (104 hours)

POSITION	CORR. PROF.	EXPT. PROF.	CNV. CORR.	DIFFERENCE
0	17.3	7.3	5.6	-1.8
1	14.1	9.9	9.9	0
2	12.7	10.5	10.4	-0.2
3	11.8	10.2	10.3	0.1
4	11.1	10	9.9	-0.1
5	10.6	9.9	9.9	0
6	9.6	9.8	9.8	0
7	8.9	9.8	9.7	-0.1
8	9	9.6	9.8	0.2
9	9	9.7	10.2	0.5
10	8.7	10.2	10.1	-0.1
11	8.9	10.5	10.8	0.3
12	9.1	11.1	11.5	0.3
13	9.6	12	12.2	0.1
14	10.6	12.7	13.1	0.3
15	10.9	13.7	14.5	0.8
16	12.2	15.4	16.1	0.6
17	22.7	17.9	19.4	1.6
18	31.8	23.1	24.8	1.7
19	42.2	30.5	30.5	0

RECALCULATED AVERAGE ICE SALINITY IS 13.2 (INCL. SKELETON LAYER)
RECALCULATED AVERAGE ICE SALINITY IS 10.6 (EXCL. SKELETON LAYER)
RECALCULATED AVERAGE SOLUTION SALINITY IS 42.9

DISTRIBUTION COEFFICIENT IS 0.28

SUM OF THE DIFFERENCES IS 4.33782 (INCL. SKELETON LAYER)
SUM OF THE ABS. DIFFERENCES IS 8.89738 (INCL. SKELETON LAYER)

PROFILE R3-8 (125 hours)

POSITION	CORR. PROF.	EXPT. PROF.	CNV. CORR.	DIFFERENCE
0	18.6	6.7	5.7	-1
1	14.8	10.3	10.3	0
2	12.8	10.5	10.6	0
3	11.1	10.1	10.2	0.1

PROFILE R3-8 (cont'd)

POSITION	CORR. PROF.	EXPT. PROF.	CNV. CORR.	DIFFERENCE
4	9.5	9.4	9.4	0
5	9.5	8.9	9.2	0.3
6	9.8	9.3	9.2	-0.1
7	9.5	9	9.1	0.1
8	8.8	9.4	9.3	-0.1
9	8.8	9.4	9.5	0.1
10	8.5	9.8	9.3	-0.4
11	7.9	9.8	9.9	0.1
12	8.9	10.4	10.4	0
13	9.5	11	10.8	-0.2
14	8.3	11.2	11.2	-0.1
15	7.4	11.6	11.6	-0.1
16	9.2	12.4	12.3	-0.1
17	11.5	14.3	14.2	-0.1
18	12.2	17	16.5	-0.5
19	24.6	19.9	20.1	0.3
20	38.4	26.7	26.7	0

RECALCULATED AVERAGE ICE SALINITY IS 11.6 (INCL. SKELETON LAYER)
RECALCULATED AVERAGE ICE SALINITY IS 10 (EXCL. SKELETON LAYER)
RECALCULATED AVERAGE SOLUTION SALINITY IS 44.1

DISTRIBUTION COEFFICIENT IS 0.26

SUM OF THE DIFFERENCES IS -1.7423 (INCL. SKELETON LAYER)
SUM OF THE ABS. DIFFERENCES IS 3.6022 (INCL. SKELETON LAYER)

PROFILE R3-9 (178 hours)

POSITION	CORR. PROF.	EXPT. PROF.	CNV. CORR.	DIFFERENCE
0	17.8	7.2	5.6	-1.6
1	15	10.2	10.1	0
2	13.8	10.9	10.6	-0.3
3	11.4	10.3	10.3	0.1
4	8.6	9.7	9.3	-0.4
5	8.8	8	8.7	0.6
6	9.2	8.9	8.6	-0.3
7	8.2	8.5	8.5	0
8	8.2	8.5	8.4	-0.1
9	8.2	8.3	8.4	0.1
10	7.7	8.2	8.3	0
11	8.9	8.9	8.8	-0.1
12	9.5	9.2	9.5	0.3
13	7	9.6	9.7	0.2
14	6.9	9.1	9.4	0.2
15	8.3	9	9.6	0.6
16	7.4	10.3	10.3	0

PROFILE R3-9 (cont'd)

POSITION	CORR. PROF.	EXPT. PROF.	CNV. CORR.	DIFFERENCE
17	8.3	10.5	11	0.5
18	10.8	12	12.2	0.2
19	12	13.1	14.2	1.1
20	12.6	15.7	16.1	0.4
21	21	17.4	18.9	1.5
22	26.5	21.2	23.5	2.3
23	35.7	28.4	28.4	0

RECALCULATED AVERAGE ICE SALINITY IS 11.5 (INCL. SKELETON LAYER)
RECALCULATED AVERAGE ICE SALINITY IS 9.7 (EXCL. SKELETON LAYER)
RECALCULATED AVERAGE SOLUTION SALINITY IS 46.3

DISTRIBUTION COEFFICIENT IS 0.27

SUM OF THE DIFFERENCES IS 5.55889 (INCL. SKELETON LAYER)
SUM OF THE ABS. DIFFERENCES IS 10.8721 (INCL. SKELETON LAYER)

PROFILE R3-10 (227 hours)

POSITION	CORR. PROF.	EXPT. PROF.	CNV. CORR.	DIFFERENCE
0	17.8	6.5	5.5	-1
1	13.9	9.9	9.9	0
2	12.1	10	10	0
3	11.7	9.6	9.8	0.2
4	10.3	9.6	9.3	-0.3
5	8.7	8.9	9	0.1
6	8.2	8.3	8.4	0.1
7	7.4	8.1	8	-0.1
8	7.6	7.8	7.9	0.1
9	8.7	8	8.1	0.1
10	8.7	8.4	8.1	-0.3
11	8.4	8.4	8.5	0.1
12	7.8	8.9	8.7	-0.2
13	7.5	8.3	8.5	0.2
14	6.8	8.5	8.5	0
15	5.9	8.3	8.5	0.3
16	7.1	8.4	8.7	0.3
17	8.2	9.4	9.5	0.1
18	8.2	10.2	10.3	0.1
19	9.1	11	11.2	0.2
20	10.5	12.2	12.5	0.3
21	10.8	13.8	14.1	0.4
22	12	15.2	15.9	0.7
23	19.7	18	18.9	0.9
24	28.9	22.3	24	1.7
25	41.1	30.1	30.1	0

PROFILE R3-10 (cont'd)

RECALCULATED AVERAGE ICE SALINITY IS 11.1 (INCL. SKELETON LAYER)
RECALCULATED AVERAGE ICE SALINITY IS 9.2 (EXCL. SKELETON LAYER)
RECALCULATED AVERAGE SOLUTION SALINITY IS 48.1

DISTRIBUTION COEFFICIENT IS 0.25

SUM OF THE DIFFERENCES IS 4.35499 (INCL. SKELETON LAYER)
SUM OF THE ABS. DIFFERENCES IS 7.82589 (INCL. SKELETON LAYER)

PROFILE R3-12 (373 hours)

POSITION	CORR. PROF.	EXPT. PROF.	CNV. CORR.	DIFFERENCE
0	16.2	5.9	5.1	-0.9
1	13.1	9.1	9.1	0
2	11.4	9.4	9.4	0
3	10.8	9.1	9.2	0.1
4	10.1	8.9	8.8	-0.1
5	8.6	8.8	8.6	-0.2
6	8.1	7.9	8.1	0.2
7	8	7.8	7.8	0
8	7.3	7.9	7.7	-0.2
9	7.2	7.2	7.5	0.3
10	6.7	7.4	7.1	-0.3
11	6.8	7	7.2	0.2
12	7.9	7.5	7.5	0
13	7.4	7.8	7.6	-0.2
14	6.4	7.3	7.3	0
15	5.8	6.9	7	0.1
16	5.5	6.9	6.9	0
17	6.7	6.9	7.1	0.2
18	7.7	7.6	7.7	0.1
19	7.2	8.3	8.5	0.2
20	8	8.9	9	0.1
21	7.8	9.3	9.5	0.2
22	6.5	10	10.1	0.1
23	8.4	10.2	10.8	0.5
24	10.5	12.2	12.3	0.1
25	10.9	13.7	14.2	0.6
26	14.7	16	16.8	0.8
27	24.8	19.3	20.3	1
28	27.4	24.9	25.6	0.8
29	30.3	29.3	29.3	0

RECALCULATED AVERAGE ICE SALINITY IS 10.2 (INCL. SKELETON LAYER)
RECALCULATED AVERAGE ICE SALINITY IS 8.5 (EXCL. SKELETON LAYER)
RECALCULATED AVERAGE SOLUTION SALINITY IS 52.5

DISTRIBUTION COEFFICIENT IS 0.28

PROFILE R3-12 (cont'd)

SUM OF THE DIFFERENCES IS 3.92637 (INCL. SKELETON LAYER)
SUM OF THE ABS. DIFFERENCES IS 7.49777 (INCL. SKELETON LAYER)

PROFILE R3-13 (468 hours)

POSITION	CORR. PROF.	EXPT. PROF.	CNV. CORR.	DIFFERENCE
0	16.2	5.1	5.1	0
1	14.2	9.5	9.3	-0.2
2	12.1	9.8	9.8	0
3	11.2	9.4	9.5	0.2
4	9.9	9.1	9	-0.1
5	8.1	8.5	8.5	0
6	7.3	7.7	7.8	0.1
7	6.9	7.3	7.4	0.1
8	7.1	7.3	7.3	0
9	7.5	7.1	7.3	0.2
10	6.6	7.4	7.1	-0.4
11	6.4	6.8	7.1	0.3
12	7.5	7.4	7.3	-0.1
13	7.4	7.4	7.4	0
14	6.8	7.4	7.3	-0.1
15	6.7	7	7.1	0.1
16	6.5	7	7	0
17	6.4	6.9	7	0.1
18	7	7.3	7.3	0
19	7.3	7.9	7.9	0.1
20	7.3	8.6	8.5	0
21	7.2	8.9	8.8	0
22	6.3	9.2	9.3	0.1
23	6.1	9.4	9.5	0.1
24	8.1	10.1	10.6	0.4
25	9.8	12.4	12.2	-0.2
26	10.3	14.2	14.5	0.3
27	13.1	16.3	16.5	0.2
28	21.1	19.6	20.6	1
29	31.2	26.2	26.2	0

RECALCULATED AVERAGE ICE SALINITY IS 9.2 (INCL. SKELETON LAYER)
RECALCULATED AVERAGE ICE SALINITY IS 8.1 (EXCL. SKELETON LAYER)
RECALCULATED AVERAGE SOLUTION SALINITY IS 53.2

DISTRIBUTION COEFFICIENT IS 0.19

SUM OF THE DIFFERENCES IS 2.15887 (INCL. SKELETON LAYER)
SUM OF THE ABS. DIFFERENCES IS 4.46504 (INCL. SKELETON LAYER)

PROFILE R3-14 (522 hours)

POSITION	CORR. PROF.	EXPT. PROF.	CNV. CORR.	DIFFERENCE
0	14	5	4.7	-0.3
1	14.1	8.6	8.6	0
2	12.2	10	9.5	-0.5
3	10.8	9	9.3	0.3
4	9.7	9	8.7	-0.3
5	7.9	8.1	8.2	0.1
6	7	7.6	7.6	0
7	7	7	7.2	0.2
8	6.8	7.2	7.1	-0.1
9	6.3	6.9	7	0
10	6.1	6.5	6.5	0
11	5.9	6.6	6.7	0
12	6.7	6.9	6.9	0.1
13	7.8	7.2	7.2	0
14	7.3	7.5	7.3	-0.2
15	6.9	7.1	7.2	0.1
16	7.2	7.1	7.1	0
17	7.2	7.1	7.1	-0.1
18	6.5	6.9	7.1	0.2
19	5.8	7.6	7.3	-0.4
20	6.9	7.3	7.5	0.2
21	6.9	8.5	8.2	-0.3
22	5.7	8.7	8.5	-0.2
23	6.1	8.6	8.8	0.2
24	7	9.6	9.5	0
25	8	10.9	10.9	0.1
26	9.4	13	12.5	-0.5
27	10.4	14.5	14.6	0.1
28	11.4	17.3	17	-0.3
29	24.8	20.8	21.4	0.5
30	40.1	28.9	28.9	0

RECALCULATED AVERAGE ICE SALINITY IS 9.1 (INCL. SKELETON LAYER)
RECALCULATED AVERAGE ICE SALINITY IS 7.8 (EXCL. SKELETON LAYER)
RECALCULATED AVERAGE SOLUTION SALINITY IS 54.4

DISTRIBUTION COEFFICIENT IS 0.19

SUM OF THE DIFFERENCES IS -0.910208 (INCL. SKELETON LAYER)
SUM OF THE ABS. DIFFERENCES IS 5.58092 (INCL. SKELETON LAYER)

PROFILE R3-15 (614 hours)

POSITION	CORR. PROF.	EXPT. PROF.	CNV. CORR.	DIFFERENCE
0	13.3	4.7	4.6	-0.2
1	14.1	8.4	8.4	0
2	12.4	9.9	9.4	-0.5

PROFILE R3-15 (cont'd)

POSITION	CORR. PROF.	EXPT. PROF.	CNV. CORR.	DIFFERENCE
3	10.2	9.1	9.2	0.1
4	9.5	8.3	8.5	0.2
5	8.4	8.4	8.1	-0.2
6	7.1	7.3	7.6	0.2
7	6	7.1	7	-0.1
8	6.4	6.5	6.7	0.2
9	7.3	6.7	6.8	0.1
10	5.7	7	6.6	-0.4
11	5.6	6.1	6.4	0.4
12	7.5	6.6	6.8	0.2
13	7.1	7.5	7.1	-0.5
14	5.8	6.7	6.8	0.2
15	6	6.4	6.5	0
16	6.4	6.3	6.4	0.1
17	6.6	6.6	6.5	-0.1
18	6.7	6.5	6.6	0.1
19	6.4	6.8	6.8	0.1
20	6	7.2	7.2	0
21	5.3	7.5	7.4	-0.1
22	4.8	7.3	7.5	0.2
23	6	7.9	8.1	0.2
24	8	9.1	9.2	0.1
25	8.7	10.5	10.5	0
26	8	11.8	11.7	-0.1
27	8.2	12.7	13	0.2
28	10	14.5	14.9	0.4
29	15.4	17.7	18.1	0.4
30	29.4	22.5	23.7	1.2
31	45.8	31.9	31.9	0

RECALCULATED AVERAGE ICE SALINITY IS 9.2 (INCL. SKELETON LAYER)
RECALCULATED AVERAGE ICE SALINITY IS 7.6 (EXCL. SKELETON LAYER)
RECALCULATED AVERAGE SOLUTION SALINITY IS 55.5

DISTRIBUTION COEFFICIENT IS 0.18

SUM OF THE DIFFERENCES IS 2.22957 (INCL. SKELETON LAYER)
SUM OF THE ABS. DIFFERENCES IS 6.68439 (INCL. SKELETON LAYER)

PROFILE R3-16 (733 hours)

POSITION	CORR. PROF.	EXPT. PROF.	CNV. CORR.	DIFFERENCE
0	11.2	4.7	4.3	-0.4
1	13.6	7.8	7.8	0
2	13.4	9.8	9.3	-0.5
3	11.2	9.7	9.5	-0.2
4	9.8	8.7	8.8	0.1

PROFILE R3-16 (cont'd)

POSITION	CORR. PROF.	EXPT. PROF.	CNV. CORR.	DIFFERENCE
5	8.5	8.3	8.2	-0.1
6	6.9	7.6	7.6	-0.1
7	6	6.8	6.9	0.1
8	6.2	6.6	6.6	0.1
9	6.5	6.6	6.6	0
10	6.1	6.5	6.4	0
11	5.8	6.4	6.4	0
12	6.5	6.5	6.6	0.1
13	7.1	6.8	6.8	0
14	5.6	7	6.7	-0.3
15	4.9	6	6.2	0.3
16	6.3	5.9	6.1	0.1
17	6.9	6.5	6.4	-0.1
18	6.6	6.7	6.6	-0.1
19	7.1	6.5	6.8	0.3
20	7.1	7.3	7.1	-0.2
21	6.3	7.5	7.6	0.1
22	6	7.8	7.9	0.1
23	5.7	7.9	8	0.1
24	6.7	8.4	8.7	0.3
25	8.1	9.6	9.6	-0.1
26	7.7	10.6	10.7	0
27	7.6	11.4	11.6	0.3
28	8.1	13	13.4	0.5
29	10.9	15	15.2	0.2
30	17.7	17.9	19.4	1.5
31	28.3	25	24.9	0

RECALCULATED AVERAGE ICE SALINITY IS 8.3 (INCL. SKELETON LAYER)
RECALCULATED AVERAGE ICE SALINITY IS 7.5 (EXCL. SKELETON LAYER)
RECALCULATED AVERAGE SOLUTION SALINITY IS 56.3

DISTRIBUTION COEFFICIENT IS 0.14

SUM OF THE DIFFERENCES IS 2.06722 (INCL. SKELETON LAYER)
SUM OF THE ABS. DIFFERENCES IS 6.16761 (INCL. SKELETON LAYER)

PROFILE R3-17 (950 hours)

POSITION	CORR. PROF.	EXPT. PROF.	CNV. CORR.	DIFFERENCE
0	11.4	4.3	4.2	-0.1
1	13.3	7.6	7.6	0
2	12.9	9.4	9	-0.4
3	10.1	9.3	9	-0.3
4	8.1	7.9	8.1	0.2
5	7	7.4	7.4	0
6	6.6	6.8	6.9	0.1

PROFILE R3-17 (cont'd)

POSITION	CORR. PROF.	EXPT. PROF.	CNV. CORR.	DIFFERENCE
7	7.5	6.6	6.8	0.2
8	7.5	7.2	7	-0.2
9	6.5	6.9	6.9	0
10	5.5	6.2	6.3	0
11	4.6	6	6	0
12	5.3	5.6	5.9	0.3
13	6.8	6.2	6.2	0
14	6.2	6.7	6.4	-0.3
15	5.2	6	6.1	0.1
16	5.4	5.7	5.8	0.1
17	6.1	5.9	5.9	-0.1
18	7	5.9	6.2	0.2
19	6.6	6.8	6.5	-0.3
20	6.5	6.4	6.6	0.2
21	6.6	7.3	7	-0.3
22	5.2	7.3	7.3	0
23	4.6	7.1	7.1	0
24	6	7.6	7.8	0.2
25	6.8	8.6	8.4	-0.2
26	6.1	9.4	9.4	-0.1
27	6.5	10.2	10	-0.3
28	6.8	11.6	11.9	0.2
29	4.9	13.4	12.7	-0.7
30	10.5	15	15.8	0.7
31	18.9	20.5	20.5	0

RECALCULATED AVERAGE ICE SALINITY IS 7.2 (INCL. SKELETON LAYER)
RECALCULATED AVERAGE ICE SALINITY IS 7 (EXCL. SKELETON LAYER)
RECALCULATED AVERAGE SOLUTION SALINITY IS 57.1

DISTRIBUTION COEFFICIENT IS 0.12

SUM OF THE DIFFERENCES IS -0.664156 (INCL. SKELETON LAYER)
SUM OF THE ABS. DIFFERENCES IS 5.75145 (INCL. SKELETON LAYER)

Z is the position of the ice below the cold-plate (cm); S is the ice salinity (o/oo); T is the ice temperature (°C); and v_b is the brine volume (o/oo) determined by the ice temperature and salinity.

	Z(cm)	S(o/oo)	T(°C)	v_b(o/oo)
Profile R2-3	0	26.8	-19.9	95.6
	1	25.3	-17.2	99.4
	2	23.2	-14.8	101.6
	3	21.1	-12.5	105.3
	4	20.0	-10.5	115.2
	5	19.0	-8.7	128.8
	6	19.0	-6.9	159.0
	7	22.5	-5.4	238.4
	8	24.2	-4.0	344.4
	9	28.5	-2.7	608.6
Profile R2-4	0	25.4	-20.6	88.5
	1	24.8	-18.9	91.3
	2	24.2	-17.2	95.0
	3	21.3	-15.5	89.9
	4	18.9	-13.9	86.4
	5	18.0	-12.4	90.1
	6	16.8	-10.9	93.4
	7	15.5	-9.5	96.8
	8	15.9	-8.1	114.4
	9	15.5	-6.8	130.8
	10	16.0	-5.5	164.8
	11	24.9	-4.4	323.1
	12	27.5	-3.2	492.6
	13	30.7	-2.4	745.3
Profile R2-5	0	28.6	-20.7	99.6
	1	23.1	-19.5	83.2
	2	22.3	-18.4	83.4
	3	20.7	-17.3	80.6
	4	17.6	-16.4	71.0
	5	15.9	-15.4	67.0
	6	15.3	-14.4	67.8
	7	13.6	-13.6	62.9
	8	12.7	-12.7	62.0
	9	13.9	-11.8	72.1
	10	12.8	-11.0	70.3
	11	11.5	-10.2	67.2
	12	13.2	-9.4	82.9
	13	13.4	-8.6	91.1
	14	12.4	-7.9	90.8
	15	12.7	-7.1	102.5
	16	13.5	-6.3	121.9
	17	14.1	-5.6	142.3
	18	15.0	-4.8	175.6
	19	21.5	-4.0	304.3
	20	26.6	-3.1	491.0
	21	35.5	-2.5	837.8
Profile R2-6	0	27.5	-20.9	95.1
	1	23.3	-19.9	82.8
	2	21.2	-18.9	77.8
	3	19.0	-18.0	71.9
	4	16.5	-17.1	64.5
	5	16.4	-16.3	66.4
	6	16.0	-15.5	67.1
	7	14.0	-14.7	61.0
	8	13.9	-13.9	63.2
	9	13.9	-13.1	66.2
	10	12.0	-12.4	59.6
	11	12.1	-11.7	63.1
	12	13.8	-11.0	75.9
	13	13.7	-10.3	79.6
	14	11.8	-9.7	72.0
	15	11.5	-9.0	74.9
	16	12.7	-8.4	88.1
	17	11.5	-7.8	85.1
	18	12.0	-7.2	95.6
	19	14.3	-6.6	123.8
	20	13.0	-6.0	122.7
	21	10.5	-5.5	107.1
	22	11.1	-4.9	126.5
	23	13.6	-4.4	172.7
	24	15.3	-3.9	219.1
	25	35.5	-3.4	609.6
	26	58.5	-3.0	1214.6
Profile R2-7	0	29.2	-20.9	101.2
	1	24.4	-20.0	86.5
	2	21.3	-19.1	77.6
	3	18.5	-18.2	69.4
	4	17.1	-17.5	65.8
	5	16.5	-16.7	65.6
	6	15.2	-15.9	62.5
	7	13.3	-15.2	56.5
	8	12.6	-14.5	55.4

	Z(cm)	S(o/oo)	T(°C)	v_b(o/oo)
	9	13.4	-13.8	61.3
	10	12.5	-13.1	59.5
	11	11.7	-12.5	57.7
	12	12.4	-11.9	63.7
	13	13.3	-11.3	71.4
	14	13.4	-10.7	75.4
	15	12.3	-10.1	72.6
	16	12.1	-9.6	74.6
	17	12.9	-9.0	84.2
	18	12.5	-8.5	85.8
	19	11.8	-8.0	85.4
	20	12.8	-7.4	99.5
	21	12.7	-7.0	103.9
	22	11.1	-6.5	97.0
	23	12.0	-6.1	111.4
	24	15.4	-5.6	155.7
	25	17.3	-5.2	188.3
	26	16.2	-4.7	193.9
	27	22.9	-4.3	302.7
	28	29.0	-3.9	427.5
	29	39.0	-3.6	637.1
Profile R2-8	0	28.5	-20.8	99.0
	1	23.5	-19.9	83.5
	2	20.5	-19.1	74.6
	3	17.8	-18.3	66.5
	4	16.0	-17.5	61.5
	5	16.1	-16.8	63.7
	6	15.0	-16.1	61.1
	7	13.0	-15.5	54.4
	8	12.9	-14.8	55.9
	9	12.4	-14.1	55.7
	10	11.1	-13.5	51.5
	11	11.3	-12.9	54.4
	12	12.3	-12.4	61.1
	13	12.9	-11.8	66.8
	14	12.8	-11.3	68.7
	15	13.0	-10.8	72.5
	16	12.9	-10.2	75.5
	17	12.1	-9.7	73.9
	18	12.2	-9.2	78.0
	19	12.8	-8.7	86.1
	20	11.6	-8.2	82.1
	21	10.6	-7.8	78.3
	22	11.1	-7.4	86.1
	23	10.9	-7.0	88.9
	24	11.8	-6.5	103.2
	25	14.5	-6.1	135.1
	26	14.1	-5.7	139.9
	27	12.1	-5.4	126.0
	28	12.4	-5.0	138.9
	29	14.0	-4.7	166.9
	30	17.4	-4.4	222.5
	31	35.8	-4.1	509.3
	32	52.7	-3.8	840.4
Profile R2-9	0	27.9	-20.7	97.1
	1	23.5	-19.9	83.5
	2	21.4	-19.1	78.0
	3	18.9	-18.4	70.4
	4	16.3	-17.5	62.7
	5	15.3	-16.8	60.5
	6	15.1	-16.1	61.6
	7	13.5	-15.4	56.8
	8	13.3	-14.8	57.6
	9	13.9	-14.1	62.5
	10	11.6	-13.6	53.5
	11	11.2	-13.0	53.5
	12	12.4	-12.4	61.6
	13	12.6	-11.8	65.2
	14	12.5	-11.3	67.1
	15	11.8	-10.8	65.7
	16	11.5	-10.3	66.6
	17	11.9	-9.8	72.0
	18	12.2	-9.3	77.3
	19	11.6	-8.8	77.1
	20	12.3	-8.4	85.3
	21	12.7	-7.9	93.1
	22	10.2	-7.5	78.1
	23	9.9	-7.1	79.6
	24	11.7	-6.7	99.5
	25	11.8	-6.3	106.2
	26	13.5	-5.9	129.6
	27	13.9	-5.5	142.6
	28	10.3	-5.1	112.8
	29	8.7	-4.8	100.7
	30	10.3	-4.5	127.2
	31	10.3	-4.1	139.1
	32	10.6	-3.8	154.2
	33	32.7	-3.6	526.5
	34	54.2	-3.4	974.0
Profile R2-10	0	26.7	-20.7	92.8
	1	23.7	-19.9	84.2
	2	21.3	-19.1	77.6
	3	18.1	-18.4	67.4

	Z(cm)	S(o/oo)	T(°C)	v_b(o/oo)
	4	16.2	-17.6	62.1
	5	16.1	-16.8	63.7
	6	14.6	-16.1	59.5
	7	13.0	-15.4	54.6
	8	13.4	-14.8	58.1
	9	13.2	-14.2	59.0
	10	11.6	-13.7	53.2
	11	10.4	-13.1	49.4
	12	10.8	-12.5	53.2
	13	12.5	-12.0	63.8
	14	12.9	-11.5	68.3
	15	11.8	-11.0	64.7
	16	11.2	-10.5	63.8
	17	11.3	-10.1	66.6
	18	11.5	-9.6	70.8
	19	11.8	-9.1	76.1
	20	11.9	-8.7	79.9
	21	11.3	-8.3	79.1
	22	11.1	-7.9	81.1
	23	11.2	-7.5	85.8
	24	10.2	-7.1	82.0
	25	11.5	-6.7	97.8
	26	13.7	-6.4	121.9
	27	11.4	-6.1	105.7
	28	10.1	-5.7	99.6
	29	11.3	-5.4	117.5
	30	9.9	-5.2	106.4
	31	8.9	-4.9	101.0
	32	10.3	-4.6	124.5
	33	12.5	-4.4	158.4
	34	18.6	-4.2	249.5
	35	42.6	-4.0	630.3
	35	64.7	-3.9	1032.3
Profile R2-11	0	28.2	-20.6	98.5
	1	23.3	-19.7	83.3
	2	20.5	-18.9	75.1
	3	18.5	-18.2	69.4
	4	16.7	-17.4	64.5
	5	15.7	-16.7	62.4
	6	15.3	-16.1	62.4
	7	13.6	-15.5	56.9
	8	11.9	-14.9	51.2
	9	12.3	-14.3	54.6
	10	11.3	-13.7	51.8
	11	9.9	-13.2	46.7
	12	10.8	-12.6	52.9
	13	12.0	-12.1	60.8

	Z(cm)	S(o/oo)	T(°C)	v_b(o/oo)
	14	12.5	-11.6	65.6
	15	12.4	-11.1	67.5
	16	11.9	-10.7	66.8
	17	11.3	-10.2	66.0
	18	11.0	-9.8	66.5
	19	10.5	-9.4	65.8
	20	9.6	-8.9	63.0
	21	10.5	-8.6	71.1
	22	11.5	-8.2	81.4
	23	11.3	-7.8	83.6
	24	11.4	-7.5	87.4
	25	12.2	-7.1	98.4
	26	12.1	-6.8	101.5
	27	10.4	-6.5	90.8
	28	9.7	-6.2	88.3
	29	9.4	-5.9	89.6
	30	8.7	-5.6	87.0
	31	8.5	-5.3	89.5
	32	8.9	-5.1	97.3
	33	10.1	-4.9	114.9
	34	11.6	-4.7	137.7
	35	20.2	-4.5	254.1
	36	30.6	-4.3	410.8
	37	45.5	-4.1	660.7
Profile R2-12	0	27.7	-20.5	97.0
	1	24.1	-19.7	86.3
	2	20.9	-18.9	76.6
	3	18.7	-18.1	70.4
	4	16.1	-17.4	62.2
	5	13.9	-16.7	55.1
	6	14.6	-16.0	59.8
	7	14.2	-15.4	59.8
	8	12.4	-14.8	53.7
	9	12.3	-14.2	54.9
	10	11.9	-13.6	54.9
	11	10.4	-13.0	49.7
	12	10.7	-12.5	52.7
	13	11.6	-12.0	59.2
	14	11.9	-11.5	62.9
	15	11.4	-11.0	62.5
	16	10.7	-10.5	60.9
	17	10.6	-10.0	62.9
	18	10.8	-9.6	66.4
	19	10.3	-9.2	65.7
	20	9.8	-8.8	65.0
	21	10.8	-8.4	74.7
	22	11.2	-8.0	81.0

	Z(cm)	S(o/oo)	T(°C)	v_s(o/oo)
	23	10.8	-7.6	81.7
	24	11.2	-7.3	88.0
	25	11.7	-7.0	95.6
	26	10.8	-6.6	93.0
	27	10.3	-6.3	92.5
	28	10.2	-6.0	95.9
	29	7.6	-5.8	73.4
	30	6.3	-5.6	62.8
	31	7.4	-5.4	76.4
	32	7.5	-5.2	80.3
	33	8.2	-5.0	91.2
	34	9.6	-4.8	111.3
	35	9.5	-4.7	112.3
	36	9.4	-4.5	115.9
	37	26.9	-4.4	350.4
	38	45.9	-4.2	651.0
Profile R2-13	0	25.4	-20.4	89.0
	1	23.1	-19.5	83.2
	2	20.2	-18.7	74.5
	3	18.7	-18.0	70.7
	4	17.4	-17.2	67.8
	5	15.0	-16.5	60.1
	6	13.7	-15.8	56.5
	7	13.1	-15.2	55.6
	8	12.7	-14.6	55.5
	9	12.2	-14.0	55.1
	10	10.7	-13.5	49.6
	11	9.7	-13.0	46.3
	12	10.4	-12.5	51.3
	13	11.4	-12.0	58.1
	14	11.8	-11.5	62.4
	15	12.2	-11.0	66.9
	16	10.9	-10.6	61.6
	17	9.4	-10.2	54.8
	18	10.5	-9.8	63.4
	19	11.4	-9.4	71.5
	20	10.7	-8.9	70.3
	21	10.4	-8.6	70.4
	22	10.3	-8.2	72.7
	23	10.5	-7.8	77.6
	24	11.1	-7.5	85.0
	25	11.0	-7.2	87.5
	26	10.8	-6.8	90.5
	27	11.4	-6.6	98.2
	28	10.2	-6.3	91.6
	29	7.7	-6.1	71.0
	30	7.9	-5.8	76.4

	Z(cm)	S(o/oo)	T(°C)	v_s(o/oo)
	31	8.3	-5.6	83.0
	32	7.7	-5.4	79.6
	33	8.1	-5.2	86.8
	34	9.4	-5.0	104.8
	35	10.0	-4.8	116.0
	36	9.3	-4.7	109.9
	37	17.7	-4.5	221.6
	38	29.5	-4.3	395.1
	39	46.9	-4.2	666.6
Profile R2-14	0	23.9	-20.3	83.9
	1	22.5	-19.5	80.9
	2	21.7	-18.7	80.2
	3	19.4	-18.0	73.4
	4	16.6	-17.2	64.6
	5	14.9	-16.5	59.7
	6	13.5	-15.8	55.7
	7	11.9	-15.2	50.4
	8	12.3	-14.6	53.8
	9	12.3	-14.0	55.5
	10	10.0	-13.5	46.3
	11	9.2	-13.1	43.6
	12	10.3	-12.6	50.4
	13	10.9	-12.1	55.2
	14	11.3	-11.6	59.2
	15	11.4	-11.2	61.5
	16	10.7	-10.8	59.5
	17	10.4	-10.4	59.7
	18	9.7	-9.9	58.0
	19	10.2	-9.6	62.7
	20	10.7	-9.1	68.9
	21	9.6	-8.8	63.6
	22	9.7	-8.5	66.3
	23	9.7	-8.2	68.4
	24	10.0	-7.8	73.8
	25	11.5	-7.6	87.1
	26	11.1	-7.3	87.2
	27	10.2	-7.0	83.1
	28	9.8	-6.7	83.1
	29	8.3	-6.4	73.2
	30	6.9	-6.2	62.6
	31	6.5	-5.9	61.7
	32	6.8	-5.7	66.7
	33	7.5	-5.5	76.1
	34	8.3	-5.2	89.0
	35	7.6	-5.1	82.9
	36	6.4	-4.9	72.3
	37	8.5	-4.7	100.3

	Z(cm)	S(o/oo)	T(°C)	v_b(o/oo)
	38	13.3	-4.6	161.7
	39	33.2	-4.4	437.9
	40	51.3	-4.3	718.6
Profile R2-15	0	23.0	-4.8	273.2
	1	20.2	-4.7	243.6
	2	19.3	-4.7	232.4
	3	18.4	-4.6	225.8
	4	15.9	-4.6	194.2
	5	14.2	-4.6	172.9
	6	14.2	-4.6	172.9
	7	13.4	-4.6	162.9
	8	12.5	-4.5	155.0
	9	12.5	-4.5	155.0
	10	11.5	-4.4	145.4
	11	10.4	-4.4	131.2
	12	11.4	-4.4	144.1
	13	12.4	-4.3	160.6
	14	11.4	-4.3	147.4
	15	10.9	-4.2	144.0
	16	10.9	-4.2	144.0
	17	10.6	-4.2	139.9
	18	11.2	-4.1	151.5
	19	10.9	-4.1	147.4
	20	10.3	-4.0	142.5
	21	10.4	-4.0	143.9
	22	10.0	-4.0	138.2
	23	9.4	-3.9	133.0
	24	10.1	-3.9	143.1
	25	11.4	-3.8	166.1
	26	12.0	-3.8	175.1
	27	11.2	-3.8	163.1
	28	9.7	-3.7	144.5
	29	8.3	-3.7	123.3
	30	7.5	-3.7	111.2
	31	7.0	-3.6	106.5
	32	7.4	-3.6	112.7
	33	8.2	-3.6	125.1
	34	8.1	-3.5	127.0
	35	8.2	-3.5	128.6
	36	7.1	-3.5	111.0
	37	8.0	-3.4	129.0
	38	16.8	-3.4	276.2
	39	29.2	-3.3	509.2
Profile R2-16	0	16.6	-4.8	194.9
	1	17.7	-4.7	212.5
	2	18.6	-4.6	228.4
	3	17.7	-4.6	216.9
	4	16.0	-4.5	199.7
	5	16.2	-4.4	206.7
	6	15.7	-4.3	204.6
	7	13.4	-4.2	177.9
	8	12.8	-4.2	169.7
	9	12.2	-4.1	165.4
	10	10.5	-4.0	145.3
	11	10.3	-3.9	146.0
	12	11.3	-3.8	160.1
	13	11.6	-3.8	169.1
	14	12.8	-3.7	192.0
	15	11.9	-3.7	178.1
	16	9.8	-3.6	150.0
	17	10.5	-3.6	161.0
	18	12.0	-3.6	184.6
	19	11.1	-3.5	175.1
	20	10.5	-3.5	165.5
	21	10.9	-3.5	171.9
	22	10.9	-3.5	171.9
	23	10.5	-3.4	170.2
	24	10.1	-3.4	163.6
	25	10.8	-3.4	175.2
	26	12.2	-3.4	198.5
	27	12.3	-3.3	206.2
	28	10.0	-3.3	166.7
	29	8.3	-3.3	137.8
	30	8.2	-3.3	136.2
	31	7.2	-3.3	119.3
	32	7.2	-3.2	122.9
	33	8.6	-3.2	147.3
	34	8.7	-3.2	149.0
	35	8.2	-3.2	140.3
	36	8.4	-3.2	143.8
	37	11.3	-3.2	194.8
	38	17.4	-3.1	314.0
	39	27.8	-3.1	514.7
Profile R2-17	0	13.0	-4.8	151.6
	1	15.2	-4.7	181.6
	2	17.0	-4.7	203.8
	3	17.0	-4.6	206.1
	4	16.6	-4.5	207.4
	5	15.8	-4.4	201.4
	6	14.9	-4.4	189.6
	7	13.9	-4.3	180.5
	8	12.5	-4.2	165.6
	9	11.6	-4.1	157.1

	Z(cm)	S(o/oo)	T(°C)	v_p(o/oo)
	10	10.9	-4.0	150.9
	11	10.9	-4.0	150.9
	12	11.1	-4.0	153.8
	13	10.5	-4.0	145.3
	14	11.0	-3.9	156.2
	15	11.8	-3.9	167.8
	16	10.5	-3.9	148.9
	17	9.7	-3.8	140.8
	18	10.4	-3.8	151.2
	19	10.9	-3.8	158.7
	20	11.1	-3.7	165.9
	21	11.3	-3.7	168.9
	22	10.4	-3.7	155.2
	23	10.1	-3.7	150.6
	24	11.5	-3.6	176.7
	25	11.8	-3.6	181.4
	26	11.9	-3.6	183.0
	27	12.1	-3.6	186.1
	28	10.7	-3.5	168.7
	29	9.7	-3.5	152.6
	30	8.4	-3.5	131.8
	31	7.1	-3.4	114.2
	32	8.0	-3.4	129.0
	33	8.5	-3.4	137.2
	34	7.7	-3.4	124.0
	35	8.3	-3.4	133.9
	36	10.5	-3.3	175.3
	37	13.0	-3.3	218.2
	38	19.2	-3.3	327.0
	39	27.5	-3.2	492.6
Profile R2-18	0	12.1	-5.1	133.0
	1	14.8	-4.9	169.8
	2	15.6	-4.7	189.0
	3	16.3	-4.5	203.5
	4	17.4	-4.4	222.5
	5	16.1	-4.3	210.0
	6	14.2	-4.3	184.5
	7	12.7	-4.2	168.4
	8	10.8	-4.2	142.6
	9	9.9	-4.2	130.5
	10	9.6	-4.1	129.5
	11	10.3	-4.0	142.5
	12	10.5	-4.0	145.3
	13	9.9	-4.0	136.8
	14	10.6	-3.9	150.3
	15	10.8	-3.9	153.2
	16	9.3	-3.8	134.9

	Z(cm)	S(o/oo)	T(°C)	v_p(o/oo)
	17	8.5	-3.7	126.3
	18	9.8	-3.7	146.1
	19	10.4	-3.6	159.4
	20	10.3	-3.6	157.8
	21	10.7	-3.6	164.1
	22	10.5	-3.6	161.0
	23	10.2	-3.6	156.3
	24	10.4	-3.6	159.4
	25	11.7	-3.5	184.8
	26	12.9	-3.5	204.3
	27	11.7	-3.5	184.8
	28	10.4	-3.5	163.8
	29	9.5	-3.5	149.4
	30	8.7	-3.4	140.5
	31	8.2	-3.4	132.2
	32	8.1	-3.4	130.6
	33	9.1	-3.4	147.1
	34	9.9	-3.4	160.3
	35	10.9	-3.4	176.9
	36	13.2	-3.4	215.3
	37	14.4	-3.4	235.5
	38	21.8	-3.4	362.6
	39	29.9	-3.3	522.2
Profile R2-19	0	12.2	-5.2	131.6
	1	13.5	-5.0	151.6
	2	14.7	-4.8	172.0
	3	15.9	-4.6	194.2
	4	16.0	-4.4	204.1
	5	15.5	-4.3	201.9
	6	14.6	-4.2	194.3
	7	12.3	-4.2	162.9
	8	10.4	-4.2	137.2
	9	10.1	-4.2	133.2
	10	8.8	-4.1	118.5
	11	7.5	-4.1	100.7
	12	8.7	-4.0	119.9
	13	10.5	-4.0	145.3
	14	10.4	-4.0	143.9
	15	10.2	-3.9	144.6
	16	10.1	-3.9	143.1
	17	9.4	-3.8	136.4
	18	9.7	-3.8	140.8
	19	9.9	-3.8	143.8
	20	10.1	-3.7	150.6
	21	10.5	-3.7	156.7
	22	10.5	-3.7	156.7
	23	10.5	-3.6	161.0

	Z(cm)	S(o/oo)	T(°C)	v_b(o/oo)
	24	10.9	-3.6	167.2
	25	11.7	-3.5	184.8
	26	12.2	-3.5	193.0
	27	10.9	-3.4	176.9
	28	10.5	-3.4	170.2
	29	10.2	-3.4	165.2
	30	8.4	-3.4	135.5
	31	8.7	-3.3	144.6
	32	9.1	-3.3	151.4
	33	8.1	-3.3	134.5
	34	8.0	-3.2	136.8
	35	9.0	-3.2	154.3
	36	12.3	-3.2	212.5
	37	22.1	-3.1	403.4
	38	34.1	-3.1	641.4
Profile R2-20	0	10.4	-4.9	118.4
	1	12.1	-4.8	140.9
	2	14.6	-4.6	177.9
	3	16.2	-4.5	202.3
	4	16.4	-4.4	209.3
	5	15.0	-4.3	195.2
	6	12.9	-4.2	171.1
	7	11.7	-4.2	154.8
	8	10.6	-4.2	139.9
	9	9.6	-4.2	126.5
	10	9.3	-4.2	122.5
	11	8.4	-4.1	113.0
	12	8.2	-4.1	110.3
	13	9.9	-4.1	133.6
	14	10.8	-4.0	149.5
	15	9.9	-4.0	136.8
	16	9.2	-4.0	127.0
	17	9.1	-3.9	128.7
	18	8.7	-3.9	122.9
	19	9.7	-3.9	137.3
	20	11.3	-3.8	164.6
	21	10.5	-3.8	152.7
	22	9.9	-3.8	143.8
	23	10.6	-3.7	158.2
	24	10.4	-3.7	155.2
	25	11.4	-3.7	170.5
	26	11.7	-3.6	179.8
	27	10.2	-3.6	156.3
	28	10.3	-3.6	157.8
	29	10.5	-3.6	161.0
	30	9.1	-3.5	143.0
	31	8.3	-3.5	130.2
	32	8.5	-3.4	137.2
	33	8.3	-3.4	129.0
	34	8.1	-3.4	130.6
	35	10.1	-3.4	163.6
	36	13.0	-3.3	218.2
	37	22.5	-3.3	386.2
	38	33.1	-3.3	582.6

	Z(cm)	S(o/oo)	T(°C)	v_s(o/oo)
Profile R3-3	0	21.7	-10.1	129.5
	1	17.1	-8.7	115.6
	2	15.8	-7.5	121.9
	3	15.5	-6.4	138.3
	4	13.8	-5.2	149.3
	5	16.8	-4.2	224.5
	6	22.3	-3.2	394.5
	7	29.1	-2.2	769.9
Profile R3-4	0	20.2	-10.1	120.3
	1	16.0	-9.2	102.8
	2	14.6	-8.3	102.6
	3	13.5	-7.4	105.1
	4	12.8	-6.5	112.1
	5	12.7	-5.7	125.8
	6	12.9	-4.8	150.4
	7	18.3	-3.9	263.7
	8	24.4	-3.1	447.9
	9	32.3	-2.2	863.5
Profile R3-5	0	22.9	-10.2	135.7
	1	16.6	-9.7	101.9
	2	13.0	-9.1	84.0
	3	11.1	-8.5	76.0
	4	11.6	-8.0	83.9
	5	10.4	-7.4	80.6
	6	9.4	-6.8	78.6
	7	10.1	-6.3	90.7
	8	10.2	-5.7	100.6
	9	9.7	-5.1	106.2
	10	10.0	-4.6	120.8
	11	11.7	-4.0	162.3
	12	12.1	-3.5	191.3
	13	24.0	-2.9	470.8
	14	36.0	-2.3	929.2
Profile R3-6	0	18.1	-10.3	105.8
	1	14.9	-9.8	90.5
	2	13.3	-9.2	85.2
	3	12.3	-8.5	84.4
	4	11.3	-8.2	79.9
	5	10.5	-7.7	78.5
	6	9.9	-7.2	78.6
	7	8.7	-6.7	73.6
	8	8.9	-6.3	79.8
	9	10.2	-5.8	99.0
	10	9.4	-5.4	97.4
	11	9.9	-4.9	112.6
	12	11.9	-4.5	147.4
	13	12.1	-4.0	168.0
	14	13.0	-3.6	200.4
	15	21.6	-3.2	381.5
	16	30.9	-2.8	639.8
	17	42.9	-2.4	1081.6
Profile R3-7	0	17.3	-10.2	101.8
	1	14.1	-9.6	87.1
	2	12.7	-9.0	82.9
	3	11.8	-8.4	81.7
	4	11.1	-8.0	80.2
	5	10.6	-7.5	81.2
	6	9.6	-7.1	77.2
	7	8.9	-6.8	74.3
	8	9.0	-6.4	79.5
	9	9.0	-6.1	83.1
	10	8.7	-5.7	85.6
	11	8.9	-5.4	92.1
	12	9.1	-5.0	101.4
	13	9.6	-4.7	113.5
	14	10.6	-4.3	136.6
	15	10.9	-4.0	150.9
	16	12.2	-3.6	187.7
	17	22.7	-3.3	389.8
	18	31.8	-2.9	636.7
	19	42.2	-2.5	1016.2
Profile R3-8	0	18.6	-10.2	109.7
	1	14.8	-9.7	90.7
	2	12.8	-9.3	81.1
	3	11.1	-8.8	73.7
	4	9.5	-8.4	65.6
	5	9.5	-7.9	69.3
	6	9.8	-7.5	74.9
	7	9.5	-7.1	76.3
	8	8.8	-6.7	74.5
	9	8.8	-6.3	78.9
	10	8.5	-6.0	79.7
	11	7.9	-5.6	78.9
	12	8.9	-5.3	93.8
	13	9.5	-5.0	105.9
	14	8.3	-4.6	100.0
	15	7.4	-4.3	94.9
	16	9.2	-3.9	130.1
	17	11.5	-3.6	176.7
	18	12.2	-3.3	204.4
	19	24.6	-2.9	483.3

	Z(cm)	S(o/oo)	T(°C)	v_s(o/oo)
	20	38.4	-2.6	877.1
Profile R3-9	0	17.8	-10.3	104.0
	1	15.0	-9.8	91.1
	2	13.8	-9.5	86.0
	3	11.4	-9.0	74.2
	4	8.6	-8.6	58.1
	5	8.8	-8.3	61.4
	6	9.2	-7.9	67.1
	7	8.2	-7.5	62.6
	8	8.2	-7.2	64.9
	9	8.2	-6.8	68.4
	10	7.7	-6.5	66.9
	11	8.9	-6.2	81.0
	12	9.5	-5.9	90.6
	13	7.0	-5.6	69.8
	14	6.9	-5.3	72.5
	15	8.3	-5.0	92.3
	16	7.4	-4.7	87.2
	17	8.3	-4.4	104.3
	18	10.8	-4.1	146.0
	19	12.0	-3.8	175.1
	20	12.6	-3.5	199.5
	21	21.0	-3.2	370.4
	22	26.5	-2.9	523.2
	23	35.7	-2.6	809.1
Profile R3-10	0	17.8	-10.3	104.0
	1	13.9	-9.9	83.6
	2	12.1	-9.5	75.2
	3	11.7	-9.1	75.5
	4	10.3	-8.8	68.3
	5	8.7	-8.4	60.0
	6	8.2	-8.1	58.4
	7	7.4	-7.7	55.1
	8	7.6	-7.4	58.7
	9	8.7	-7.1	69.8
	10	8.7	-6.8	72.6
	11	8.4	-6.5	73.1
	12	7.8	-6.2	70.8
	13	7.5	-5.9	71.3
	14	6.8	-5.6	67.8
	15	5.9	-5.4	60.8
	16	7.1	-5.1	77.4
	17	8.2	-4.8	94.8
	18	8.2	-4.5	100.8
	19	9.1	-4.3	117.1
	20	10.5	-4.0	145.3
	21	10.8	-3.7	161.3
	22	12.0	-3.5	189.7
	23	19.7	-3.2	346.3
	24	28.9	-3.0	554.7
	25	41.1	-2.7	909.3
Profile R3-12	0	16.2	-20.5	56.1
	1	13.1	-19.7	46.4
	2	11.4	-18.9	41.4
	3	10.8	-18.1	40.4
	4	10.1	-17.4	38.8
	5	8.6	-16.7	33.9
	6	8.1	-16.0	32.9
	7	8.0	-15.4	33.4
	8	7.3	-14.8	31.4
	9	7.2	-14.2	32.0
	10	6.7	-13.6	30.8
	11	6.8	-13.0	32.3
	12	7.9	-12.5	38.8
	13	7.4	-12.0	37.6
	14	6.4	-11.5	33.6
	15	5.8	-11.0	31.6
	16	5.5	-10.5	31.1
	17	6.7	-10.0	39.6
	18	7.7	-9.6	47.2
	19	7.2	-9.2	45.7
	20	8.0	-8.8	52.9
	21	7.8	-8.4	53.7
	22	6.5	-8.0	46.7
	23	8.4	-7.6	63.3
	24	10.5	-7.3	82.4
	25	10.9	-7.0	88.9
	26	14.7	-6.6	127.3
	27	24.8	-6.3	227.9
	28	27.4	-6.0	264.8
	29	30.3	-5.8	303.9
Profile R3-13	0	16.2	-10.4	93.7
	1	14.2	-10.0	84.7
	2	12.1	-9.6	74.6
	3	11.2	-9.3	70.9
	4	9.9	-8.9	65.0
	5	8.1	-8.5	55.2
	6	7.3	-8.2	51.3
	7	6.9	-7.9	50.1
	8	7.1	-7.6	53.4
	9	7.5	-7.4	57.9
	10	6.6	-7.1	52.8

	Z(cm)	S(o/oo)	T(°C)	V_B(o/oo)
	11	6.4	-6.9	52.5
	12	7.5	-6.6	64.3
	13	7.4	-6.4	65.2
	14	6.8	-6.2	61.7
	15	6.7	-5.9	63.6
	16	6.5	-5.7	63.7
	17	6.4	-5.5	64.9
	18	7.0	-5.2	74.9
	19	7.3	-5.0	81.1
	20	7.3	-4.8	84.3
	21	7.2	-4.5	88.4
	22	6.3	-4.3	80.6
	23	6.1	-4.1	81.7
	24	8.1	-3.9	114.3
	25	9.8	-3.7	146.1
	26	10.3	-3.5	162.2
	27	13.1	-3.3	220.0
	28	21.1	-3.1	384.2
	29	31.2	-2.8	646.6
Profile R3-14	0	14.0	-10.4	80.7
	1	14.1	-10.0	84.1
	2	12.2	-9.6	75.2
	3	10.8	-9.3	68.3
	4	9.7	-8.9	63.7
	5	7.9	-8.6	53.3
	6	7.0	-8.3	48.7
	7	7.0	-8.0	50.3
	8	6.8	-7.7	50.6
	9	6.3	-7.5	47.9
	10	6.1	-7.2	48.2
	11	5.9	-6.9	48.4
	12	6.7	-6.7	56.5
	13	7.8	-6.5	67.8
	14	7.3	-6.2	66.2
	15	6.9	-6.0	64.5
	16	7.2	-5.8	69.5
	17	7.2	-5.6	71.8
	18	6.5	-5.4	67.0
	19	5.8	-5.2	61.9
	20	6.9	-5.0	76.6
	21	6.9	-4.8	79.6
	22	5.7	-4.6	68.3
	23	6.1	-4.4	76.3
	24	7.0	-4.2	91.8
	25	8.0	-4.0	110.1
	26	9.4	-3.8	136.4
	27	10.4	-3.6	159.4
	28	11.4	-3.4	185.2
	29	24.8	-3.2	441.4
	30	40.1	-3.0	792.3
Profile R3-15	0	13.3	-10.4	76.6
	1	14.1	-10.0	84.1
	2	12.4	-9.6	76.4
	3	10.2	-9.3	64.4
	4	9.5	-8.9	62.3
	5	8.4	-8.6	56.7
	6	7.1	-8.3	49.4
	7	6.0	-8.0	43.1
	8	6.4	-7.8	47.0
	9	7.3	-7.5	55.6
	10	5.7	-7.3	44.4
	11	5.6	-7.0	45.3
	12	7.5	-6.8	62.5
	13	7.1	-6.6	60.8
	14	5.8	-6.4	51.0
	15	6.0	-6.2	54.3
	16	6.4	-6.0	59.8
	17	6.6	-5.8	63.7
	18	6.7	-5.5	67.9
	19	6.4	-5.3	67.2
	20	6.0	-5.1	65.2
	21	5.3	-5.0	58.6
	22	4.8	-4.8	55.2
	23	6.0	-4.6	72.0
	24	8.0	-4.4	100.5
	25	8.7	-4.2	114.4
	26	8.0	-4.0	110.1
	27	8.2	-3.8	118.7
	28	10.0	-3.6	153.1
	29	15.4	-3.5	245.3
	30	29.4	-3.3	512.9
	31	45.8	-3.1	887.6
Profile R3-16	0	11.2	-10.4	64.3
	1	13.6	-10.0	81.0
	2	13.4	-9.6	82.7
	3	11.2	-9.3	70.9
	4	9.8	-9.0	63.7
	5	8.5	-8.7	56.8
	6	6.9	-8.4	47.5
	7	6.0	-8.1	42.6
	8	6.2	-7.8	45.5
	9	6.5	-7.5	49.5
	10	6.1	-7.3	47.6

	Z(cm)	S(o/oo)	T(°C)	v_b(o/oo)
	11	5.8	-7.1	46.4
	12	6.5	-6.8	54.1
	13	7.1	-6.6	60.8
	14	5.6	-6.4	49.2
	15	4.9	-6.2	44.3
	16	6.3	-6.0	58.8
	17	6.9	-5.8	66.6
	18	6.6	-5.5	66.9
	19	7.1	-5.3	74.6
	20	7.1	-5.1	77.4
	21	6.3	-5.0	69.8
	22	6.0	-4.8	69.1
	23	5.7	-4.6	68.3
	24	6.7	-4.5	82.2
	25	8.1	-4.3	104.0
	26	7.7	-4.1	103.5
	27	7.6	-3.9	107.1
	28	8.1	-3.7	120.3
	29	10.9	-3.6	167.2
	30	17.7	-3.4	291.6
	31	28.3	-3.2	508.0
Profile R3-17	0	11.4	-10.1	67.2
	1	13.3	-9.7	81.3
	2	12.9	-9.3	81.8
	3	10.1	-9.0	65.7
	4	8.1	-8.6	54.7
	5	7.0	-8.3	48.7
	6	6.6	-8.0	47.4
	7	7.5	-7.7	55.8
	8	7.5	-7.5	57.2
	9	6.5	-7.2	51.3
	10	5.5	-6.9	45.1
	11	4.6	-6.7	38.7
	12	5.3	-6.5	45.9
	13	6.8	-6.3	60.7
	14	6.2	-6.1	57.0
	15	5.2	-5.9	49.2
	16	5.4	-5.7	52.8
	17	6.1	-5.5	61.8
	18	7.0	-5.4	72.2
	19	6.6	-5.2	70.5
	20	6.5	-5.0	72.1
	21	6.6	-4.8	76.1
	22	5.2	-4.7	61.0
	23	4.6	-4.5	56.2
	24	6.0	-4.3	76.8
	25	6.8	-4.1	91.2
	26	6.1	-4.0	83.7
	27	6.5	-3.8	93.7
	28	6.8	-3.6	103.4
	29	4.9	-3.5	76.3
	30	10.5	-3.3	175.3
	31	18.9	-3.1	342.3

t is the time (hr) and h is the ice thickness (cm).

Run 2:

$0 \leq h < 32$

$$t = A1(h) + A2(h)^2 + A3(h)^3 + A4(h)^4$$

where A1 = 0.100717
A2 = 0.123590
A3 = -2.43955×10^{-3}
A4 = 7.27394×10^{-5}

correlation coefficient = 0.999955
standard error of the estimate = 0.467297

$32 \leq h < 38$

$$t = B1 + B2(h) + B3(h)^2$$

where B1 = 2978.20
B2 = -192.477
B3 = 3.23026

correlation coefficient = 0.999497
standard error of the estimate = 2.34285

$38 \leq h$

$$t = C1 + C2(h)$$

where C1 = -4028.36
C2 = 115.657

correlation coefficient = 0.991538
standard error of the estimate = 15.0075

Run 3:

$0 \leq h < 22$

$$t = A1(h) + A2(h)^2 + A3(h)^3 + A4(h)^4$$

where A1 = 0.241555
A2 = 0.312351
A3 = -1.38347×10^{-2}
A4 = 6.41655×10^{-4}

correlation coefficient = 0.999898
standard error of the estimate = 0.520213

$22 \leq h$

$$t = B1 + B2(h) + B3(h)^2 + B4(h)^3$$

where B1 = -13393.2
B2 = 1669.29
B3 = -69.0424
B4 = 0.961763

correlation coefficient = 0.993944
standard error of the estimate = 17.9179

k_{eff} is the effective distribution coefficient and v* is the growth velocity at the bridging layer (cm/sec).

$v^* \geq 2.0 \times 10^{-5}$ cm/sec:

k_{eff}	$v^* \times 10^6$ (cm/sec)
0.72	280.
0.66	234.
0.60	201.
0.56	177.
0.53	158.
0.52	143.
0.49	124.
0.44	105.
0.43	91.1
0.42	102.
0.38	80.3
0.35	58.4
0.34	33.8
0.34	63.5
0.31	24.2
0.30	41.5
0.29	35.2

$v^* < 2.0 \times 10^{-5}$ cm/sec:

k_{eff}	$v^* \times 10^6$ (cm/sec)
0.28	18.9
0.27	19.4
0.27	14.1
0.26	16.7
0.25	13.7
0.22	6.92
0.20	5.96
0.19	10.2
0.19	2.25
0.19	3.04
0.18	1.72
0.15	2.40
0.15	2.40
0.14	1.72
0.13	2.40
0.12	1.72